12-1-2014

GIS Framework for Spatiotemporal Mapping of Urban Flooding and Analyze Watershed Hydrological Response to Land Cover Change

Sayed Joinal Hossain Abedin
University of Nevada, Las Vegas, hossain2@unlv.nevada.edu

GIS FRAMEWORK FOR SPATIOTEMPORAL MAPPING OF URBAN FLOODING AND ANALYZE WATERSHED HYDROLOGICAL RESPONSE TO LAND COVER CHANGE

By

Sayed Joinal Hossain Abedin

Bachelor of Science in Water Resources Engineering

Bangladesh University of Engineering and Technology

2009

A thesis submitted in partial fulfillment of the requirements for the

Master of Science in Engineering – Civil and Environmental Engineering

Department of Civil and Environmental Engineering and Construction

Howard R. Hughes College of Engineering

The Graduate College

University of Nevada, Las Vegas

December 2014

UNLV | GRADUATE COLLEGE

We recommend the thesis prepared under our supervision by

Sayed Joinal Hossain Abedin

entitled

GIS Framework for Spatiotemporal Mapping of Urban Flooding and Analyze Watershed Hydrological Response to Land Cover Change

is approved in partial fulfillment of the requirements for the degree of

Master of Science in Engineering -- Civil and Environmental Engineering

Department of Civil and Environmental Engineering and Construction

Haroon Stephen, Ph.D., Committee Chair

Sajjad Ahmad, Ph.D., Committee Member

Jacimaria Batista, Ph.D., Committee Member

Zhongbo Yu, Ph.D., Graduate College Representative

Kathryn Hausbeck Korgan, Ph.D., Interim Dean of the Graduate College

December 2014

ABSTRACT

Urban flooding is a manmade disaster, and a recurrent problem in cities around the globe. Increased surface imperviousness due to urbanization along with inadequate drainage infrastructure system are the chief culprits for urban flooding. Flooding in an urban area brings about severe economic, structural, and environmental damages, and can be associated with casualties too. In order to evade flooding, an efficient flood model is imperative to study current flooding, and analyze flooding behavior to urban surface characteristics.

This research aims to develop a framework using Geographic Information System (GIS) to perform modeling and mapping of flood spatiotemporal variation in urban micro-watersheds. Moreover, watershed hydrologic response to the flood remediation measures through land cover changes is analyzed. The GIS-framework includes a workflow of several methods and processes including delineating urban watershed, generation of runoff hydrograph, and time series mapping of inundation depths and flood extent. The developed GIS-framework is used to study urban watershed hydrologic response to the change in land surface characteristics. This framework is tested in areas previously known to have experienced flooding at the University of Nevada Las Vegas (UNLV) main campus including Blacklot parking lot and East Mall. Calibration is performed with Digital Elevation Model (DEM) resolution, rainfall temporal resolution, and clogging factors whereas validation is performed using news reports and photographic evidence.

The testing at Blacklot site resulted in calibration at 5m DEM resolution and clogging factor of 0.83. The flood model produces a peak flood depth error of 24% between the estimated (26 inches) and actual flood depth (34 inches) for the Blacklot. The observed inundation points are found to be within the estimated flood extents. The flood beginning time (1:53 PM) is found consistent with the actual timing of 2:00 PM. East Mall site shows consistent results. The GIS framework provides spatiotemporal maps of flood inundation for visualization of flood dynamics. Through the calibration against DEM and rainfall resolution, it is observed that DEM resolution follows an irregular trend against errors, while rainfall resolution produces higher errors with increasing resolution.

The response of an urban watershed to land cover change is also analyzed. The tests are conducted in the Blacklot area, and the land cover types include porous asphalt, gravel and grass swale strips, grass pavers, and concrete grid pavers. The analysis shows that the watershed flooding reduces with a decrease in curve numbers of the surface materials. Flooding is reduced by 26% for porous asphalt, and only 2.90% for grass and gravel swale strips. The flooding is most reduced for grass pavers (by 46%), while flooding is reduced to none for concrete grid pavers. Concrete grid pavers are found to be the optimum land cover in the Blacklot area to avoid flooding.

This research provides insight into flood modeling, and mapping for a storm drain inlet based watershed. It also provides intuition on calibration against DEM and rainfall temporal resolution, and on soft validation techniques. Finally, it provides understanding on watershed hydrologic response to flood remediation land surfaces.

ACKNOWLEDGMENTS

I would like to thank Dr. Haroon Stephen for his continuous support and contributions that have made this research possible. I also express my appreciation towards Dr. Sajjad Ahmad, Dr. Jacimaria Batista, and Dr. Zhongbo YU for their participation and inputs. My gratitude will always be given to my family and friends. Their support and encouragement throughout my graduate studies have helped me to obtain this invaluable accomplishment.

TABLE OF CONTENTS

ABSTRACT iii
ACKNOWLEDGMENTS v
TABLE OF CONTENTS vi
LIST OF TABLES viii
LIST OF FIGURES ix
CHAPTER 1: INTRODUCTION 1
1.1 Research Motivation 3
1.2 Research Objectives 5
1.3 Research Approach 6
1.4 Thesis Outline 7
1.5 Thesis Contribution 7
CHAPTER 2: LITERATURE REVIEW 8
2.1 Causes of urban flooding: Climate Change and Urbanization 8
2.2 Flooding in Las Vegas 10
2.3 Issues to be considered in Hydrological Modeling 14
2.4 GIS Integration with Hydrologic Models: Practices, Problems and Prospects 15
2.5 GIS-framework Studies 17
2.5.1 Studies on Watershed Delineation 17
2.5.2 Studies on Rainfall to runoff conversion 20
2.5.3 Studies on Runoff to flow conversion 23
2.5.4 Studies on Inundation Estimation and Mapping 29
2.5.5 Calibration and Validation 35
2.6 Relating Watershed's Hydrologic Response to Land cover Change 39
2.6.1 Studies on Permeable Pavement System for Urban Stormwater Management 40
2.6.2 Studies on Recognized Porous Pavement Systems for Flood Reduction 43
2.6.3 Porous Asphalt Pavement 43
2.6.4 Gravel Pavers 45
2.6.5 Grass Pavers 45
2.6.6 Concrete Grid pavers (CGP) 46
2.7 Concluding Statements 46
CHAPTER 3: STUDY AREA AND DATA 48
3.1 Study Area 48
3.1.1 Blacklot Parking Area 48
3.1.2 East Mall Area 51
3.2 Data 53
3.2.1 Remote Sensing Data 53
3.2.2 Hydrological Data 55
CHAPTER 4: GIS-FRAMEWORK 60
4.1 Research Approach 60
4.2 Flood Mapping GIS Framework 61
4.2.1 Urban watershed Delineation 62
4.2.2 Rainfall to Runoff Conversion 64
4.2.3 Runoff to Flow Conversion 66

4.2.4 Inundation Estimation and Mapping 68
4.2.5 Calibration and Validation 71
4.3 Summary 74
CHAPTER 5: CASE STUDIES 76
5.1. Black Parking Lot of UNLV 76
5.1.1. Results 76
5.1.2. Discussion 94
5.2. East Mall 99
5.2.1 Results 99
5.2.2. Discussion 113
5.3 Sensitivity Analysis 115
5.4 Summary of Discussion 118
CHAPTER 6: RELATING THE WATERSHED'S HYDROLOGIC RESPONSE TO THE LAND COVER CHANGE 120
6.1 Introduction 120
6.2 Research Approach and Methodology 120
6.2.1 Research Approach 120
6.2.2 Methodology 122
6.3 Results 127
6.3.1 Porous Asphalt Pavement 127
6.3.2 Gravel Swale Strip 129
6.3.3 Grass Swale Strip 131
6.3.4 Grass Pavers along the Parking Aisles 133
6.3.5 Concrete Grid Pavers (CGP) 135
6.4 Discussion 136
6.5 Summary 140
CHAPTER 7: SUMMARY AND CONCLUSION 141
7.1 Summary 141
7.2 Conclusions 143
7.2.1 Limitations 146
7.3 Recommendations 146
APPENDIX 148
REFERENCES 150
VITA 161

LIST OF TABLES

Table 2.2-1: Peak depths and discharges at various CCRFCD stations 12
Table 3.2-1: Peak rainfall intensity distribution for Station 4574 57
Table 6.2-1: Area coverage and curve numbers for land covers 122
Table 6.4-1: Summary of outputs for land cover analysis 136

LIST OF FIGURES

Figure 2.2-1: Flooding in Las Vegas in 1975 (Randerson, 1976) 10
Figure 2.2-2: Flooding in UNLV Blacklot (RebelYell, 2013)..... 13
Figure 2.5-1: Watershed delineation process (modified from Zhang et al., 2011)..... 18
Figure 2.5-2: Snapping pour point (modified from Trent University Library, 2012)..... 19
Figure 2.5-3: Graphical representation of a runoff hydrograph..... 23
Figure 2.5-4: Translation hydrograph construction (modified from Usul and Yilmaz, 2002) 27
Figure 2.5-5: Grate inlet (left); Curb opening inlet (middle) and Combination inlet (right) 30
Figure 2.6-1: Porous asphalt (top left corner); Concrete grid pavers (top right corner); Gravel pavers (bottom left corner) and Grass pavers (bottom right corner) (Hunt and Collins, 2008)..... 42
Figure 2.6-2: Typical cross section of porous pavement system in a parking area (modified from UNHSC, 2009) 44
Figure 3.1-1: Blacklot study area (on the right) and Las Vegas Valley (on the left)..... 49
Figure 3.1-2: Location of drain inlet (on top) and the drain inlet (at bottom) 50
Figure 3.1-3: Study area for East Mall's drain inlet (along with East Mall) 51
Figure 3.1-4: Storm drain inlet at the East Mall area..... 52
Figure 3.2-1: Land Cover map for East Mall study area 54
Figure 3.2-2: Rainfall Hyetograph for September 11, 2012 56
Figure 3.2-3: Soil map for the East Mall study area..... 57
Figure 4.1-1: GIS-framework for modeling and mapping urban flood 61
Figure 4.2-1: Flowchart of watershed delineation processes..... 63
Figure 4.2-2: Graphical representation of Inundation estimation processes; typical runoff hydrograph along with rating curve (tope left corner); flood volume vs. time plot (top right corner); Stage-volume curve (lower left corner); and flood depth vs. time curve (lower right corner)..... 69
Figure 4.2-3: Flowchart of methodology for estimating time series of flood depths 71
Figure 5.1-1: Black lot study area DEM of 5 meter resolution and its errors..... 77
Figure 5.1-2: Reconditioned 5m DEM of the Blacklot study area 78
Figure 5.1-3: Stream Network in the Blacklot study area 78
Figure 5.1-4: Delineated watershed in Black lot for the pour point 79
Figure 5.1-5: Velocity coefficient map of the Black lot watershed..... 81
Figure 5.1-6: Slope map of the Black lot watershed..... 81
Figure 5.1-7: Velocity map of the Black lot watershed..... 82
Figure 5.1-8: Travel time map of the Blacklot watershed 82
Figure 5.1-9: Time area histogram of the Blacklot watershed..... 83
Figure 5.1-10: Runoff hydrograph for the 1st rainfall subevent in Blacklot watershed.... 84
Figure 5.1-11: Hydrograph for the complete rainfall event..... 85
Figure 5.1-12: Stage discharge curve for Blacklot drain inlet..... 85
Figure 5.1-13: Stage capacity curve for the Blacklot watershed 86
Figure 5.1-14: Flood depth variation over time in Blacklot watershed 87
Figure 5.1-15: Inundation extent at 30 minute after rainfall in Black lot watershed..... 88
Figure 5.1-16: Inundation extent at 60 minutes after rainfall in Blacklot watershed 89

Figure 5.1-17: Inundation extent after 124 minutes of rainfall in Blacklot watershed..... 89
Figure 5.1-18: Inundation extent after 590 minutes of rainfall in Blacklot watershed..... 90
Figure 5.1-19: Inundation extent after 500 minutes of rainfall in Blacklot watershed..... 90
Figure 5.1-20: Calibration and validation against DEM resolution in Blacklot watershed 91
Figure 5.1-21: Calibration and validation against rainfall resolution in Blacklot watershed 92
Figure 5.1-22: Calibration and validation against clogging factor in Blacklot watershed 92
Figure 5.1-23: Image used for validation and calibration in Blacklot (RebelYell, 2013) 93
Figure 5.1-24: Geographic location of inundation points at Black parking lot 94
Figure 5.2-1: Reconditioned 5m DEM of the East Mall study area 99
Figure 5.2-2: Delineated watershed for the East Mall area 100
Figure 5.2-3: Velocity coefficient map for the East Mall watershed..... 102
Figure 5.2-4: Slope map of the East Mall watershed..... 102
Figure 5.2-5: Velocity map of the East Mall watershed 103
Figure 5.2-6: Travel time map of the East Mall watershed 104
Figure 5.2-7: Time area histogram of the East Mall watershed..... 104
Figure 5.2-8: Runoff hydrograph for the 1st rainfall subevent in East Mall watershed.. 105
Figure 5.2-9: Final runoff hydrograph for the East Mall watershed..... 106
Figure 5.2-10: Stage discharge curve of the East Mall drain inlet..... 106
Figure 5.2-11: Stage capacity curve of the East Mall watershed..... 107
Figure 5.2-12: Flood depth variation over time in East Mall watershed 108
Figure 5.2-13: Inundation extent after 60 minutes of rainfall in East Mall watershed... 109
Figure 5.2-14: Inundation extent after 185 minute of rainfall in East Mall watershed .. 109
Figure 5.2-15: Inundation extent after 480 minute of rainfall in East Mall watershed .. 110
Figure 5.2-16: Inundation extent after 650 minute of rainfall in East Mall watershed .. 110
Figure 5.2-17: Inundation extent after 700 minute of rainfall in East Mall watershed .. 111
Figure 5.2-18: Calibration against DEM resolution for East Mall watershed 112
Figure 5.2-19: Image for calibration and validation in East Mall (RebelYell, 2013)..... 112
Figure 5.3-1: Runoff sensitivity to the total rainfall 116
Figure 5.3-2: Flooding sensitivity to the total rainfall 117
Figure 5.3-3: Sensitivity of peak flood depth, flood duration and peak runoff to rainfall 118
Figure 6.2-1: Flowchart of research methodology for determining impacts of land cover change on flooding..... 121
Figure 6.2-2: Schematic map of gravel and grass swale strip along main flowpath 124
Figure 6.2-3: Curve number distribution map for gravel and grass swale strips..... 125
Figure 6.2-4: Schematic presentation of parking aisle filled with grass pavers 126
Figure 6.3-1: Runoff hydrograph for the porous asphalt land cover 127
Figure 6.3-2: Flood depth variation over time for porous asphalt land cover 128
Figure 6.3-3: Peak inundation extent for the porous asphalt land cover 128
Figure 6.3-4: Runoff hydrograph for the gravel swale strip 129
Figure 6.3-5: Flood depth variation over time for gravel swale strip 130
Figure 6.3-6: Peak inundation extent for gravel swale strip 130
Figure 6.3-7: Runoff hydrograph for the grass swale strip..... 131
Figure 6.3-8: Flood depth variation over time for grass swale strip..... 132

Figure 6.3-9: Peak inundation extent for grass swale strip 132
Figure 6.3-10: Runoff hydrograph for the gravel pavers along the parking aisles 133
Figure 6.3-11: Flood depth over time for the grass pavers along the parking aisles 134
Figure 6.3-12: Peak inundation extent for the grass pavers along the parking aisles 134
Figure 6.3-13: Runoff hydrograph for the concrete grid pavers 135
Figure 6.3-14: Flood depth variation over time for concrete grid pavers 136

CHAPTER 1: INTRODUCTION

Urban flooding is a common problem in cities resulting from excessive water flows accompanied with impaired or limited drainage infrastructure. The excessive flows can result from various sources including runoff from precipitation or snowmelt, flows from coastal and riverine overtopping; and leaks from failure of water storage or conveyance structures. In case of rapid flows of excess water, urban flash floods can occur that pose additional challenges. Usually, urban flash floods occur when there is heavy rainfall for a short duration. Generally, flash floods are most common in cities. That is why urban flash floods are frequently referred as urban floods.

Urban areas are prone to flooding mainly because of excessive impervious surface made of watertight materials like asphalt, concrete, bricks etc. that do not let the water to infiltrate, and thus produce higher amount of runoff (Chen et al., 2009). Moreover, impervious surfaces accelerate runoff because of their low surface friction. Thus, there is a large amount of runoff in short time duration, and when the existing drainage system is unable to remove this excessive and rapid runoff, flooding occurs. Urban floods can be caused by sediments too. The sediments in an urban area are produced from land site construction, deterioration of road surfaces, street trashes etc. (NRCS, 2008). The urban runoff carries sediments, and passes through the drainage system that includes drainage pipes, detention basins etc. Sediments can corrode the pipes resulting in structural failure, and can reduce the water holding capacity of the reservoirs resulting floods in upstream. Besides, the sediments carried by the runoff poses great threats to the downstream aquatic life (NRCS, 2008).

Though urban floods occur for a short duration they may cause serious economic damage by interrupting and shutting off the local businesses. Floods can also cause structural damages, such as damages to buildings, streets and the drainage system. Urban floods can also affect the daily life of people, such as interruption of the electric power supply. Floods also pose threat to human health through the contamination of drinking water, and threat of various waterborne diseases. In addition, floods may result in shutting down of educational institutions, and hindering the religious activities. Urban floods can cause environmental damages by affecting the downstream aquatic ecosystem. Finally, in extreme cases, floods can be fatal and result in causalities. The consequences of these damages are very high providing that around 50% of the world's total population live in urban areas, which is over 80% for United States (Chen et al., 2009). Thus, in order to prevent flooding, it should be ensured that either runoff does not exceed the capacity of the drainage system or there is adequate capacity of drainage system.

Storm drainage inlet is the point of a drainage system where stormwater enters the system. Drain inlet is a stormwater collection component (Guo et al., 2007), and if not efficient in collecting storm water, becomes prone to flooding. The efficiency of a storm inlet greatly depends on urbanization. Most often, updating the location and capacity of the storm drain inlets are required with the change in urbanization. This is because urbanization is a dynamic process that tends to increase the runoff, and changes the stream network and watershed boundaries. Besides, urban area produces waste materials like debris, rubbishes, and litters that are carried by the runoff and clog the storm inlets, and thus reducing capacity (Urban Storm Drainage Criteria Manual, Chapter 6, 2002).

Floods can be prevented or reduced through several approaches, such as reducing the urbanization, building flood prevention structures like retention basin, updating the drainage system and changing land cover (Konrad, 2003). Stopping the growth of urbanization is an unlikely solution to avoid flooding. Other solutions like updating the drainage system and constructing a detention basin require extensive drainage and structural studies. However, the alternative solution based on hydrological modeling is considered in this research. In order to implement such a solution, the mechanism of flooding in an urban watershed as well as hydrologic response of the watershed to the changes in land cover should be well understood.

This thesis presents research to better understand urban flooding. It is done through developing tools to estimate flows and overflows and analyzing flood behavior over time. Moreover, a systematic approach is developed to test remediation measures to reduce flooding.

1.1 Research Motivation

The research is undertaken because of the following motivations:

1. To devise an approach for better understanding of floods: Urban flooding is a complex phenomenon due to inhomogeneous nature of urban surfaces (Jing, 2010). Moreover, urban landscape is very dynamic that modulates the spatio-temporal behavior of flooding further complicating its progression. Hence, understanding an urban flood is very challenging and no effective flood remediation measures can be undertaken without an insightful understanding about the floods. A comprehensive approach should be

developed to understand flooding in an urban watershed, which may differ from watershed to watershed. This research devises an approach to better understand flooding.

2. Using GIS for spatially distributed flood modeling: Generally, the process of developing a flood model is complex, and time consuming. Typically, there are two types of hydrological models available to model a flood: spatially lumped models and spatially distributed models. Distributed model is considered to be more accurate than lumped model to map spatio-temporal behavior of floods in an urban watershed (Kilgore, 1997). Moreover, distributed models are computationally intensive than lumped models.

There are numerous hydrologic modeling software (HEC-HMS, SWAT, etc.) available for urban flood modeling. But the major problems of most of them are they cannot delineate watershed for an area and are not able to do modeling on distributed scale conveniently. Hence, they are not able to perform spatio-temporal analysis. Moreover, they are not able to visualize the outputs. Geographic Information System (GIS) technology provides capabilities to process and visualize spatio-temporal phenomenon. Since, the model needs to behave as much accurate as possible, and a better understand of flooding needs to be obtained through the analysis and visualization of flood's spatio-temporal outputs, there is a strong motivation to use GIS for developing flood model.

3. To make the model user friendly: The motivation behind this is to make model user friendly so that it can be used by the flood management authorities with ease. To do this, optimal amount of data and methods are utilized to create computationally efficient

approach. Besides, publicly available data and simple hydrologic methods are used to ensure uncomplicated implementation.

4. To develop a flood model: The motivations behind developing a flood model is to better understand an urban flood event, ascertain the relationship between the changes in urban landscape and the flooding, and prevent flooding. To accomplish this task, a flood model that produces the variation of flood depths and areas with time and space using various geographic information of the watershed, such as elevation, soil and land cover needs to be developed. Through the analysis of outputs the flooding can be well understood. Since the model uses land cover information, the relationship between the changes in urban landscape and the flooding can also be easily ascertained, and as well as the optimum land cover can be found to avoid flooding.

5. To investigate the impacts of data resolution on flood modeling accuracy: It is recommended to use high resolution data to produce accurate results (Chen et al., 2009; Wang et al, 2009; Goulden et al., 2014). Consequently, people tend to buy high resolution data from various sources that can lead to unnecessary time and money consumption, and misleading results too, where actually using publicly available data of relatively lower resolution can be more advantageous. Therefore, investigations need to be made to find out the impact of hydrologic data resolution on flood modeling accuracy.

1.2 Research Objectives

The goal of this research is to study urban flooding through development of GIS based modeling tools. In order to achieve this goal, following objectives are investigated in this research.

1. Develop a GIS-based framework for urban flood modeling to map the spatiotemporal behavior of floods in urban micro watersheds.

   Hypothesis: It is hypothesized that a GIS based framework of a hydrological model can provide spatiotemporal maps and visualization of urban floods. The basis is that GIS provides platform to perform hydrologic analysis in both spatial and temporal domain simultaneously.

2. Analyze hydrological response of urban micro watershed to remediation measures of runoff modification through land cover change.

   Hypothesis: It is hypothesized that flooding behavior in a watershed changes with the change in land cover. The basis is that flooding depends on the infiltration capacity of the land cover; the more the infiltration through land surface, the less the flooding.

1.3 Research Approach

To accomplish the first objective, GIS platform, i.e., GIS tools and techniques are used to develop the framework. A flood model inside the framework is constructed by generating runoff hydrograph, and estimating the flood depths and areas. Gridded Soil Conservation Service (SCS) Curve Number method along with time area approach is used to produce runoff hydrograph, which is compared to the discharge hydrograph of the watershed outlet to produce time series of flood depths and areas. These outputs are mapped in GIS to visualize the spatio-temporal behavior of the flood. To accomplish the second objective, GIS-framework is used for various land cover change scenarios for flood remediation at a test site. The outputs are analyzed to observe the watershed hydrologic response to the change in land cover.

1.4 Thesis Outline

This thesis is organized as follows. Chapter 1 introduces the research background, motivation, and objectives. Chapter 2 describes about the studies reviewed to conduct this research. Chapter 3 describes about the study area, and data that are used in this research. Chapter 4 explains extensively the methods to develop the GIS-framework, and Chapter 5 highlights and explains the results obtained through testing the framework in study sites. Chapter 6 highlights and explains the outputs for land cover change analysis, and Chapter 7 summarizes the thesis, and provides conclusions and recommendations.

1.5 Thesis Contribution

The followings are the contributions of this research:

1. This research provides a GIS framework and workflow for developing an urban flood model for the inlet-based small-scale watersheds.
2. A flooding analysis of Blacklot and East Mall areas of UNLV campus is provided, giving an insight into the spatio-temporal behavior of flooding.
3. GIS framework is applied to test multiple land cover scenarios for retrofitting Black Lot to reduce flooding.

CHAPTER 2: LITERATURE REVIEW

This chapter provides a review of studies that are consulted to conduct the research. Since the study sites are in the City of Las Vegas, a brief history of some reckoned flash flooding in Las Vegas is provided at the beginning. This section is followed by addressing contemporary issues in hydrological modeling that need to e addressed before starting modeling. Since this research aims at using GIS to develop flood model, and to map spatiotemporal variation of flooding, and therefore, studies are reviewed on practices and problems of integrating GIS with hydrological models that followed by how to use GIS techniques and tools to create a framework in GIS. The final section of this chapter describes about the studies consulted in order to study watershed response to land cover change. The section basically also talks about various runoff reducing surface materials.

2.1 Causes of urban flooding: Climate Change and Urbanization

Flooding is a common natural disaster in cities. The intensity of flooding has increased over the last few years. The reasons for increased flooding intensity in urban areas are several, and interrelated (Genovese, 2006). However, they can be attributed to two main factors: i) urbanization and ii) climate change (Genovese, 2006).

Feyen et al. [2008] demonstrated the impacts of urbanization on the future flooding in Europe. They also showed the impacts of global warming alongside of urban development. Actually, the goal of their research was to assess the impacts of global warming and land use change on future flooding in Europe. The authors combined HIRHAM climate model with a hydrological model called 'LISFLOOD'. For the climate

model, the authors used SRES A2 greenhouse emission scenario. The authors estimated future flood depths and extents which were later transformed into monetary damage using flood depth-damage function and land use information. For each country expected annual damages (EAD) were computed from the damage-probability functions. The authors found that most countries in Europe will face an increase in EAD in the coming century. The authors found in conclusion that the effect of urbanization is far more significant than global climate change on local urban flooding.

Huong & Pathirana [2013] ran a similar study like Feyen et al. (2008). The goal of their research was to obtain the combined effects of change of internal and external factors on urban flooding system. The external factor was considered to be the climate change while the internal factor was considered to be the urban growth itself. The contribution of climate change was considered to be the sea level rise and increase in flow. The contribution of urbanization was considered to be the effect of urbanization on local extreme rainfall pattern. Eventually, both contributions from climate change and urbanization were integrated to estimate their combined effects on urban flooding. Various scenarios were run by combining the effects of urbanization and climate change. All the scenarios were run for until the year of 2100. According to the authors, one of the unique features of this study that make it distinct from other typical climate change impact studies is that this study integrated the contributions from both internal and external contributors of the urban system flooding. The authors found in conclusion that the impact of urbanization on urban rainfall intensities is an important factor to cause flooding in local scale.

From the literature review it is found that both climate change, and urbanization

are culprits for causing urban floods. Urbanization have more impacts on flooding in a local scale (like cities) than climate change. However, this research only considers urbanization as a crucial factor for urban flooding, and therefore, impacts of climate change on floods is not considered within the scope of this research although several studies have indicated that climate change will impact flows and floods in the western USA (Sagarika et al., 2014; Dawadi and Ahmad, 2012; Kalra and Ahmad 2012; Carrier et al., 2011; 2013). In fact in a study to evaluate flood control infrastructure in the Las Vegas Valley in response to climate change, Forsee and Ahmad (2011a; 2011b) have demonstrated that intensity and frequency of floods will change. However, considering climate change would require extensive climate studies, and due to time constraint, climate change is not considered in the research to develop urban flood model.

2.2 Flooding in Las Vegas

The City of Las Vegas has a long history of flash flooding (CCRFCD, 2013). It has been receiving flash flooding almost every year since 1990, and almost all of them

Figure 2.2-1: Flooding in Las Vegas in 1975 (Randerson, 1976)

found to be occurred between the months of July and August (CCRFCD, 2013). The main cause of flooding is sudden severe rainfall during the period from July to August that exceeds the capacity of the drainage facilities and lack of sufficient vegetative cover in the area (CCRFCD, 2013). The first flash flood in the city was reported to occur on July 15, 1905, and between the year of 1905 and 1975, the U.S. Soil Conservation Service recorded a total of 184 flooding events that resulted in private property and public facilities damages (CCRFCD, 2013). Of them, the flooding of 1975 seems to be the one of the most catastrophic events, and the associated estimated damage was reported to be then 4.5 million US dollars (Randerson, 1976).

Randerson [1976] analyzed the meteorological data to identify the flood locations, and estimate the intensity of the rainstorms that caused the flash flooding in the Las Vegas Valley on July 3, 1975. The heavy rainfall that caused the flash flood was found to cover an area of 550 km^2. The total amount of rainfall was estimated to be 3 inch (75% of annual average rainfall of the Valley) that results in 4.19 x 10^7 m^3 of total rainfall. The total amount of runoff was estimated to be 2.3 x 10^7 m^3 resulting in only 45% of losses throughout the valley. This high amount of runoff volume produced the flooding in the Valley, and the then central business district was the mostly affected area due to its high amount of urbanization. Thus, it can be said that urbanization augments flooding in the area, and therefore, urbanization needs to be checked in proper way.

Recently, on September 11, 2012 another devastating flood event occurred in Las Vegas. The flooding event was reported and published by Timothy Sutko, an Environmental Mitigation Manager of CCRFCD in 2012. According to the author, on September 11, 2012, severe weather with heavy rain moved through the Las Vegas

Valley, and other parts of Clark County causing deadly flooding. The findings are summarized below:

- The National Weather Service (NWS) officially recorded 1.18 inches of rain, the most rainfall ever recorded for any September day since records began to be kept in 1937.
- Flood flows at the Desert Rose Golf Course drowned and killed a landscaper. At least 80 instances of flood damage to property reported in the area.
- A flash flood warning for the entire valley expired at around 9 p.m.
- Maximum depth and associated peak discharge in some of the CCRFCD stream gage stations are provided in Table 2.2-1:

Table 2.2-1: Peak depths and discharges at various CCRFCD stations

Location	Max depth (ft)	Peak discharge (cfs)
Tropicana wash at Swenson	4.3	5215
Flamingo wash at Nellis	4.6	3230
Las Vegas Wash at Cheyenne	6.7	5170
Las Vegas Wash at Las Vegas Blvd.	4.6	4730
Las Vegas Wash at Lake Mead Blvd.	6.4	6325
Las Vegas Wash at Sahara	7.3	9150
Las Vegas Wash at Vegas valley Dr.	7.5	10900
Las Vegas Wash at Rainbow Garden Weir	8.5	12000

- In the UNLV campus there were approximately 20 flood damages to property. Vehicles parked in the Thomas & Mack parking lot and buildings on the UNLV campus were extensively flooded. In addition, several businesses along Maryland Parkway suffered heavy flood damages. Figure 2.2-2 shows flooding at Thomas & Mack parking lot.

It is found through the reviews that Las Vegas is prone to flash flooding when

Figure 2.2-2: Flooding in UNLV Blacklot (RebelYell, 2013)

there is heavy rainfall. This is certainly because of high urbanization (high surface imperviousness), and inadequate drainage capacity. Therefore, either urbanization needs to be checked in an optimal way to stop flooding through changing land cover or the drainage system capacity needs to be increased. This research investigates the response of flooding to the change in land cover in a small scale. The land covers are such that they can easily replace the highly impenetrable surface, but their performance is same as the impenetrable ones.

2.3 Issues to be considered in Hydrological Modeling

A global hydrological model would be difficult to create as hydrological processes vary from region to region and from time to time. There exist numerous hydrological models, and choosing an appropriate hydrological model can be hard. It depends on several issues like the availability and accuracy of data, resolution of data, complexity of the hydrological process in the study area etc.

Urbonas [2007] has mentioned of several important issues in his keynote paper that should be considered in hydrological modeling. According to the author, a distributed rainfall-runoff model should have calibration scheme to obtain accuracy, and to achieve accuracy the most important thing is the modeler's skill and understanding of the hydrology in the study sites. The modeler has to decide which model or method should be used based on the complexity of the study area, and availability and resolution of data, and as wells as reputation of the method. Moreover, the author gave importance to check the data, and the values of the calibrating parameters that are found from responsible sources. The author also provided various examples on issues like how the model's output can be affected by the spatial rain gage density, temporal rainfall data density, and use of radar rainfall data over rain gage data, incorrect calibrated data, and uncalibrated model. The author also suggested that to achieve minimum level of accuracy in urban runoff simulations, rainfall data should have at least a temporal resolution of 15 minutes. He also found that radar rainfall data are not suitable for small catchments unless they have very high resolution. The author also strongly recommended not to use blindly local criteria for modeling without calibration. This research considers the issues mentioned above for its flood model construction.

2.4 GIS Integration with Hydrologic Models: Practices, Problems and Prospects

Integration of GIS with hydrologic models has been applied in various aspects of urban watershed analysis such as runoff estimation, runoff pollutant estimation, flood control etc. The following paragraphs talk about some of its application areas, problems and future prospects.

Greene and Cruise [1995] integrated hydrologic models with GIS to manage urban watersheds. The authors used TIN technique to delineate watershed from the DEM. SCS Curve Number method was used to estimate rainfall excess, and the discharge was routed using a standard kinematic wave model. This integration of GIS with hydrologic model approach was tested in various lots, blocks and multi-blocks. The authors found that GIS could be used successfully for a realistic analysis of runoff in an urban watershed.

Ellis & Viavattene [2013] developed a GIS-based integrated approach for the management of urban surface water flooding. In order to construct the approach, an integrated model was developed. The major outputs of the model were the identification of 'critical drainage areas', i.e., areas susceptible to flooding in case of extreme rainfall events, and visualization of the flooded areas and associated damages before, and after the implementation of flood control measures. According to the authors, integration of GIS with hydrologic models is an effective way of mean to model and control flooding in an urban watershed.

Estiri at al. [2002] developed a GIS-based landuse model to estimate stormwater runoff and pollutant concentration at parcel and watershed levels for the City of Seattle, Washington through the use of 'simple method' equation. The model took into

consideration the local precipitation data, pollutant coefficients from the National Stormwater Quality Database (NSQD), and impervious coefficients from other national studies. This model developed in the paper can be used successfully to identify 'hot spots' of pollutant contamination within urban areas.

Miller at al. [2002] built a tool using GIS for watershed analysis called Automated Geospatial Watershed Assessment (AGWA) tool. This tool can perform both spatial and temporal analysis. This tool can be used to generate input parameter files for the Soil Water Assessment Tool (SWAT) and KINEmatic Runoff and erosion model (KINEROS2) using basic input data, such as: elevation, land cover, soil and precipitation data. This tool is an extension of ESRI's ArcView 3.X version. The tool can also be applied in ungauaged watersheds conveniently.

Unlike the previous researchers, Sui and Maggio [1999] reviewed the practices, the problems and the prospects of integrating GIS with hydrological modeling. According to the authors, the integration of GIS with hydrological modeling was essentially technology-driven. The authors asserted that the integration of hydrological modeling with GIS should proceed in a way that is compatible for both GIS and hydrological models. According to the authors, GIS- based hydrological modeling would not only assist us with new computing platforms, but also would free us from the constraints of existing hydrological models. This exchangeable GIS-based hydrological modeling would also lead us to a variety of wide-range applications with ease. However, the authors warned about the uncertainties that may occur during the integration of GIS with hydrological models, and called for future researches to develop ways to administer such uncertainties.

Through the literature review on integrating GIS with hydrologic models, it is noticed that GIS can be integrated with hydrologic model successfully, and through the integration the urban watershed analysis has become easier and more accurate than before. This is mainly due to the suitability of the spatial-temporal framework embedded in the present generation of GIS that permits it to conduct spatiotemporal analyses. Considering the fact, the research aims at integrating GIS with hydrologic model/ method to develop its flood model.

2.5 GIS-framework Studies

This section, through the following subsections, describes about the literatures reviewed to build each component of the GIS-framework.

2.5.1 Studies on Watershed Delineation

Previous studies have used GIS for watershed delineation using DEM that is built from digital elevation data. The accuracy of watershed delineation greatly depends on the accuracy of DEM. Therefore, it should be made sure that the errors in DEM are minimized as much as possible before delineating watershed. The following paragraph provides some details about the study consulted on how to remove errors from DEM in GIS, and followed by the next paragraph that talks about the study reviewed to delineate watershed using DEM.

Prodanović et al. [2009] developed DEM-based GIS algorithms for hydrologic analysis where they actually focused on how to remove errors from DEM data. The DEM had a large number of flat areas in the catchment but according to the authors, river areas lie in flat zones. The authors used low-pass filtering on flat pixels that are located at

boarder of larger flat regions to correct the horizontal areas. The DEM also had ponds or depressions, which were removed to define stream network. An algorithm was developed to delineate the boundary of the depressions, and determine the outlet points. Then DEM is changed in such a way that all pond pixels should have the elevation equal to the elevation of the exit cell. In this research GIS tool is used that utilize built-in algorithms for low-pass filtering to remove elevation errors.

Zhang et al. [2011] demonstrated in their paper how to delineate watershed from DEM. According to the authors, filling of the DEM is also required to remove errors from the DEM, i.e., to create a depressionless DEM. Through filling any imperfections (sinks) in the DEM is removed. This filled DEM is used to find the flow direction of the cells which is used to find out the flow accumulation cells, i.e., to create accumulation raster. The flow accumulation value of a cell is the number of upstream cells that contribute their flows to the cell. Using this flow accumulation raster along with the

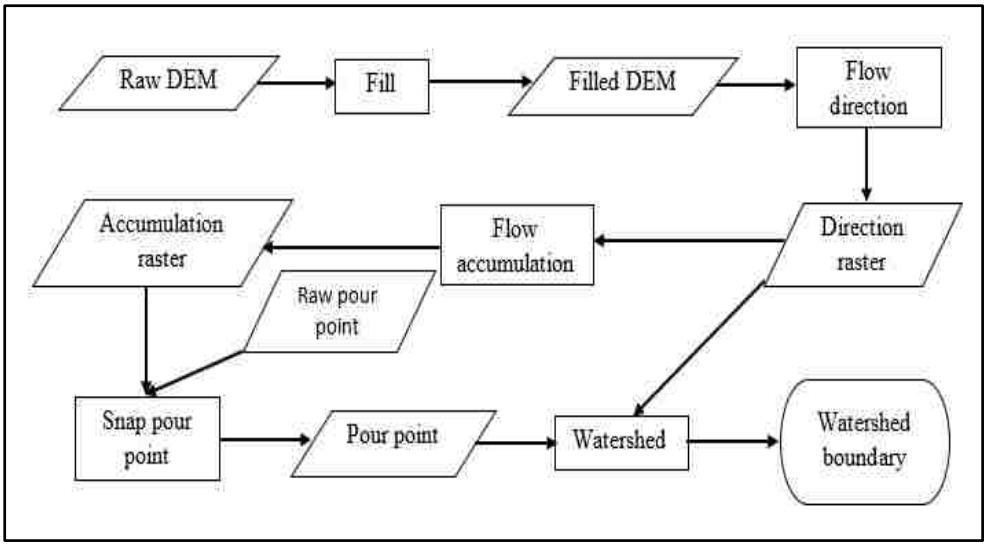

Figure 2.5-1: Watershed delineation process (modified from Zhang et al., 2011)

given pour point, watershed is delineated. Figure 2.5-1 shows the general process of delineating watershed drawn by Zhang et al., 2011. A pour point is the point based on which the watershed will be created, i.e., the point acts as the watershed outlet. These given pour points may be the points located at stream gauge stations, storm drain inlets or other hydrometric stations. However, it is found that the outlet point positions taken from hydrometric stations commonly do not coincide with stream locations extracted from digital elevation models (DEMs), and this creates serious error when delineating watershed (Lindsay et al., 2008). Sometimes there is a location error for the outlet pour points generated from the inaccurate GPS/GIS data. In such cases, a filed visit might be necessary. The most widely used automatic technique for repositioning outlets or pour points is the Snap Pour Point tool available in ArcGIS, a renowned commercial GIS package that moves outlets to the grid cell of highest flow accumulation within a specified search distance (Lindsay et al., 2008). Although Snap Pour Point is effective at

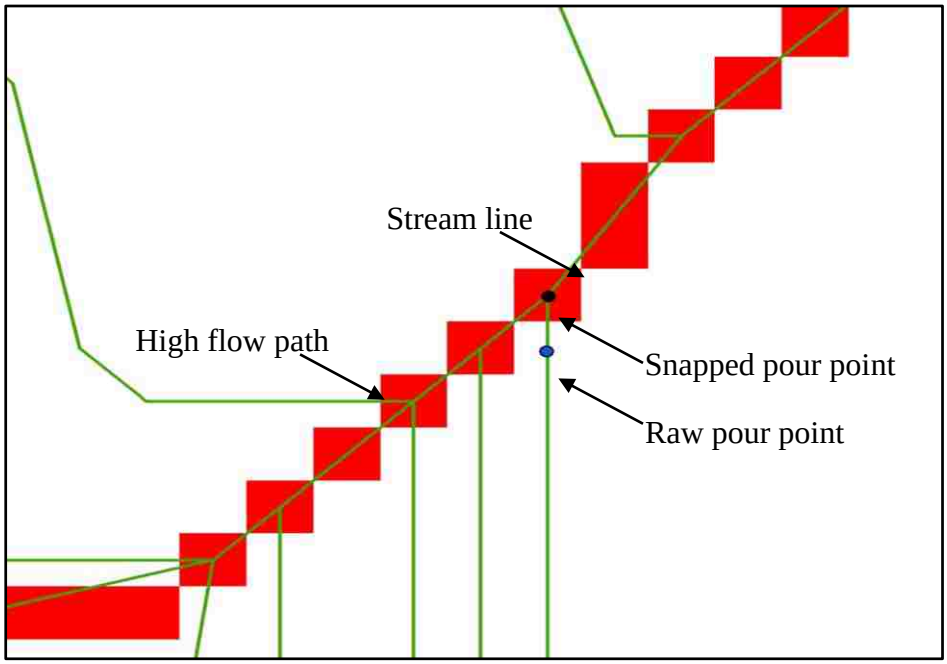

Figure 2.5-2: Snapping pour point (modified from Trent University Library, 2012)

delineating watershed, but they are highly sensitive to the search distance, and it is usually difficult to determine a suitable value for this parameter beforehand (Lindsay et al., 2008). Therefore, it is recommended to fix a search distance large enough (Lindsay et al., 2008). However, snapping is not needed if the given pour point is located at higher flow accumulation cell than its surrounding cells, and the delineated watershed for this point is not very small within the study site extent. If it is important to the analysis that the given pour points remain at the exact cell location they are placed, then the Snap Pour Point tool should run with a search distance of '0'. However, if the original pour point is displaced to the new nearby location, no hamper to the outputs are found since the accuracy of the mapped watershed is more important than the positioning of the outlet with respect to its true location. (Lindsay et al., 2008). Figure 2.5-2 demonstrates how the snap pour point tool works.

After reviewing the studies on watershed delineation, it is observed that the errors in DEM should be removed by both low pass filtering and filling processes to obtain higher accuracy, and Snap Pour Point tool should be used to find out the pour point. This research uses low pass filtering and filling processes together to make DEM error free, follows the watershed delineation process using Snap Pour Point tool.

2.5.2 Studies on Rainfall to runoff conversion

There are numerous methods available to convert rainfall into runoff. This section describes about the studies considered to choose a rainfall-runoff method for this research.

Soil Conservation Service (SCS) Curve Number (CN) method is a widely used method to estimate runoff from rainfall (Kumar et al., 2010). Ponce et al. (1996) investigated the maturity of SCS CN method to estimate runoff from rainfall. The authors examined critically the Curve Number method, delineated its capabilities, limitations and uses and identified the areas of further research in the method. According to the authors, the SCS method is apparently more of a lumped model but can be used successfully for distributed modeling. It is an infiltration loss method, and should not be used for long term analysis of a watershed.

The advantages of SCS Curve Number methods are:

1. It is simple, predictable and conceptually stable than any other rainfall-runoff model
2. It relies only on one parameter, CN
3. It has well documented environmental inputs
4. It is a well-established method around the globe

The disadvantages of Curve Number method are:

1. It was developed using regional data of Midwestern US. So cautions are recommended while using in other geographic or climatic regions.
2. This method is better applicable for the site where there is negligible base flow.
3. The method is applicable for small and midsized catchments, but can be used with caution when applied to larger watersheds, such as that have area greater than 100 sq. mi, or 250 sq km
4. Investigations should be made for initial abstraction ratio (Υ) as Υ can be interpreted as a regional parameter

5. The method lacks guidance on how to vary the antecedent moisture condition, and it does not consider the temporal variability of abstraction losses

The authors concluded that this method is a well-matured method considering the following factors:

1. The method is widely understood and accepted throughout the world
2. It is chosen widely by the engineers and hydrologists for hydrologic design
3. There is no other superior method available than SCS CN method to estimate runoff

However, when using SCS CN method it is imperative to decide whether to use it as a lumped model or a distributed model based on the complexity of the watershed. This is done through considering either the homogeneity or the heterogeneity of Curve Number (CN) as CN is the most important spatial parameter of the method. This decision plays an important role on the accuracy of results. Soulis and Valiantzas [2012] proposed a method for identification of the SCS-CN parameter spatial distribution using rainfall-runoff data in heterogeneous watersheds. In this study, authors showed that spatial distribution of CN within the watershed provides more accurate runoff response than a single value of CN for a heterogeneous watershed, i.e., for such watersheds gridded / distributed SCS CN method should be used.

Based on these studies it can be concluded that, though the SCS CN method has some disadvantages, but this is the most superior and widely recognized method to compute runoff from rainfall, and this method produces better results when utilized in distributed modeling. Since GIS provides efficient tools to process spatially distributed

hydrological models, the distributed SCS CN method is used as hydrologic method for rainfall-runoff conversion in this research.

2.5.3 Studies on Runoff to flow conversion

This section describes about the studies considered to convert runoff into flow at the watershed outlet. This conversion means routing the runoff from the watershed cell through its flow path to the outlet to generate flow. When contribution of runoff from all grid cells, and the time to reach the outlet of the cells is known, a runoff hydrograph at the outlet can be constructed by plotting runoff flow against time. Figure 2.5-3 shows a typical runoff hydrograph along with its components. The definition of the components are given below (Boudreau, 2006):

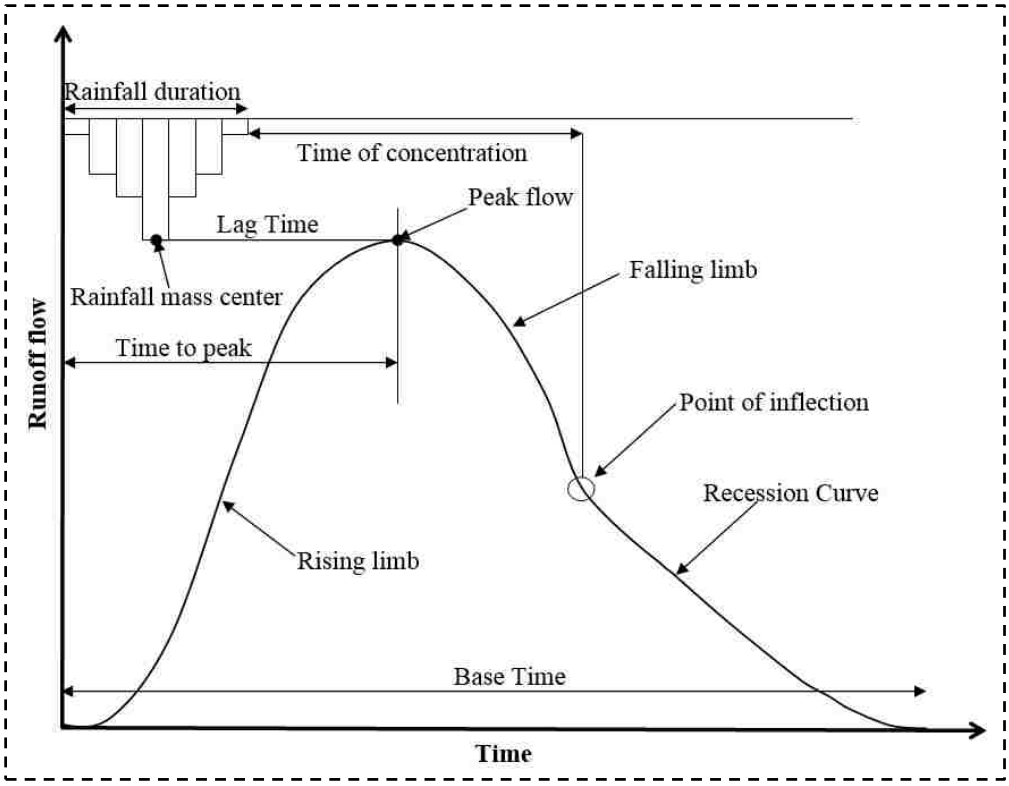

Figure 2.5-3: Graphical representation of a runoff hydrograph

Base time: Total duration of the hydrograph is termed as Base time, and is generally denoted by T_b

Point of inflection: The point on a hydrograph that separates the falling limb from the recession curve. At this point the concavity of the curve changes.

Lag time: The time distance between the center of the rainfall mass and the peak of the hydrograph. It is generally denoted by T_L

Peak flow: The highest point on the hydrograph. It is also called peak discharge, and is typically denoted by Q_P

Time to peak: The time it takes for the hydrograph to reach its peak flow. It is typically denoted by T_P

Time of concentration: It is the time taken by the water to reach the watershed outlet from its hydraulically furthest point. In a hydrograph, it is the time distance between the end of rainfall and inflection point. It is generally denoted by T_C

Rising limb: The rising portion of the hydrograph is called the rising limb.

Rainfall mass center: The center of the total rainfall mass, or simply total rainfall.

Falling limb: The falling portion of the hydrograph is called the falling limb. It is terminated after the point of inflection.

Recession curve: It is the portion of the hydrograph where runoff is preeminently generated from watershed storages like subsurface flows, small depressions etc.

However, the routing of runoff in an urban watershed poses great challenges to modeling urban flood (Chen et al., 2009), and therefore, can make a flood model complex. The following subsections describe various procedures to accomplish this task.

2.5.3.1.Runoff Routing using Stochastic Methods

Stochastic methods have been investigated for runoff routing. Olivera and Maidment [1999] proposed a complex stochastic method for routing spatially distributed excess precipitation over a watershed to produce runoff hydrograph at its outlet. The authors derived a routing response function for each cell of a digital elevation model of watershed. Total runoff at the watershed outlet was estimated through the integral convolution of rainfall excess intensity with the watershed response function for each cell, and then multiplied by time steps and drainage area. The outlet discharge response of the watershed to a unit input to a watershed cell is called the flow path response function [T -1]. Flow path response functions represent the translation (advection) and redistribution (dispersion) processes in the flow path, i.e., lag time from the watershed cell to the watershed outlet and spreading around the centroid of the mass element. The response function for each cell has two parameters: flow time and dispersion coefficients. Flow time and dispersion coefficients were calculated using First-Passage-Time distribution, a moment-based approximation of convolution integral to obtain response function for each cell. The developed runoff routing model was applied to the Waller Creek gauged watershed in the city of Austin, Texas with an area of 14.8 km2. 88% of the total rainfall was found to produce direct runoff attributed to the imperviousness of an urban watershed.

Smedt et al. [2000] also established a stochastic method to simulate spatially distributed runoff in a river catchment using detailed physical characteristics of the catchment. In this method, physical characteristics accounted for included soil moisture, topography, soil cover and land cover. A complex probabilistic approach was used to determine the river discharge for each grid cell along the flow paths. The total river discharge at the outlet was estimated by the combination of contributions of discharge for all cells. In the research, SCS method is used to estimate runoff from rainfall at each grid cell. However, due to the complexity of these stochastic methods, they are not followed to route runoff in this research.

2.5.3.2.Runoff Routing using Deterministic Methods

Runoff can be routed using deterministic methods. Translation hydrograph method is a widely used deterministic method for routing runoff in GIS. The following paragraphs details about the studies looked at for translation hydrograph construction in GIS.

Ashour [2002] presented a simplified distributed hydrological model in GIS to generate runoff records for Wadi Rajil watershed, situated in the eastern arid part of Jordan using translation hydrograph method. The author used GIS tools to route the rainfall excess/runoff to produce a unit runoff hydrograph at the watershed outlet. For each time step of the input rainfall event, two grids were generated using GIS tools; the isochronal grid and the total runoff grid. The isochronal grid is the equal time-of-flow grid representing the group of cells with same travel time. The isochronal grids were constructed by routing the runoff, i.e., determining the flow path for each cell to the outlet, and estimating velocity at each cell using Manning's equation. Flow paths were

determined by estimating flow length for each cell using GIS tool. Total discharge grid was produced by estimating rainfall excess at each cell using water-budget equation. Rainfall excess for each cell was then translated to generate runoff at the outlet by subtracting conveyance losses from rainfall excess. The contributions of runoff from the cells were added to estimate total runoff at the outlet. By merging the two grids, the isochronal and total runoff, a new grid was produced that included attributes, the time of travel and the total runoff, for each time zone. This grid represented the catchment response corresponding to one time step of the input rainfall event. The final hydrograph corresponding to the rainfall event was generated by shifting in time the hydrograph of a given input time step over that of the previous time step, and summing up the values according to the specified hydrograph time step.

Usul and Yilmaz [2002] used Clark's technique to produce an Instantaneous Unit Hydrograph (IUH) at the basin outlet using GIS. The authors estimated the three

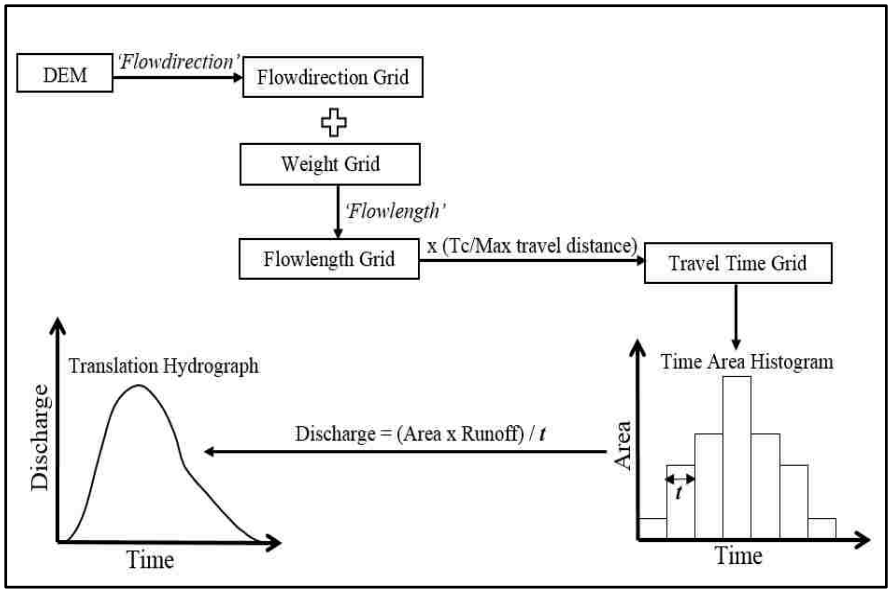

Figure 2.5-4: Translation hydrograph construction (modified from Usul and Yilmaz, 2002)

parameters that are required to use Clark's technique: time of concentration, storage coefficient and time-area histogram of the basin. Time of concentration was estimated using SCS lag equation. Storage coefficient was estimated using observed hydrograph while DEM was used to compute time-area histogram. The time-area histogram was converted to translation hydrograph that was routed using linear reservoir equation/model at the basin outlet to produce IUH. The model was tested in the Ulus basin of Turkey, close to the Black sea coastline with an area of 950 km^2. Figure 2.5-4 demonstrates the process. This whole process is actually similar to the Ashour (2002) until creation of IUH, and this process is called the time-area approach or translation hydrograph approach. The major concern in the translation hydrograph method is the calculation of velocity to estimate travel time. There are various formulas to estimate velocity like Manning's N equation, land use equation, flow type equation etc. Sorrell and Hamilton [1991] proposed the following equation to compute velocity:

$$V = K * S^{1/2} \qquad \text{Equation 2.5-1}$$

where V = velocity (fps); K = coefficient depending on type of flow or land uses; and S = slope of the flow path (%). When using flow type equation it should be noted that there are three types of flow regime according to USGS: i. Small tributary ii. Waterway and iii. Sheet flow. According to Sorrell and Hamilton [1991]:

1. Permanent or intermediary streams of USGS map is termed as small tributary. Man-made channels and swales demonstrated on engineering drawings should also be considered as small tributaries.

2. A travel or flow path that does not have a blue streamline indicating a defined channel in USGS map can be considered as waterway.

3. Any overland flow path that is not compatible with the waterway definition can be called sheet flow. Sheet flows can have maximum flow length of 300 feet. The remaining downstream portion of the flow path should be considered as waterway for modeling purposes.

Also, the authors suggested of using $\Upsilon = 0.2$ for small scale watershed. Because of simplicity of this deterministic translation hydrograph approach to route runoff, this research utilizes this method for runoff routing. Also, flow type equation for estimation of velocity and initial abstraction of 0.2 is used in the research.

2.5.4 Studies on Inundation Estimation and Mapping

Once a runoff hydrograph is produced, the next step is to create a discharge hydrograph that is compared to the runoff hydrograph for inundation estimation. If a watershed flows into a storm drain inlet, the stage discharge curve of the inlet acts as a discharge hydrograph. This following section describes about the literatures that are reviewed to construct a stage discharge curve for a storm drain inlet, and followed by the section that describes about the GIS studies on flood modeling and mapping.

2.5.4.1.Stage Discharge Curve Construction Studies

A drainage inlet is an important component of urban stormwater collection and component system. The interception capacity of a drainage inlet acts as the discharge

Figure 2.5-5: Grate inlet (left); Curb opening inlet (middle) and Combination inlet (right)

capacity for the watersheds that flow into a drainage inlet. A stage-discharge curve of an inlet acts as the discharge hydrograph for such watersheds. Hence, the drainage of the runoff depends upon the drain inlet capacity. When the flows of a runoff hydrograph overpass the discharge capacity of the inlet, flooding in the catchment starts to occur. Generally, a stage-discharge curve is developed when a drain inlet is constructed. Therefore, it is possible to find a rating curve for an inlet from responsible authorities. However, when such information is unavailable, a rating curve for an inlet needs to be constructed.

In order to develop a rating curve for an inlet, it is imperative to identify the type of the inlet of interest first. There are four types of inlets (Brown et al., 1996):

1. Grate inlets
2. Curb-opening inlets
3. Slotted inlets
4. Combination inlets

Grate inlets are openings covered by a horizontal grate, curb-opening inlets are vertical openings in the curb, and covered with a top slab, slotted inlets are long inlet, and consists of a series of horizontal bars with openings among them, and combination inlet

is a combination of a curb-opening inlet and a grate inlet. Figure 2.5-5 shows the various types of inlets (Brown et al., 1996). Through the field visit it is found that the drainage inlet of this research study areas are located at the lower point on the study sites, and therefore they can be called 'Sump Inlet' (Urban storm drainage criteria manual, 2002). Therefore, only those researches are looked at that particularly provide information on estimating discharge capacity of a sump inlet.

Guo et al. [2009] conducted a research in the laboratory to estimate discharge capacity of street sump inlet. The paper presented a laboratory investigation of the discharge capacities of several various types of sump inlets. It included bar and vane grates, and 3- and 5-ft curb opening inlets. New formulas and procedures were developed for estimation. All these formulas and procedures are explained in the following paragraphs. The following equation is used to estimate the hydraulic capacity of the sump drainage inlets (Guo et al., 2009):

$$Q_t = Q_g + Q_c - K\sqrt{Q_g Q_c} \qquad \text{Equation 2.5-2}$$

where Q_t is total interception capacity of the combination drainage inlet (cfs), Q_g is interception capacity of the grate inlet (cfs), Q_c is interception capacity of the curb opening inlet(cfs) and K is reduction factor. Guo et. al. (2009) derived the following equation to estimate the interception capacity of an inlet that can be used for any inlet regardless of its type. The equation was derived considering the fact that, in practice for a given water depth, the interception capacity is the smallest among the weir, orifice, and mixing flows.

$$Q_g = \min(Q_{wg}, Q_{mg}, Q_{og}) \quad \text{Equation 2.5-3}$$

$$Q_c = \min(Q_{wc}, Q_{mc}, Q_{oc}) \quad \text{Equation 2.5-4}$$

where Q_{wg} is interception capacity of the grate inlet for weir flow (cfs), Q_{mg} *and* Q_{og} are interception capacity of the grate inlet for mixing flow (cfs) and orifice flow (cfs) respectively, Q_{wc} is interception capacity of the curb inlet for weir flow (cfs) and Q_{mc} *and* Q_{oc} are interception capacity of the curb inlet for mixing flow (cfs) and orifice flow (cfs) respectively. Q_{mg} and Q_{mc} are computed using equations (2.4-5) and (2.4-6) (Guo et. al., 2009) while Q_{wg} , Q_{og} , Q_{wc} , Q_{oc} are determined using the equations (2.4-7) through (2.4-10) (Guo et al., 2009).

$$Q_{mg} = C_m\sqrt{Q_{wg}Q_{og}} \quad \text{Equation 2.5-5}$$

$$Q_{mc} = C_m\sqrt{Q_{wc}Q_{oc}} \quad \text{Equation 2.5-6}$$

where C_m is mixing flow coefficient that is equal for both curb opening inlet and grate inlet (Guo et. al., 2009).

$$Q_{wg} = N_w C_{wg}\sqrt{2g}(2W_g + L_g)d^{3/2} \quad \text{Equation 2.5-7}$$

where N_w is grate length opening ratio after subtracting steel bars, C_{wg} is weir discharge coefficient for grate inlet, W_g is grate width (ft), L_g is grate length (ft) and d is depth of water (ft).

$$Q_{og} = N_o C_o W_g L_g\sqrt{2gd} \quad \text{Equation 2.5-8}$$

where N_o is orifice area opening ratio, and C_o is orifice discharge coefficient.

$$Q_{wc} = C_{wc}\sqrt{2g}L_c d^{3/2} \quad \text{Equation 2.5-9}$$

$$Q_{oc} = C_o\sqrt{2gd}L_cH_c$$ Equation 2.5-10

where C_{wc} is weir discharge coefficient for curb inlet and H_c is curb opening height(ft).

The drainage capacities computed by the above equations do not consider clogging effect. But in real situation, all the inlets are affected by clogging (Urban Storm Drainage Criteria Manual, 2002). Therefore, a clogging factor should be applied to the inlet capacity of a grate or curb inlet using the following equation (Urban Storm Drainage Criteria Manual, 2002):

$$C_g or\ C_c = \frac{KF}{N}$$ Equation 2.5-11

where C_g is combined clogging factor for multiple units of grate inlet, C_c is combined clogging factor for multiple units of curb inlet, K is clogging coefficient that depends on the number of units, F is clogging factor for single unit of either grate and curb inlet, and N is the number of units. For a single unit of inlet, C_g and C_c become equal to F. The following equations are used to compute effective grate inlet capacity (Q_g') and curb inlet capacity (Q_c') for clogging effects in cfs:

$$Q_g' = Q_g * (1 - C_g)$$ Equation 2.5-12

$$Q_c' = Q_c * (1 - C_c)$$ Equation 2.5-13

The clogging factor for grate, C_g and curb opening inlet, C_c is computed individually, and then added to obtain the clogging factor for a combination inlet. Thus, the equation (2.4-2) becomes the following equation to estimate the drainage capacity of a combination inlet:

$$Q' = [(1 - CF) * (Q_g + Q_c - K\sqrt{Q_g Q_c})]$$ Equation 2.5-14

where Q' is the drainage capacity of a combination inlet (cfs), and *CF* is the clogging factor of the combination inlet that is estimated by the equation below:

$$CF = C_g + C_C$$ Equation 2.5-15

Using the equations demonstrated above, discharges through an inlet for various water depths are obtained, and a stage discharge curve for the respective inlet is constructed by plotting the discharges against the water depths.

2.5.4.2.Flood Modeling and Mapping

Discharge hydrograph along with runoff hydrograph at the catchment outlet is developed to model floods. But there exist other numerous ways for building urban flood models. Various empirical (Ahmad et al. 2009; 2010), statistical (Ahmad and Simonovic 2001a; 2005; Mosquera-Machado and Ahmad, 2007), and hydrodynamic models (Ahmad and Simonovic, 1999) are utilized to model floods. Besides, there have been other innovative attempts to describe flood flows over land surface, for example, using spatial system dynamics (Ahmad and Simonovic 2001b, 2004). However, this research focuses on creating an empirical flood model using GIS tools and techniques.

Wang et al. [2008] presented a method of developing a grid-based distributed hydrologic model for storm-inundation simulation using GIS and remote sensing for flood emergency planning. Chen et al. [2009] developed a GIS-based model for urban flood inundation named 'GUFIM'. The authors used water budget equation to produce runoff from the rainfall. A routing algorithm was developed to map the flood inundation

using the runoff. They considered the cells as the starting point of routing which has low flow accumulation values. Flat water model was assumed for the research. For the validation of the model, the authors selected the main campus of University of Memphis because of its known flooding history. Jing [2010] developed a convenient and manageable method for flood inundation using GIS. The study showed that through the inundation modeling by combining DEM and observed floodwater level values and maximum discharge, the inundated area can be accurately simulated. The author selected the Wenshan city, which is located in Yunnan Province in southwestern China as a sample study area.

All these studies do not talk about comparing runoff hydrograph with discharge hydrographs for flood modeling. Besides, no straightforward literature review is found available on how to map the inundation in GIS. Therefore, these studies are not followed in this research, since it aims to compute inundation outputs through comparing the runoff hydrograph with discharge hydrograph, and as well as devises a new technique to map inundation.

2.5.5 Calibration and Validation

This section describes about literatures reviewed for calibrating and validating the framework. It actually details the calibrating parameters accounted for this research.

2.5.5.1.DEM resolution as a Calibrating Parameter

DEMs are created from point cloud elevation data like LiDAR data. The LiDAR data that are collected using Light Detection And Ranging (LiDAR) remote sensing technology have become popular in hydrological analyses. DEMs can have various

resolutions depending on the user's choice and need. Goulden et al. (2014) conducted a review study on LiDAR- derived DEM where they mentioned of several studies that dealt with the resolution of LiDAR- derived DEM in performing hydrological analyses. The findings from those studies are summarized below.

It was found in one of the studies that the 2 m LiDAR DEM provided more accurate drainage networks than the National Hydrography Dataset (NHD) derived DEM. It was also found that among the three data sources: LiDAR, Photogrammetry and Public Digital Contour Data at 5 m and 25 m resolutions, watershed derived from the LiDAR-derived DEM is more accurate. In another study, the authors found that the 1 m LiDAR-derived DEM provides the most accurate stream network. Goulden at al. mentioned of another study that found that the high resolution LiDAR DEM provides a better stream network. However, in another study mentioned in the paper of Goulden at al. (2014), it is found that for low lying areas, the increased resolution of LiDAR-derived DEM might not have significant effect.

The majority of studies mentioned in the paper of Goulden et al. (2014) came to a conclusion that fine-resolution LiDAR DEMs offer better results than the DEMs of other sources. However, an optimum DEM resolution for LiDAR-derived DEMs cannot be determined, and the optimum DEM resolution is required for accurate watershed modeling with less computational burden (Goulden et al., 2014). Determination of optimum DEM resolution depends entirely on the user providing that the modeled results derived from the DEM best matches with the field data, and thus DEM resolution should be considered as a calibrating parameter. Therefore, this research considers DEM resolution as a calibrating parameter.

Goulden et al. [2014], by themselves, investigated the effects of various interpolation methods to create DEM from raw LiDAR data on the delineation of watershed area and stream networks. Inverse Distance Weighting (IDW), Moving Average (MA), Universal Kriging (UK), Natural Neighbor (NN), and Triangular Irregular Networks (TIN) were used as interpolation methods for the inspection process. The authors could not reach to a fix solution. In some cases the IDW method showed good results while in some cases it failed to produce good accuracy. This characteristic was also found true for other interpolation methods. Thus, it can be concluded that, it is entirely dependent on the user which interpolation method is to be used. The user should run all the available interpolation methods and compare the outputs with observed or filed data to find out which interpolation method's outputs best match the observed data. This research does not consider interpolation technique for calibration, and therfore uses GIS-default Linear interpolation method to build DEM.

2.5.5.2.Temporal Resolution of Rainfall

Temporal resolution of rainfall plays an important role in determining the hydrological response of basins, and it can be considered as one of the most crucial elements in rainfall-runoff models (Wang et al., 2009). The available temporal resolution of rainfall data usually have lower resolution than the model requirements, and thus compromise accuracy of the model (Aronica et al., 2005). Wang et al. [2009] determined the impacts of temporal resolution of hydrological data on river discharge estimation. The authors applied a typical rainfall-runoff model for long-term and short-term runoff prediction using various temporal resolution rainfall data: daily, hourly, and of 10 minutes interval. The authors found that shorter temporal resolution produce better results

in short term storm discharge estimation. They obtained the most accurate results using 10-minute interval rainfall data. The authors concluded that the model performance is greatly influenced by the temporal resolution of hydrologic data, and therefore need to be calibrated.

Aronica et al. [2005] preformed an uncertainty analysis of the influence of rainfall temporal resolution in the urban drainage system modeling. They actually evaluated the effect of rainfall temporal resolution on the response of urban environments. They mentioned that the interpolated hyetograph shape and time-to-peak can influence the hydrograph shape and timing, and as well as can affect the hydrograph peak. The authors also emphasized on considering rainfall resolution as a calibrating parameter. Based on these studies, this research considers rainfall temporal distribution for calibration.

2.5.5.3.Clogging Factor

Clogging factor is always one of the important parameters for any urban watershed study in the case of the watershed drains into a storm drain inlet. The operation of an inlet is subject to the clogging due to urban debris that obstruct the runoff to get discharged through the drainage system. Inlets are generally clogged by the first-flush of runoff (Urban Storm Drainage Criteria Manual, 2002). The amount of urban debris varies with location and season, and therefore clogging factor of an inlet may change every time a hydrologic analysis is conducted (Guo and MacKenzie, 2012). Clogging factor selection mainly depends the debris and wastes condition in an area (Urban Storm Drainage Criteria Manual, 2002). Conservatively, a clogging factor of 0.5 is recommended for a single grate and 0.1 for a single curb-opening inlet (Guo and MacKenzie, 2012). They also observed that the clogging factor for multiple inlets in

serial reduces as the number of inlet units increases. However, clogging factor estimation formula for a combination inlet is not found available. To get an average estimate of clogging factor for a combination inlet, equation 2.4-15 is used. Thus, there is no specific formula to obtain clogging factor, it depends on the user to pick a one. Besides, as mentioned earlier, clogging depends on the location of the inlet, watershed surface characteristics and season. Since the watersheds of this research are delineated for storm drain inlets which mean they will flow into storm drain inlets, clogging factor as a calibrating parameter is considered.

2.6 Relating Watershed's Hydrologic Response to Land cover Change

Changing land cover that leads to urbanization, if uncontrolled, can have severe impacts on flooding. It affects flooding in various ways, such as it can increase the peak discharge of floods and flood frequency. Feyen et al. [2008] demonstrated the impacts of land cover change, i.e., urbanization on the future flooding in Europe. Huong & Pathirana [2013] ran a similar study like Feyen et al. (2008). Konrad [2003] mentioned of various effects of urban development on floods. According to the author, urbanization reduces vegetation, forces the elevation of land surfaces to change, and increases drainage networks construction which all together increase runoff. The author mentioned of various approaches on how to reduce floods in urban areas. According to him, flood-prone areas can be used for parks and playgrounds that can withstand occasional flooding. Buildings and bridges can be elevated, protected with floodwalls and similar structures. They can also be designed to withhold temporary inundation. Drainage infrastructure can be updated to increase discharge capacity. However, the author also emphasized on implementing infiltration techniques like installing infiltration trenches,

replacing porous pavements with the impervious ones, reducing impermeable surfaces to minimize runoff in watersheds etc.

This research focuses on infiltration techniques suggested by Konrad (2003) to reduce runoff, and thereby minimize flooding in the urban watersheds. This research aims at analyzing the watershed response to land cover change through replacing the impermeable landcover of the Blacklot study site by the permeable ones. Therefore, literature reviews are made for pervious land cover treatments.

2.6.1 Studies on Permeable Pavement System for Urban Stormwater Management

Permeable or porous pavement systems, instead of traditional impervious pavements, have been used to reduce runoff, and to control its quality for almost last two decades (Putman, 2010). Impacts of porous pavements on watershed behavior change, and their durability, strength, performance against the traditional impervious systems have already been analyzed by the researchers.

Brattebo and Booth [2003] analyzed the long term performance of porous pavement systems on stormwater quantity and quality. They mainly examined the long term effectiveness of these pavements against the traditional impermeable asphalt pavement in parking sites. They investigated in terms of the pavements structural durability, infiltration capacity, and the quality of infiltrated water from the pavements after 6 year of daily use. The authors addressed some commonly raised questions about pervious pavements. The questions are as follows:

1) Do permeable pavements have the same structural durability like impervious asphalt?

2) Do they get clogged over time?

3) Do they help to improve the runoff quality?

Four permeable pavement systems were considered. They are:

i) Grass pavers

ii) Gravel pavers

iii) Turfstone (similar to concrete grid pavers with 40% opening)

iv) UNI Eco-Stone (small concrete block with only 10% opening)

For quality control purposes, Copper, Zinc, Motor oil, Hardness and Conductivity of the runoff samples were measured. In terms of durability they found that both grass and gravel pavers dislodged from the ground, but no rutting, settling or shifting was observed for Turfstone and UNI Eco-Stone. Thus, grass and gravel pavers might need maintenance for withstanding traffic loads. In terms of runoff quantity reduction, all the systems worked fine, and far better than the classic impervious asphalt. In fact they virtually infiltrated all precipitation which included some major storm events too. For almost all the storms, runoff quality for these pervious systems was found be significantly improved than the impervious asphalt. However, though the porous pavements showed favorable results for stormwater quality and quantity control and as well as in terms of durability, the authors did not guarantee the same performance in everywhere. Rainfall intensities, soil condition etc. can play an important role on deteriorating their performance. Besides, according to the authors, financial consideration would play vital role on replacing them with existent impervious pavements.

Putman [2010] conducted a study on evaluating field performance of porous pavements. They considered ten parking areas as test sites, and 9 of them were covered with concrete grid pavers (the reaming one was covered with porous asphalt). Functional performance was evaluated for these pavements using their infiltration capacity.

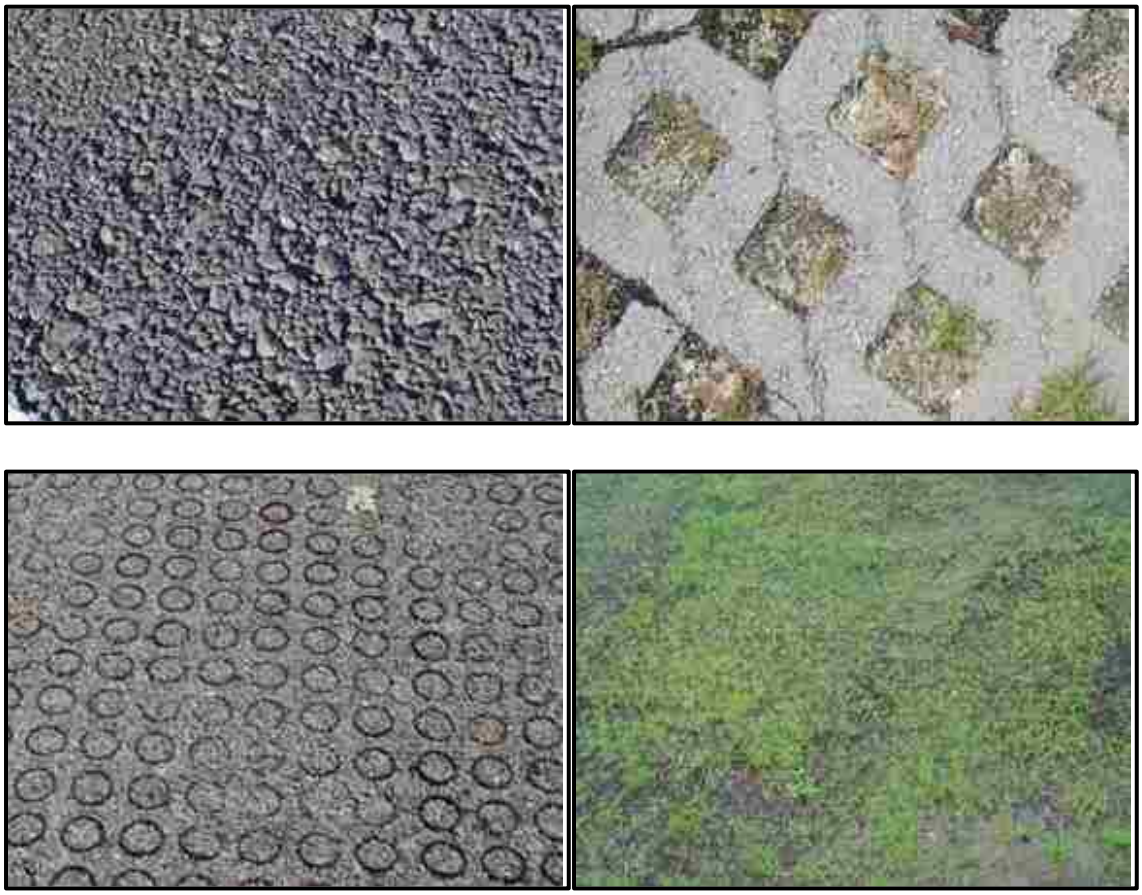

Figure 2.6-1: Porous asphalt (top left corner); Concrete grid pavers (top right corner); Gravel pavers (bottom left corner) and Grass pavers (bottom right corner) (Hunt and Collins, 2008)

Structural performance was evaluated by inspecting of cracklings on them, and surface performance was evaluated by inspecting raveling of the pavement surfaces. In terms of runoff reduction, almost same results are observed as in Brattebo and Booth (2003). However, in some places the pavements were not able to infiltrate as expected. The main

reasons behind this are found to be the clogging of voids, and poor construction. The authors concluded that though the porous pavements perform better in stormwater management, they must be maintained throughout their service life which is a disadvantage over traditional impervious pavements. These pavements showed great structural performance as no cracking was observed. This indicates that these are as good as impervious ones for load bearing. On the other hand, some small reveling were observed in 70% of the study site pavements.

Through the literature reviews, it is observed that porous pavements perform favorably well for stormwater management in urban areas than traditional impervious pavements mostly constructed with impermeable concrete, asphalt etc. The pervious pavements (except grass and gravel pavers) like concrete grid pavers have the same load bearing capacity as impervious ones. The main disadvantage is that the pervious pavements needed to be maintained properly and timely against clogging; otherwise their performance would degrade with time.

2.6.2 Studies on Recognized Porous Pavement Systems for Flood Reduction

The following pervious pavements or land cover treatments (figure 2.6-1) are widely used for reducing flood in parking lots (Hunt and Collins, 2008):

i) Porous asphalt

ii) Gravel pavers

iii) Grass pavers

iv) Concrete grid pavers

2.6.3 Porous Asphalt Pavement

Porous asphalt pavement is widely used now a days for managing storm water. This pavement, used mostly for parking lots, allow water to drain through the pavement surface (NAPA, 2014). Figure 2.6-2 shows the typical cross section of a pavement built with porous asphalt. Porous asphalt's primary advantages are (The UNH Stormwater Center, 2014):

1. Runoff quantity control
2. Runoff quality control
3. Groundwater recharge
4. Minimizes stormwater infrastructure
5. Can be used efficiently in cold-climate.

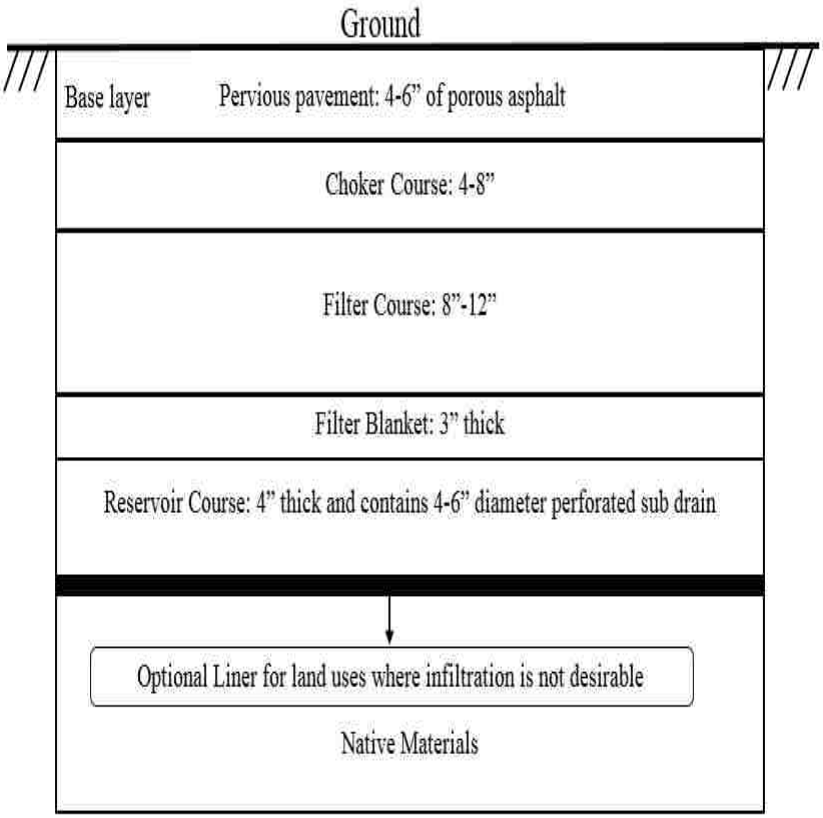

Figure 2.6-2: Typical cross section of porous pavement system in a parking area (modified from UNHSC, 2009)

2.6.4 Gravel Pavers

Gravel paver is another type of porous pavement mainly built with gravel as a base layer. This type of pavement allows to park, drive, and walk on a beautiful decorative gravel surface. The main benefits of a gravel pavement are (http://www.invisiblestructures.com/gravelpave2.html):

1. Runoff quantity reduction
2. Provides a good load bearing surface
3. Runoff quality control

This system is also widely used now-a-days for stormwater management in urban areas.

2.6.5 Grass Pavers

Grass paver, like the gravel pavers allows to park, and drive on a beautiful grass surface. It is a structure which provides good load bearing strength as the gravel pavers, and it also allows for vegetation by holding the runoff (http: //www.invisiblestructures. com/grasspave2.html). The benefits of using grass pavers are almost same as the gravel pavers.

Some of its application are (http: //www.invisiblestructures. com/grasspave2.html):

1) Overflow, stadium and event parking
2) Church parking
3) On-street parking like at grass shoulders
4) Bolstering infiltration basins
5) Helicopter landing pads

2.6.6 Concrete Grid pavers (CGP)

Concrete grid pavers like the grass and gravel pavers provide a solution for managing stormwater in parking areas. They can be used for vehicular and emergency access areas, high traffic parking areas, residential driveways, and help to reduce urban surface temperature (ICPI, 2014). These grid pavers generally have 9 cm (3.5 in) thickness, and 20 to 50 percent open or void area that can contain topsoil and grass, sand, or aggregate (Hunt and Collins, 2008). The minimum average compressive strength of concrete grid pavers is found to be higher than 35 MPa (5,000 psi) which is generally higher than the gravel and grass pavements (Hunt and Collins, 2008).

2.7 Concluding Statements

It is observed through the reviews that none of the flood model is applicable in modeling floods for an inlet-based ungauged urban catchment. But watershed area of an inlet represents stormwater collection area, and the city of Las Vegas consists of lots of such collection areas. Flooding in such areas damages properties heavily. Therefore, these areas should be well protected against flooding. In the literature review studies no guidelines are found about calibration and validation is case of barely available historic data. Also no straightforward procedure is found in the studies about flood mapping using GIS. However, through the studies, it is found that what land cover materials should be used or widely used to reduce runoff and flooding in a parking area. Bedsides, it is also understood that when modeling flood for an inlet based micro watershed using rainfall-runoff model, rainfall temporal resolution and as well as clogging factor should be considered as important hydrologic parameter along with DEM resolution since they

have the greatest impacts on modeling floods using GIS in an urban watershed. This research develops an approach to model urban floods inside a GIS-framework for inlet-based catchments which can conveniently utilized by the users with minimum amount of computational requirements. It also provides information about soft calibration and validation for insufficient historic data, and as well as straightforward technique to map floods in GIS. The model can be used by the Las Vegas flood management authorities to protect the drainage areas of inlets from flooding.

CHAPTER 3: STUDY AREA AND DATA

The GIS-framework developed in this thesis is tested using a known flood event in two study areas. This chapter describes the study areas of the known flood event, and the data used to accomplish the research work.

3.1 Study Area

This research project is conducted over two small study sites of the main cumpus of University of Nevada Las Vegas (UNLV) that is situated at the center of the Las Vegas Valley. The study sites are:

1. Blacklot parking area of UNLV
2. East Mall area of UNLV

These study sites are chosen since they are the two mostly devastated places of UNLV campus that were damaged by the flooding event on September 11, 2012. Moreover, flooding information of these sites is also available. These study areas are described in the following subsections.

3.1.1 Blacklot Parking Area

The parking lot is commonly called 'Black Lot' and is in front of the Thomas & Mack Center [See Figure 3.1-1]. The parking lot is located at 36° 6' 8.6436" N, 115° 8' 41.2722" W. It has Tropicana Parking garage and Red Lot on the east, Thomas and Mack Dr. on the west, Thomas and Mack Center on the north and East Tropicana Ave on the south. This parking lot represents a typical endorheic catchment with outlet into a drainage inlet. Such catchments evolve from changes to surface topography from

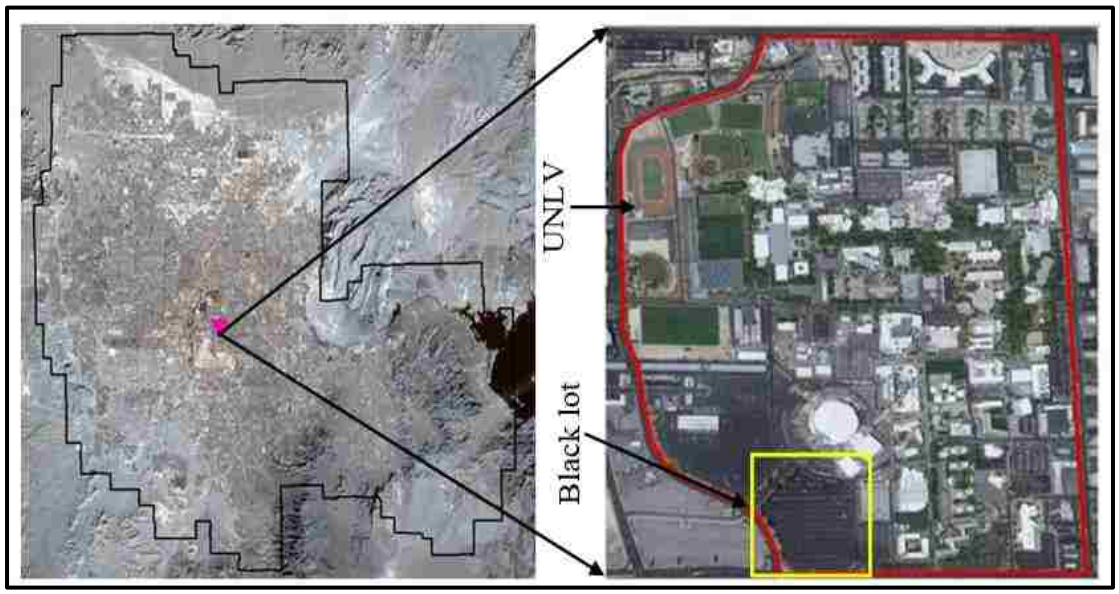

Figure 3.1-1: Blacklot study area (on the right) and Las Vegas Valley (on the left)

continuous urban development. Thus, drainage inlets that were originally designed for a certain capacity may render insufficient for the evolved catchment. The surface or land cover type of the parking lot is asphalt which is an impervious material. The lot has an approximate area of about 0.57 square kilometers. It can accommodate around 2000 vehicles at a time. There is no drainage inlet inside of the parking lot. Insufficient drainage inlets along with the impervious cover type make the parking area vulnerable to flash flooding.

Figure 3.1-2 shows the storm drain inlet location in the study area along with the drain inlet itself. Through a GPS field survey, it is found that the drain inlet of the parking lot is located at 36° 6' 10.9008" N and 115° 8' 37.2876" W and is at the lowest elevation in the catchment area. It is a 'Street Sump Inlet' with equal length combination of grate and curb-opening inlet. It is 116 inch long and 18 inch wide with a curb-opening height of 6

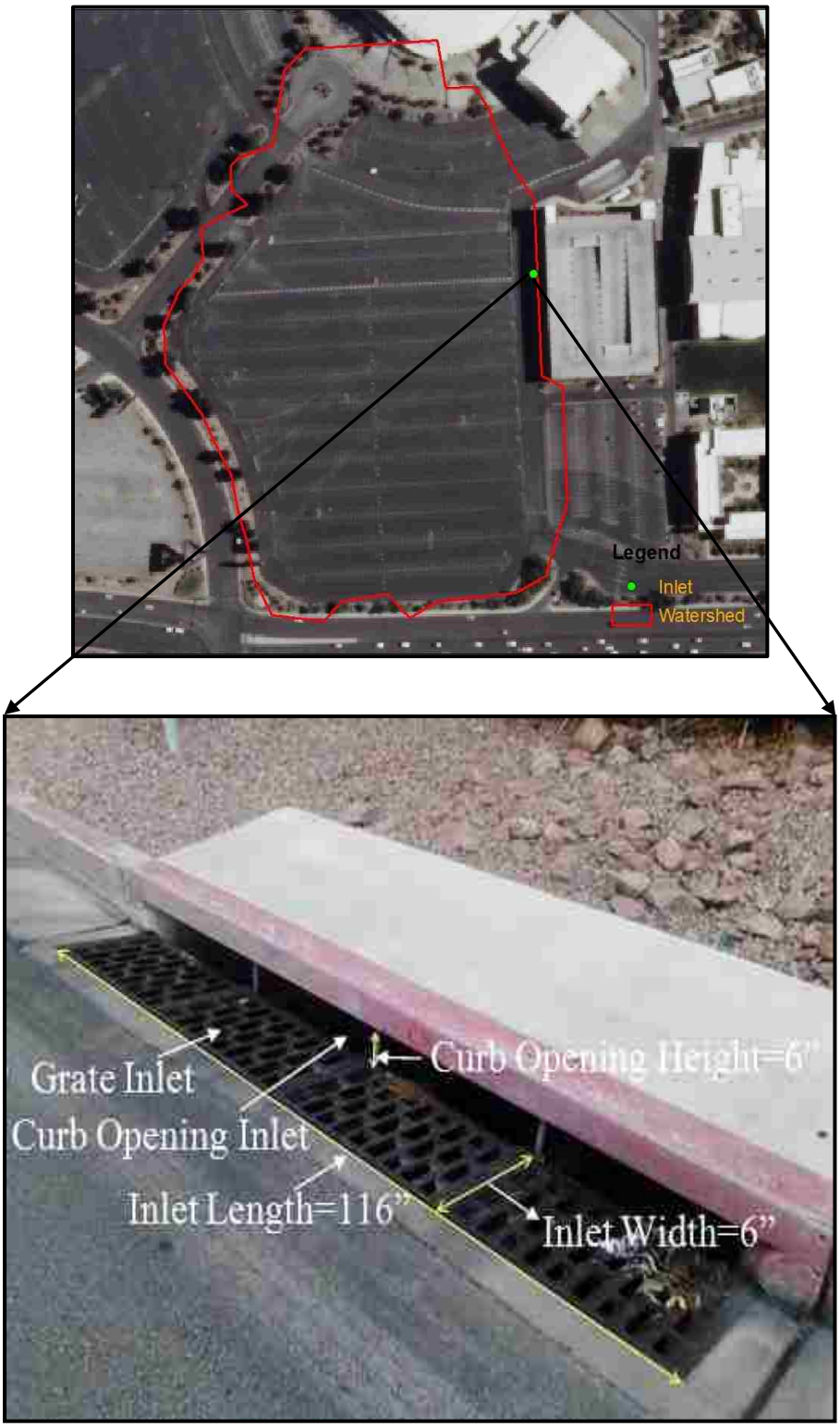

Figure 3.1-2: Location of drain inlet (on top) and the drain inlet (at bottom)

inch [See Figure 3.1-2]. The inlet is also identical to the Combination inlet Type 16, as its each segment consists of vane grate and a curb opening (Guo et al., 2009).

3.1.2 East Mall Area

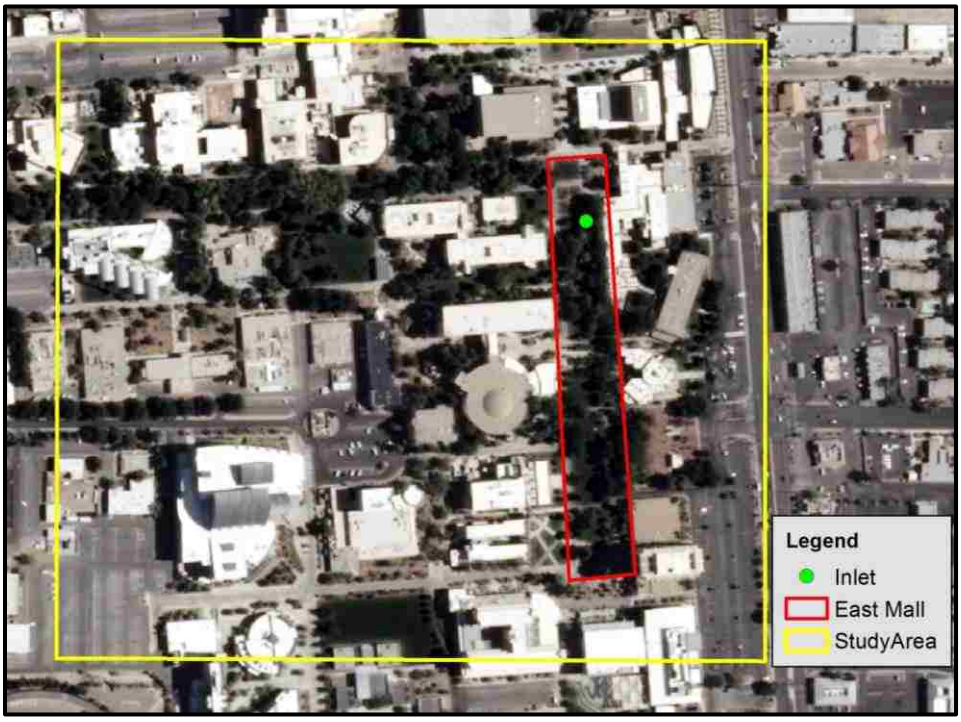

Figure 3.1-3: Study area for East Mall's drain inlet (along with East Mall)

The East Mall area is actually a strip line located on the east side of UNLV campus that runs north-south [See Figure 3.1-3]. The geographic location of the center of this strip line is 36°06'32.6"N and 115°08'20.9"W. This area is fully covered with vegetation. The area serves as a site for many student functions, like afternoon concerts and organizational recruiting, as well as campus tours, receptions, and conferences etc. The area contains Lee Pascal Memorial Rose Garden on its north side. It has Donna

Beam Fine art gallery on its east side, William D. Carlson Education building on the west side, and Student Union the south side. Since it is a strip line, and that the contributing area of the drain inlet of interest is assumed to be beyond its boundary, a bigger study area is chosen in this case which is shown in figure 3.1-3. This study area is mainly covered with vegetation, asphalt (parking areas), concrete (buildings) and gravels.

The drain inlet of the East Mall area is found to be located at 36°06'32.9"N and

Figure 3.1-4: Storm drain inlet at the East Mall area

115°08'20.6"W through the field visit. It is also found that the drain inlet's location is at the lowest elevation area of the study site. Therefore, it is considered to be a 'Sump Inlet'. The inlet is a curb opening inlet [See Figure 3.1-4]. The inlet is 42 inch long with a curb-opening height of 6.5 inch. The inlet is identical to the Type R curb opening inlet (Guo and MacKenzie, 2011).

3.2 Data

This research is performed using various remote sensing data and hydrological data that are described in the following sub-sections.

3.2.1 Remote Sensing Data

This section describes the remote sensing data utilized in this research..

3.2.1.1.LiDAR Data

LiDAR data are remote sensing data that are collected utilizing Light Detection And Ranging (LiDAR) technology. LiDAR data are used in this research to obtain elevation information. LiDAR data is a point cloud elevation data. This data is acquired by illuminating a target with laser light pulse, and measuring the time taken for the pulse to get back to the satellite. LiDAR-derived DEM provide accurate information for hydrological analyses of basin (Petroselli et al., 2012). The accuracy of DEM data is important, especially in an urban catchment, because all the hydrological analyses are based on this core data. These publicly available DEM data may be too coarse for urban flood-modeling application (Chen et al., 2009). Our research utilizes high resolution LiDAR data that have average point spacing of 1.66 m. The LiDAR data are collected from Southern Nevada Water Authority (SNWA).

3.2.1.2.National Land Cover Dataset (NLCD)

The latest version of National Land Cover Dataset that was published in 2011 utilized for creating land cover maps of the study sites. National Land Cover Database is a land cover dataset which is used throughout the whole United States, and has a spatial resolution of 30 meters. The dataset were first established in 2001. Later, it was

republished in 2006 with modification, and the latest version was published in 2011. The dataset is divided into 16 land cover classes, which is downloaded from Multi-Resolution Land Characteristics (MRLC) Consortium website (http://www.mrlc.gov/nlcd11_data.php). The dataset is created using the data collected by Landsat satellite (MRLC, 2014). Each land class of the dataset has a unique classification code. The 16 land cover classifications along with the codes (shown in square parentheses) of the NLCD 2011 are listed as follows:

1. Open Water [11]
2. Perennial Ice/Snow [12]
3. Developed, Open Space (lawns, parks, golf courses, cemeteries etc.) [21]

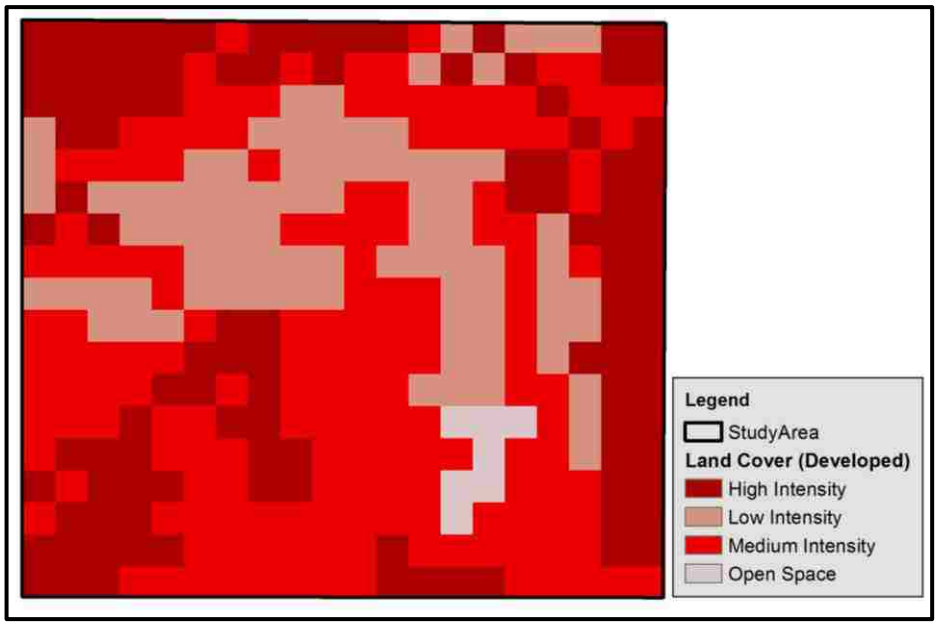

Figure 3.2-1: Land Cover map for East Mall study area

4. Developed, Low Intensity (Impervious surfaces = 20% to 49%) [22]
5. Developed, Medium Intensity (Impervious surfaces= 50% to 79%) [23]
6. Developed, High Intensity (Impervious surfaces = 80% to 100%) [24]

7. Barren Land (Rock/Sand/Clay) [31]
8. Deciduous Forest [41]
9. Evergreen Forest [42]
10. Mixed Forest [43]
11. Dwarf Scrub [51]
12. Shrub/Scrub [52]
13. Grassland/Herbaceous [71]
14. Sedge/Herbaceous [72]
15. Lichens [73]
16. Moss [74]

The dataset is extracted to the study sites. It is found that the Blacklot study area possesses Developed-Medium Intensity and Developed-High Intensity land covers. The East Mall study area possesses Developed-Open Space, Developed-Low Intensity, Developed-Medium Intensity and Developed-High Intensity land covers. Figure 3.2- 1 shows the land cover map/data created for the East Mall study site by extracting the original NLCD data to the study site.

3.2.2 Hydrological Data

The hydrological data includes rainfall data, surface hydrological soil group information, and surface curve number information.

3.2.2.1.Rainfall Data

Rainfall data are collected from the website of Clark County Regional Flood Control District (CCRFCD), i.e., the data are from their rainfall gage stations. CCRFCD

provides near real-time weather information via the Internet (http://www.ccrfcd.org/raingauges.htm). It provides weather reports for the cities of Clark County, Nevada. CCRFCD is selected as a data source because of its reliability, and relatively higher temporal resolution of rainfall data than other data sources. Precipitation data of the day of 11th September, 2012 are collected for a gage station only (Station ID: 4574). The station is located at Flamingo Wash trail that is near the Spencer.

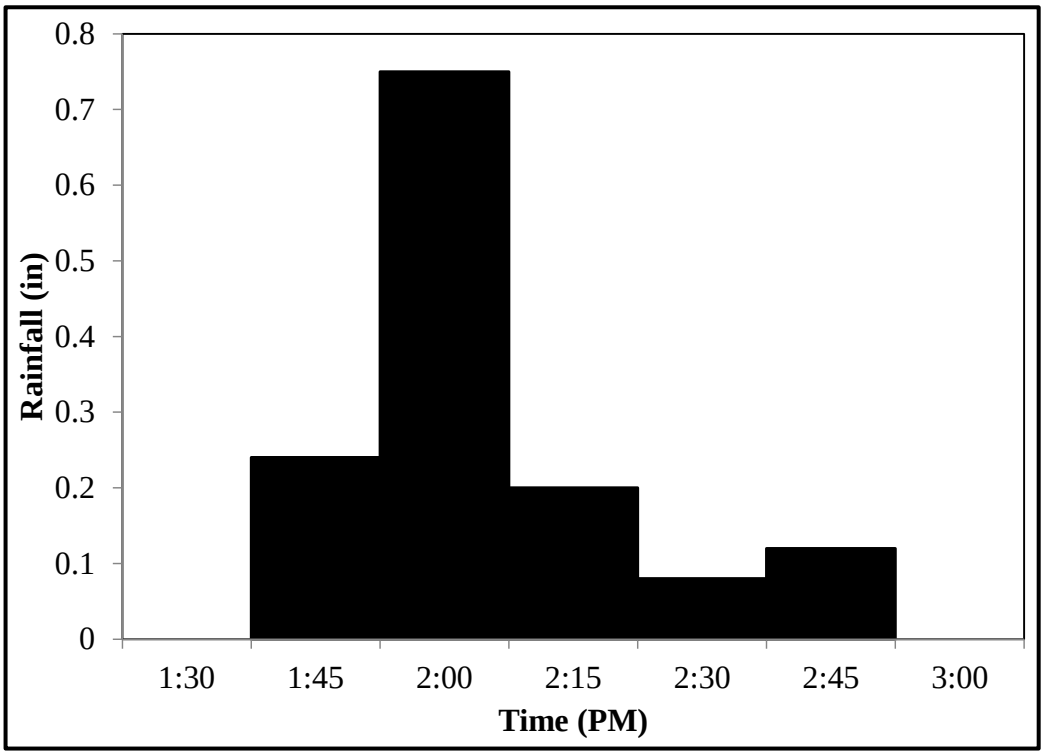

Figure 3.2-2: Rainfall Hyetograph for September 11, 2012

This station is chosen because of its close vicinity to the UNLV main campus. The distribution of the rainfall data is shown in figure 3.2-2. The peak rainfall intensities for this station at various times are provided in Table 3.2-1. However, it is observed from the figure that the rainfall started after 1:30 PM, and ended after 2:45 PM. The peak occurred between 1:45 PM and 2:00 PM. The peak rainfall recorded was 0.75 inches, while the

total amount is recorded as 1.38 inches which is 35% of the total average annual rainfall of the Las Vegas Valley (4 inches).

Table 3.2-1: Peak rainfall intensity distribution for Station 4574

Time (minutes)	Peak rainfall intensities (inches)
5	0.31
10	0.59
15	0.75
30	0.98
60	1.22
120	1.34

3.2.2.2.Soil Data

Soils are classified into Hydrologic Soil Group (HSG) to indicate the infiltration

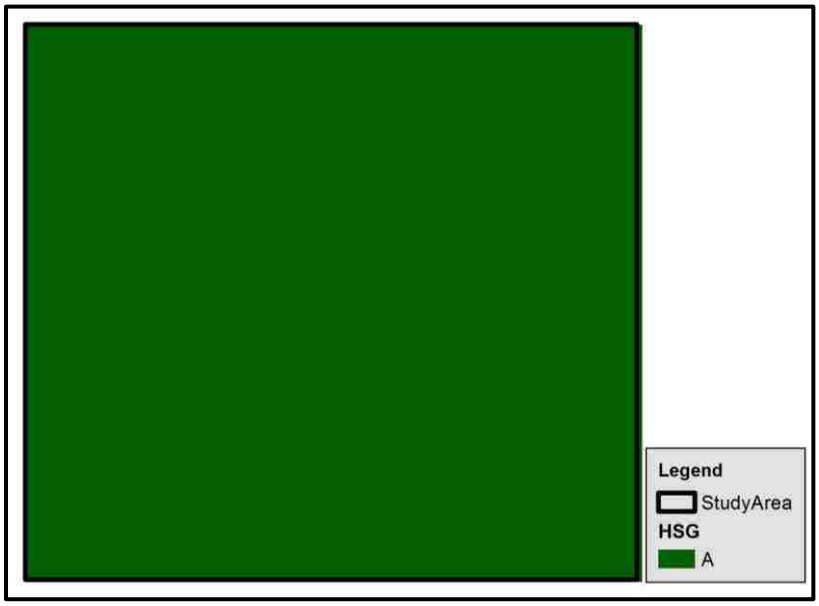

Figure 3.2-3: Soil map for the East Mall study area

rate (Cronshey, 1986). According to Cronshey [1986], soils are categorized into four groups according to their infiltration rate, namely: A, B, C and D. Group A has highest infiltration rate while Group D has lowest infiltration rates among the groups. Hydrologic soil group data are collected from Soil Survey Geographic Database (SSURGO) that is maintained by Natural Resources Conservation Service (NRCS) of United States Department of Agriculture (USDA). The SSURGO database contains information about soil collected by the National Cooperative Soil Survey (NCSS). The information or data were collected by field survey, while many soil samples were collected and sent ot the laboratories for analysis (USDA-NRCS, 2014). The data are downloaded from Web Soil Survey website (http://websoilsurvey.sc.egov.usda.gov/App/HomePage.htm) that contains SSURGO database. The SSURGO dataset for the whole US is downloaded as GIS shapefile. The dataset contains many soil physical and engineering properties other than the HSG which is considered to be as an engineering property. The Hydrologic Soil Group information are extracted from the downloaded data to create a HSG map. This HSG map is then extracted to the study areas to create their corresponding soil maps [See Figure 3.2-3]. A uniform HSG of A is found for both the study areas.

3.2.2.3.Curve Number

SCS curve number method is based on empirical rainfall-runoff relationships for various surface characteristics. SCS method requires curve number which is determined using surface characteristics information. It is an empirical parameter, and used to characterize the runoff properties for a particular soil and land cover (Cronshey, 1986). Determining CN requires soil and land cover data. They are determined using the relationship between soil and land cover. CN data are collected from various sources

(GISHydroNXT User's Manual, 2014; Wehmeyer et al., 2011; USDA-TR 55 Manual; Mishra and Singh, 2003). A curve number table is created using the NLCD land classes and HSGs. The table is shown in Appendix. From the table it is estimated that the Blacklot study site has two curve numbers which are 86 and 95 since the study area has Developed-Medium Intensity and Developed-High Intensity as land classes and Group A as the HSG. Similarly, the East Mall study site has four curve numbers that are 49 (Fair/Average condition), 66, 86, and 95. It should be noted this research considers the average moisture/hydrologic condition that is termed as Fair in the table. Distributing the curve numbers among the study site cells curve number map is created for the study sites. The curve number maps are similar to the one shown in figure 3.2-1. The only exception is that the land cover classes are replaced by the corresponding curve numbers.

All the data collected are utilized to test the GIS-framework in study sites. The next chapter details about developing the GIS-framework.

CHAPTER 4: GIS-FRAMEWORK

This chapter provides the research approach, and details of the methods used to develop the GIS-framework for urban flood modeling, and mapping the spatiotemporal behavior of the floods in urban micro watersheds. It includes urban watershed delineation for a drainage inlet, hydrological approach to compute runoff, and convert runoff to flow at the inlet; and to generate time series of inundation depths, and techniques for spatiotemporal mapping of urban floods, and calibration and validation.

4.1 Research Approach

In this research, a GIS-framework is developed for urban flood modeling, and mapping spatiotemporal variation of the flood in micro watersheds. The framework is divided into six components, namely: i) urban watershed delineation, ii) rainfall to runoff conversion, iii) runoff to flow conversion, iv) inundation estimation and mapping, and v) calibration and validation. Of them, the first four components are together called 'Urban Flood Model'. Figure 4.1-1 shows the framework. Watershed is delineated for a point of interest, which can be a drain inlet or a low elevation point. The inundation is analyzed at this point that acts as the outlet for the delineated watershed. Rainfall is converted to runoff and flow to generate a runoff hydrograph at the watershed outlet, which is compared with the discharge hydrograph of the drain to estimate flood depth. The flood depth is contoured at several times to map spatiotemporal variation of the flood. Calibration and validation of model is performed by comparing the model output with the observed data. This research approach is tested over several study areas located in Las Vegas Valley for a flood event that resulted from a 25-year 1-hour rainfall event on September 11, 2012. The results of these tests are presented in Chapter 5. The modeling

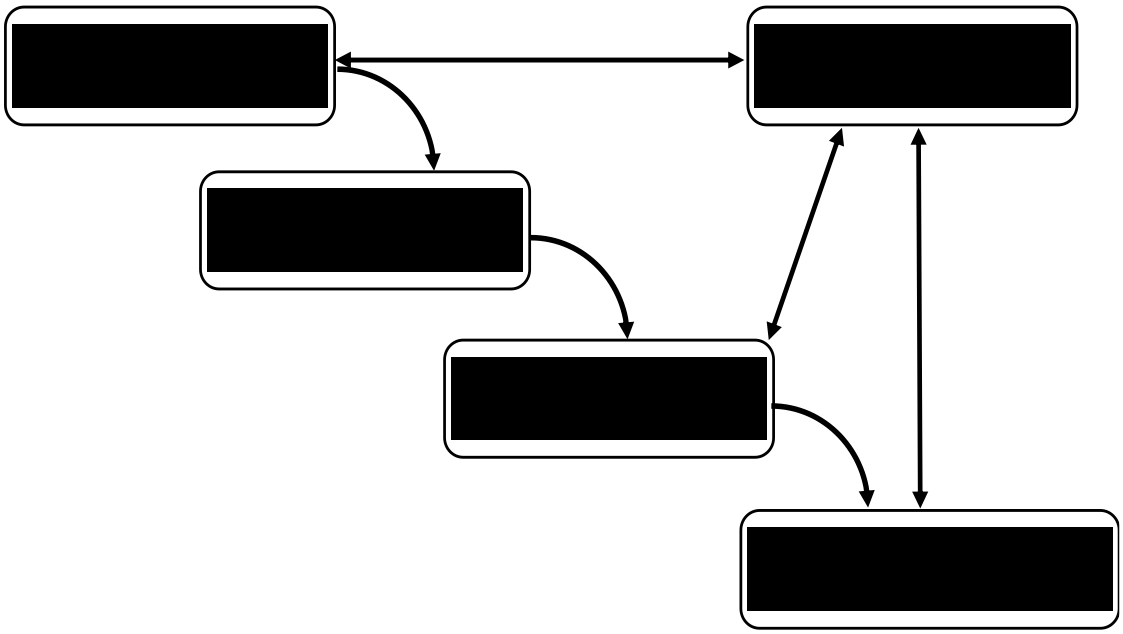

Figure 4.1-1: GIS-framework for modeling and mapping urban flood

framework is developed using ArcMap 10.1, a GIS software that provides the GIS tools, modules, methods and functions for spatial analysis, and using Python (version 2.7) language, a media that provides custom programming capability.

4.2 Flood Mapping GIS Framework

This section provides the details of methods utilized to construct the GIS-framework to model and map spatiotemporal behavior of urban floods. GIS tools and techniques are used to delineate urban watershed for a drain inlet, convert rainfall into runoff, translate runoff into runoff flow at the inlet, and produce time series of inundation depths and areas, and as well as inundation mapping along with calibration and validation. The following sections describe in details the various components of the GIS-framework.

4.2.1 Urban watershed Delineation

This section describes the procedures to produce outputs for the first component of the GIS-framework, i.e., to delineate urban watershed using GIS. The inputs for this process include the elevation data of the study site and a pour point for which the watershed will be delineated.

Watersheds for the storm drain inlets of the study areas are generated in GIS-platform using DEM. DEM map is developed from LiDAR point elevation data. The default interpolation technique of GIS, 'Linear' is used to create DEM. The DEM is presented on a regular grid, and reconditioned (made error free) to prepare data for watershed creation. The reconditioning processes include low pass filtering and filling process. Low pass filtering process is done to smooth the data, which in turn helps to remove abnormal peaks and flat areas in the DEM. This filtering is run using the Filter tool of GIS. The filling process includes removing small sinks or depression areas in the filtered DEM, and then elevate their elevations to the adjacent lowest cell. This filling process is performed using the Fill tool. The reconditioned DEM is further processed to determine direction of flow in each cell. The flow direction of a cell is obtained by finding out its adjacent lowest elevation cell, and the flow from the cell will be toward the lowest cell. Flow Direction tool is used to do this task. This is followed by creating Flow Accumulation map. The flow accumulation technique assigns to each cell, the number of upstream cells that contribute their flows to the cell. The flow accumulation grid can be used to generate the stream network. In this process, first the cells exceeding a threshold accumulation are identified and considered to form streams. The Con tool (Conditional selection) is used that utilizes a conditional statement ('if-then-else'

statement) using a threshold value. This threshold value is used to differentiate stream cells (waterway) from sheet flow cells (NOHRSC, 2014). The threshold value can be the number of cells equivalent assumption of sheet flow length in a watershed (NOHRSC, 2014). For example, for a 3m DEM resolution and 100 m long sheet flow, the threshold can be set to 33 (i.e. 100m divided by 3m). The next step is to run the GIS Watershed tool. This tool requires the pre-created flow direction grid and the pour point. A pour

Figure 4.2-1: Flowchart of watershed delineation processes

point is the point based on which the watershed will be created, i.e., the point acts as the watershed outlet. The drain inlet is primarily considered as the pour point. It is crucial that the inlet point is located on the primary streamlines of stream network, if not; Snap Pour Point tool of GIS should be used. This tool finds out the closest stream cell to the pour point using a specified search or snap distance, and moves the pour point to the center of that cell. This newly located pour point acts as the watershed outlet. Thus, using

the GIS processes and tools mentioned above, watersheds at the study areas for their corresponding storm drain inlets are delineated. Figure 4.2-1 shows the processes in brief.

4.2.2 Rainfall to Runoff Conversion

This section describes the hydrological method used to convert rainfall into runoff depth, or simply runoff, i.e., to produce outputs for the second component of the framework. The necessary equations for this conversion process are also provided.

SCS Curve Number method is used to convert rainfall into runoff, which is equal to rainfall excess. By definition, rainfall excess is the volume of rainfall that is available for surface runoff, and it is equal to the total rainfall minus interception, depression storage, and absorption (Searcy and Hardison, 1950).Runoff is calculated at each cell using the following SCS runoff equation (USDA TR-55, 1986):

$$q_{(x,y)} = \frac{\left(R_{(x,y)} - I_{(x,y)}\right)^2}{R_{(x,y)} - I_{(x,y)} + S_{(x,y)}} \qquad \text{Equation 4.2-1}$$

where $q_{(x,y)}$ is runoff (in) at any grid cell, $R_{(x,y)}$ is rainfall (in) in the grid cell, $I_{(x,y)}$ is initial abstraction (in), and $S_{(x,y)}$ is maximum soil retention (in) in the cell. Initial abstraction, the amount of initial rainfall retained by the watershed soil before the runoff begins (Yuan et. al., 2011), has a linear relationship with soil retention that is demonstrated below (USDA TR-55, 1986):

$$I_{(x,y)} = \gamma_{(x,y)} S_{(x,y)} \qquad \text{Equation 4.2-2}$$

where $\gamma_{(x,y)}$ is the initial abstraction ratio at each grid cell. Thus, initial abstraction ratio is the ratio of initial abstraction to maximum soil retention, and maximum soil retention, S is the maximum amount of rainfall that the watershed soil can abstract (Ponce et al., 1996). It is reported that γ varies from storm to storm and watershed to watershed (Yuan et. al., 2011), but it is also reported that 50% of the γ measurements, measured by SCS throughout the US, fall in the range of 0.095 to 0.38, and this led SCS to consider a standard value of 0.2 for γ in US (Ponce et al., 1996). Therefore, 0.2 as initial abstraction ratio is considered. Thus, equation (4.2-2) becomes:

$$I_{(x,y)} = 0.2S_{(x,y)} \qquad \text{Equation 4.2-3}$$

Putting equation (4.2-3) into equation (4.2-11), the following runoff equation to estimate runoff is obtained:

$$q_{(x,y)} = \frac{\left(R_{(x,y)} - 0.2S_{(x,y)}\right)^2}{R_{(x,y)} + 0.8S_{(x,y)}} \qquad \text{Equation 4.2-4}$$

The only unknown parameter in the equation is S, that depends on the soil hydrological group and the land cover class, and is represented using a curve number. Thus, S is estimated by finding out the curve number at each cell and using the equation provided below (USDA TR-55, 1986):

$$S_{(x,y)} = \frac{1000}{CN_{(x,y)}} - 10 \qquad \text{Equation 4.2-5}$$

where $CN_{(x,y)}$ is curve number of the grid cell. It is noted that low curve number results in higher S, and thus, results in lower amount of runoff in the watershed, and *vice versa*. The curve numbers that are used in the research are for average Antecedent Moisture Condition (AMC) or AMC II, which is also referred to Antecedent Runoff Condition

(ARC) to put more emphasis on runoff than soil moisture (Ponce et al., 1996). AMC II to generate runoff for this research is considered since AMC II represents a typical situation, while AMC I (dry condition) and AMC III (wet condition) result in lesser runoff and greater runoff respectively (Ponce et al., 1996). It is noted that the presented GIS framework can be customized for any AMC value.

Thus, equation (4.2-5) is used to estimate S at each grid cell, and equation (4.2-4) to estimate cell runoff for a given rainfall which is considered to be uniform throughout the watersheds. The rainfall event is divided into several sub-events, and runoffs in the watersheds are estimated for every sub-event.

4.2.3 Runoff to Flow Conversion

This section describes about the methods accounted for converting the previously estimated runoffs into flows at the watershed outlet. In other words, this section details the methods about creating a runoff hydrograph at the watershed outlet which is the final output of the framework's third component.

The runoff of a single cell in the catchment is translated through the cell's flow path to the outlet to generate runoff flow for that unit cell. This conversion of flow from runoff provides a runoff hydrograph at the watershed's outlet. A runoff hydrograph exhibits the relationship between the surface runoff and the travel time. A runoff hydrograph for each rainfall sub-event is estimated using time-area approach, i.e., through developing a time-area histogram for each sub-event. A time-area histogram exhibits a relationship between the travel time and a portion of a basin that contributes runoff during that travel time (Nilsson, 1998). Travel time (T_t) is the time it takes water to

travel from one location to another in a watershed (Cronshey, 1986). The travel time for a unit cell to reach the watershed outlet is estimated using the Flow Length tool of GIS. Before using this tool, velocity at each cell should be estimated that is computed using the following equation (Sorell and Hamilton, 1991):

$$V_{(x,y)} = K_{(x,y)} M_{(x,y)}^{1/2} \qquad \text{Equation 4.2-6}$$

where $V_{(x,y)}$ is the velocity at each cell (fps), $K_{(x,y)}$ is the velocity coefficient for a particular flow type at a cell , and $M_{(x,y)}$ is the slope at the cell in percent. Slope is estimated using the Slope tool of GIS. Next a weight grid is created, i.e., weights are given to each cell based on their velocity that is basically dividing the traverse distance of a cell, i.e., the resolution of the DEM by velocity, and the equation is given by:

$$W_{(x,y)} = \frac{L_{(x,y)}}{V_{(x,y)}} \qquad \text{Equation 4.2-7}$$

where $W_{(x,y)}$ is the weight at each cell (s) and $L_{(x,y)}$ is the flow length at each cell (m). The flow length at each cell is considered to be equal to the resolution of the cell. Thus, a weight is actually a travel time for each cell to cross the distance of the cell, not the time the water requires to reach the outlet from the cell. This weight grid and pre-developed flow direction grid are used as inputs for Flow Length tool that results in travel time grid. The stream cells have lower travel time than the sheet flow cells. The travel time grid is now used to generate the time-area histogram for the basin. The watershed is divided into equal travel time zones that are called Isochrones. Each isochrone represents the part of watershed that takes the same travel time to drain the excess rainfall, i.e., the runoff at the outlet (Usul and Yilmaz, 2002). The plot of the areas of the isochrones with respect to corresponding time values of the isochrones give the time-area histogram of the

watershed (Usul and Yilmaz, 2002). The areas are then multiplied by the runoff to obtain contributing runoff volume at the outlet. The volume is then divided by the time interval to compute runoff flow. Finally by plotting these flow values at the midpoint of time intervals the runoff hydrograph for each rainfall sub-event is produced (Usul and Yilmaz, 2002). These runoff hydrographs are accumulated by shifting according to the sub-event intervals to construct the final runoff hydrograph. Let $\{i_n\}$ be a sequence of rainfall measurements, i.e., rainfall sub-events for a given storm where each measurement corresponds to a time interval Δt. If nth element of the sequence produces $q_n(t)$ runoff hydrograph, then the total runoff hydrograph is $Q(t)$ is given by:

$$Q(t) = \sum_{n=1}^{N} q_n(t) \qquad \text{Equation 4.2-8}$$

where N is the cardinality of sequence $\{i_n\}$.

4.2.4 Inundation Estimation and Mapping

This section is divided into several sub-sections that are described below. It provides the step by step procedure for estimating flood depths and areas at various time intervals, and mapping the flood inundated areas. Figure 4.2-2 demonstrates the research approach for inundation estimation graphically. The figure also shows a typical runoff hydrograph, a stage discharge curve for a drain inlet, flood volume variation over time, typical watershed's stage volume curve and flood depth variation over time.

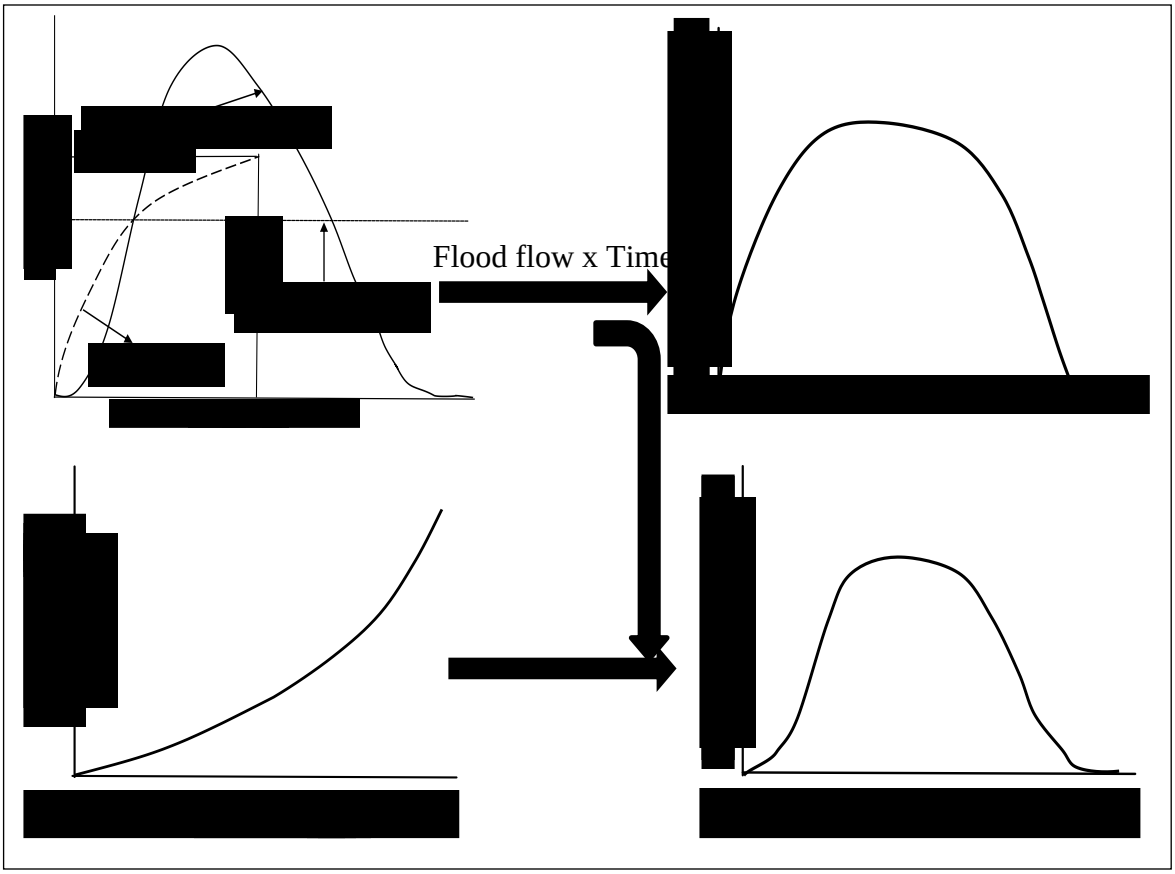

Figure 4.2-2: Graphical representation of Inundation estimation processes; typical runoff hydrograph along with rating curve (tope left corner); flood volume vs. time plot (top right corner); Stage-volume curve (lower left corner); and flood depth vs. time curve (lower right corner)

4.2.4.1.Stage Discharge Curve Construction

This section describes about how to construct a stage-discharge curve for a storm drain inlet in sump condition. This is because; the drain inlets of our study areas are sump inlets. A stage-discharge curve, also referred as a rating curve of a storm drainage inlet exhibits the relationship between the discharge capacity of the inlet and its upstream flow depth, i.e., runoff depth. This research follows the processes and equations demonstrated in Guo et al. (2009) to estimate the drain capacity of the storm drain inlets of the study areas. The equations along with the procedures are already described in section #2.7.1. A

typical stage discharge curve for a storm drain inlet is shown in figure 4.2-2 (top left graph).

4.2.4.2.Time Series of Flood Inundation and Spatiotemporal Mapping of the Flood

Flood discharges at the inlet are obtained by subtracting the discharge capacity of the inlet from the hydrograph flows of the runoff hydrograph at each interval of time. These discharges are then multiplied by the time to estimate flood volume. Flood volumes for each interval are added to obtain cumulative flood volume in the watersheds. These cumulative flood volumes are plotted against time to construct flood volume vs. time graph.

A stage-volume curve for the watershed is produced that exhibits the relationship between the watershed volume and its depth [See Figure 4.2-2]. First, the elevation of the pour point of a watershed is subtracted from the elevation of other watershed cells to obtain the depths of the cells that are available to be filled with water. These depths are multiplied by the corresponding cell's area to obtain volume. All the cells that have the same depth, their volumes are added that is equal to the total volume of the watershed at that depth. Thus, a stage-volume curve for each watershed is constructed by obtaining watershed volume at various depths, and plotting the volumes against the corresponding depths. Now for any flood volume the time is known from the flood volume vs. time graph and for the same volume, depth is estimated from the stage volume curve. Thus, the flood depths are estimated for different intervals of time to produce a time series of inundation depths. Figure 4.2-3 shows the research approach for estimating time series of flood depths in simplistic way. A time series of inundated areas is also generated by dividing the watershed volume at the inundation depths by the corresponding flood

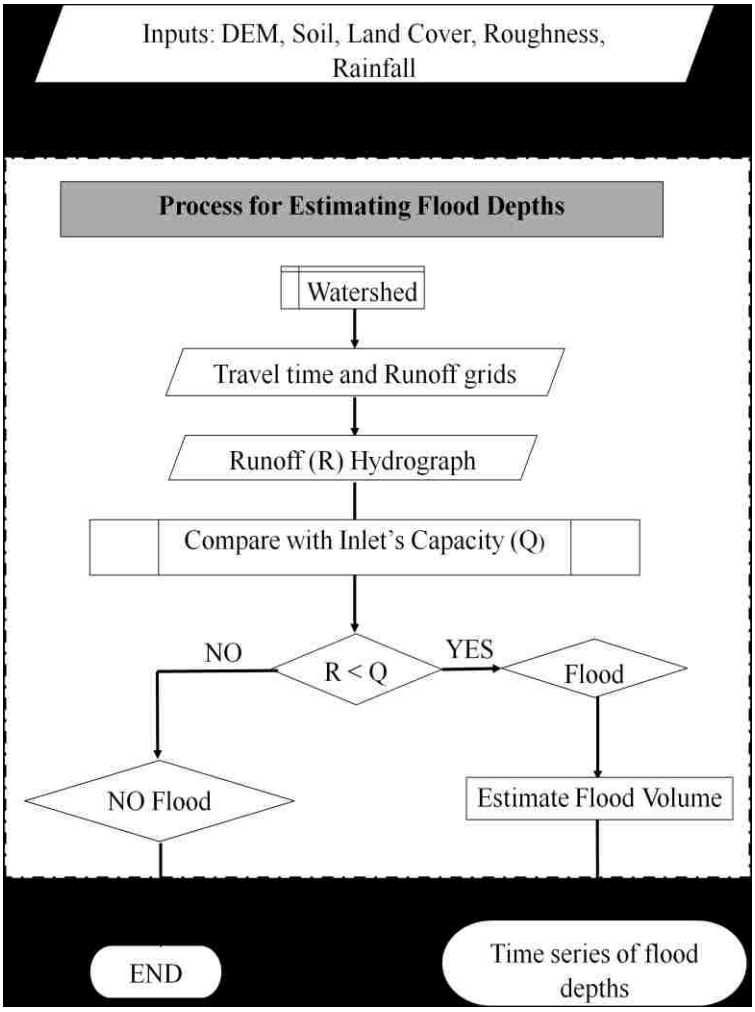

Figure 4.2-3: Flowchart of methodology for estimating time series of flood depths

depths. Later, flood inundation maps are created by contouring the flood depths of different time intervals which eventually results in spatiotemporal mapping of the flood. Spatial Contour tool of GIS is used for creating the maps.

4.2.5 Calibration and Validation

This section describes the processes of calibrating and validating the urban flood model already developed inside the GIS-framework. This final component of the framework consists of comparing the flood model's outputs with the actual information.

A hydrological study using modeling is meaningless without an acceptable calibration and validation of the results. The calibration and validation generally use historical data to ensure an accurate and valid model. If measured inundation and flow data are not available, soft calibration and validation using qualitative data can be performed e.g., photographic records of the flood event, flood reports, and news articles. Such sources can provide indicators about peak discharge, depth and duration of a flood, and hints about flood inundated areas. Although small, this can be vital information for calibration and validation of an urban hydrological model.

Since the watersheds are ungauged, indirect methods are used to calibrate and validate, i.e., soft calibration and validation techniques are utilized. Photographic evidences, newspaper reports and articles, reports from flood management authorities that provide valuable information on the flood depth, extent and duration are collected. Besides, several field visits are also made to find out information. These information with the estimated ones are compared to calibrate and validate this research approach of developing the GIS-framework for urban flood modeling and mapping. For calibration, the calibrating parameters are needed to be chosen. This research approach of developing the GIS-framework for urban flood modeling and mapping is tested against its three most important parameters, i) DEM resolution of the study areas, and ii) rainfall temporal resolution, and iii) clogging factor of the drain inlets, to calibrate and validate the approach.

4.2.5.1.Calibration Parameter: DEM Resolution

The main reason behind choosing DEM resolution as calibration parameter is due to its great amount of significance on the flood models outputs (Goulden et al., 2014).

However, it always depends on the researcher to pick up the DEM resolution to work with for an uncalibrated study area. In such case, the researcher needs to go through creating, and using several DEMs with various resolutions, and match the estimated results with the observed results for each DEM resolution to find out which DEM is the best one for his study area. If the study area is previously calibrated with any DEM, then the user should use that known DEM. However, in case of an uncalibrated study area, it is essential to calibrate the area with a known DEM.

4.2.5.2.Calibration Parameter: Rainfall Temporal Resolution

It is commonplace that to use the rainfall data in the research as they are collected. Generally, they should be used as they are if they have high temporal resolution. But if they have low resolution, analyses should be made by changing the low resolution to higher resolution to find out the closest outputs to the observed ones since rainfall temporal variation is considered as one of the most crucial elements for rainfall–runoff models, and shorter temporal resolution provide better performance in storm discharge estimation (Wang et al., 2009).

4.2.5.3.Calibration Parameter: Clogging Factor

Storm drain inlets are always affected by clogging effects, and selection of a clogging factor reflects the condition of debris and trash in the drainage area (Urban Storm Drainage Criteria Manual, 2002). Conservatively, a clogging factor of 0.5 is assumed for a single grate and 0.1 for a single curb-opening inlet (Guo and MacKenzie, 2012). Guo and MacKenzie [2012] estimated the clogging factor for multiple inlets in serial with the observed phenomenon that the clogging factor decays as the number of inlet units increases. They found that with clogging decay coefficient of 0.25 for curb

opening inlet and 0.5 for grate inlet provide good estimates of clogging factor, and equation (2.4-13) is a simplified version of their findings. However, clogging factor estimate for a combination inlet is not found available. Therefore, to get an average estimate of clogging factor for a combination inlet, equation (2.4-13) is used to find clogging factors for curb opening and grate inlet individually, and later the factors are added to obtain combined clogging factor which is demonstrated by equation (2.4-17). Since there is no specific true value for clogging factor, i.e., the values are either assumed or unavailable, and the factor changes with the location of the inlet, watershed surface characteristics, season and amount of debris etc., the clogging factor is considered as a calibrating parameter (Urban Storm Drainage Criteria Manual, 2002). Therefore, the flood model in the GIS-framework is run for various clogging factors to find out the optimum factor for the inlets of the study sites.

4.3 Summary

In this chapter, a GIS-framework for urban flood modeling and mapping is developed. GIS tools and procedures are used to develop a workflow for urban flood modeling and mapping. The framework provides mechanism to analyze a flood spatiotemporal behavior and perform calibration and validation. As part of the procedures, the methodology for creating error free DEM out of point cloud elevation data, and delineating watershed for a drain inlet using GIS tools and techniques is detailed. Moreover, the techniques for converting rainfall into runoff, and runoff into flow at the inlet using the GIS-suitable hydrologic approaches are also explained. The methodology for estimating the discharge capacity of a drain inlet at various water depths, and creating a stage discharge curve for the inlet out of the estimations is also

described. Next, the techniques for estimating flood depths at various time intervals by comparing the runoff flows with the stage discharge curve values, and for mapping the flood using the depth information are described. By products, the techniques for calibrating and validating a model against insufficient data are explained. This developed GIS-framework is tested in two small study sites of UNLV main campus. They are: i) Blacklot parking area and ii) East Mall area. The findings of testing the framework in these two study areas are highlighted in the next chapter.

CHAPTER 5: CASE STUDIES

The approach of developing the GIS-framework is tested in two study areas: i) Black parking lot and its surrounding area of UNLV and ii) East Mall and its surrounding area of UNLV. This chapter describes and analyses the results of these case studies.

5.1. Black Parking Lot of UNLV

This section highlights and describes the important outputs derived from the testing of the developed GIS-framework in the Black parking lot area of UNLV. This section consists of the following sub-sections: i) Results and ii) Discussion. The final outputs of the flood model of the GIS-framework along with other important intermediate results, as well as results of calibration and validation of the model inside the framework are demonstrated in the Results sub-section, while they are elaborately explained in the Discussion section.

5.1.1. Results

This sub-section highlights the results of the corresponding components of the developed GIS-framework produced by the testing of the framework in the Black lot study area.

5.1.1.1. Watershed Delineation

Figure 5.1-1 shows a DEM for the Black parking lot study area. The resolution of the DEM is 5 meter. This DEM is chosen arbitrarily to be created from the LiDAR data. The highest elevation in the study area for the 5m DEM is 936 m, and the lowest elevation is 590 meter. Considering the irregularities shown in figure 5.1-1 as well as

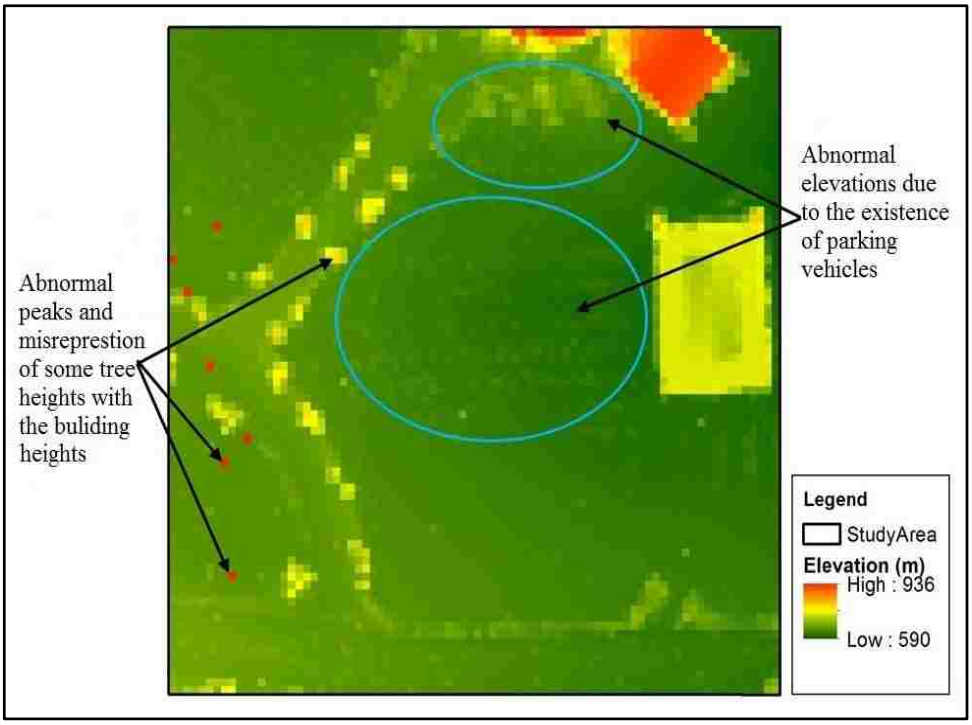

Figure 5.1-1: Black lot study area DEM of 5 meter resolution and its errors

the fact that the heights of buildings and trees relative to the surrounding low areas may cause extra elevation irregularities, and thus causing problems in delineating watershed, this DEM is reconditioned using the GIS Filter and Fill tool to smooth the data. The reconditioned DEM is presented in figure 5.1-2. Compared to the original DEM, the filtered DEM is smoother, i.e., the abnormalities and irregularities of the DEM elevation are reduced. It is observed that the irregularity effect due to the parking vehicles is almost gone. The heights of the buildings and trees are also reduced, and the heights of their surrounding low areas are also elevated making the study area more even. It is observed that the elevation in the area decreases from west to east, and that suggests runoff in the area flow from west to east where the drain inlet lies. Using this reconditioned DEM, flow direction of the grid cells is delineated, and that are used to

estimate the flow accumulation value of the cells that range from 0 (boundary cells) to 3830 (lowest cell).

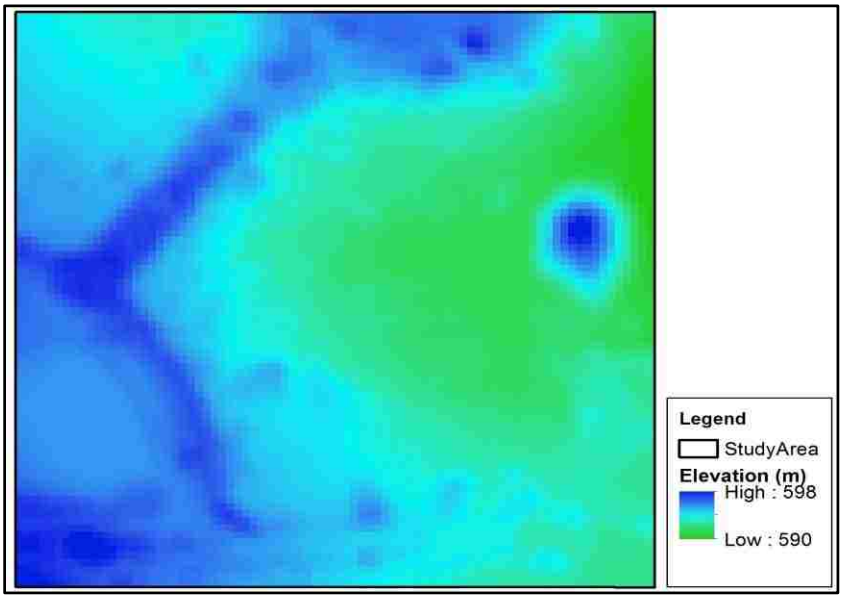

Figure 5.1-2: Reconditioned 5m DEM of the Blacklot study area

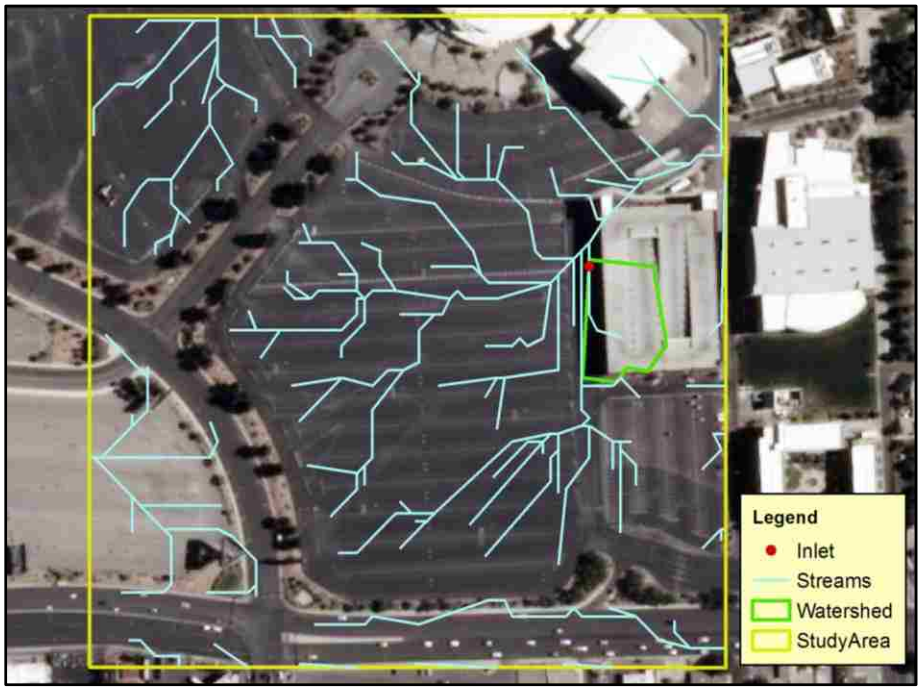

Figure 5.1-3: Stream Network in the Blacklot study area

Using the flow accumulation values and an accumulation threshold value of 20 (100m/5m), the stream network in the study area is created which is shown in figure 5.1-3. This network might be different from the real stream network. One of the reasons might be sediments deposited that are carried by runoff. Using this network and the drain inlet as the pour point watershed is created for the inlet [see figure 5.1-3]. It is observed

Figure 5.1-4: Delineated watershed in Black lot for the pour point

that the delineated watershed for the drain inlet is too small which indicates that the accumulation value of the grid cell located at the inlet's location is too small. Therefore, Snap Pour Point tool of GIS is utilized to find out the highest flow accumulation cell to the nearest of the inlet. Various snap distances of 5meters, 15 meters and 20 meters are used, and among them 15 meter snap distance finds out the closest pour point that

produces the most representable watershed [See Figure 5.1-4]. The distance between the new pour point and the inlet is estimated to be 9.86 meters using the Measure tool of GIS. This new pour point acts as the outlet of this watershed. The watershed has an area of 78136 m^2 (19.31 acres).

5.1.1.2.Rainfall to Runoff Conversion

The soil and land cover data are extracted to the watershed to estimate the curve number for the watershed. The soil group of the watershed is A, and the land covers are the type "Developed" with high and medium intensity. Thus, there exist two curve numbers in the watershed, and they are 86 and 95 for Developed with medium and high intensity respectively. 12% of the total watershed cells possess a curve number of 86, and the remaining 88% possess 95. The original rainfall data are converted to runoff using equation (4), and the soil retention values are estimated using equation (5) as 1.63 and 0.53 which is considered to be 0.1 (Pandit and Heck, 2009). Using equation (4) it is found that the first rainfall event produces runoff that range from 0 in (no runoff) to 0.15 in, for the second one the range varies from 0 in to 0.64 in of runoff, the third one produces 0 in to 0.05 in of runoff, the fourth one produces 0 in to 0.023 in runoff, and the fifth one produces 0 in to 0.12 in of runoff.

5.1.1.3.Runoff to Flow

The runoffs are converted to flow using time area approach, i.e., by estimating travel times of the watershed cells. In order to estimate the travel time of the watershed grid cells, a velocity map needs to be produced that requires velocity coefficient (K) and slope values of the cells (in percent) beforehand according to equation (6). The K map (figure 5.1-5) is produced by distributing the K values of 1.2 and 0.48 along the stream

and overland flow cells of the watershed respectively. The slope map is produced using the watershed DEM as input for Slope tool of GIS. The map is shown in figure 5.1-6. It shows that the watershed has horizontal areas with 0% slope, and high areas with 19% slope. Using the two intermediate k and slope maps, the velocity map of the watershed is

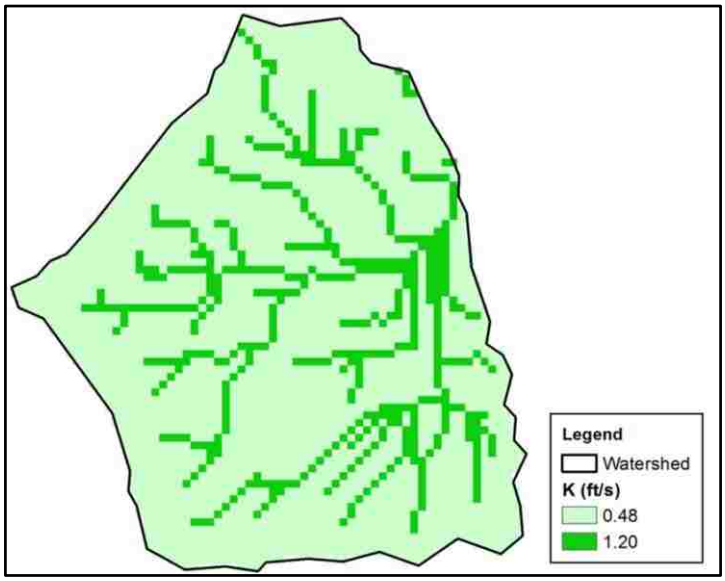

Figure 5.1-5: Velocity coefficient map of the Black lot watershed

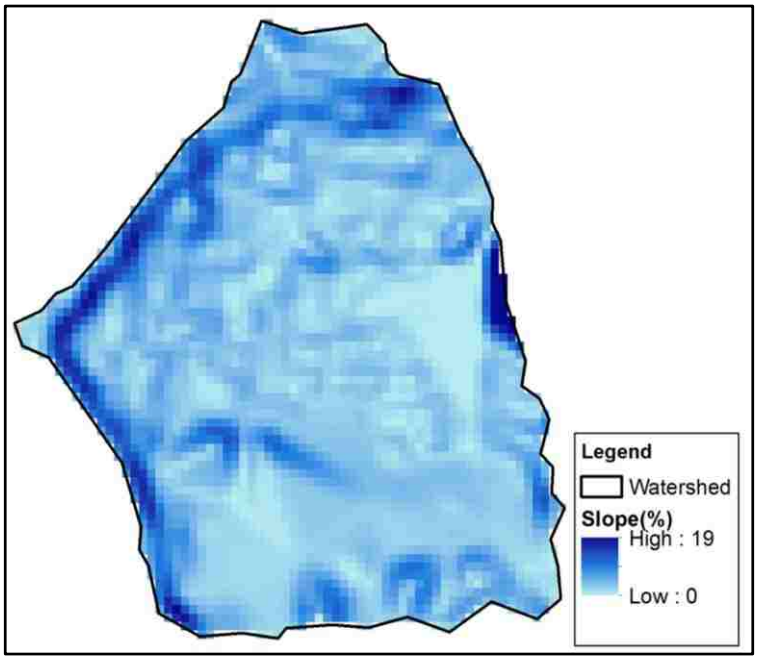

Figure 5.1-6: Slope map of the Black lot watershed

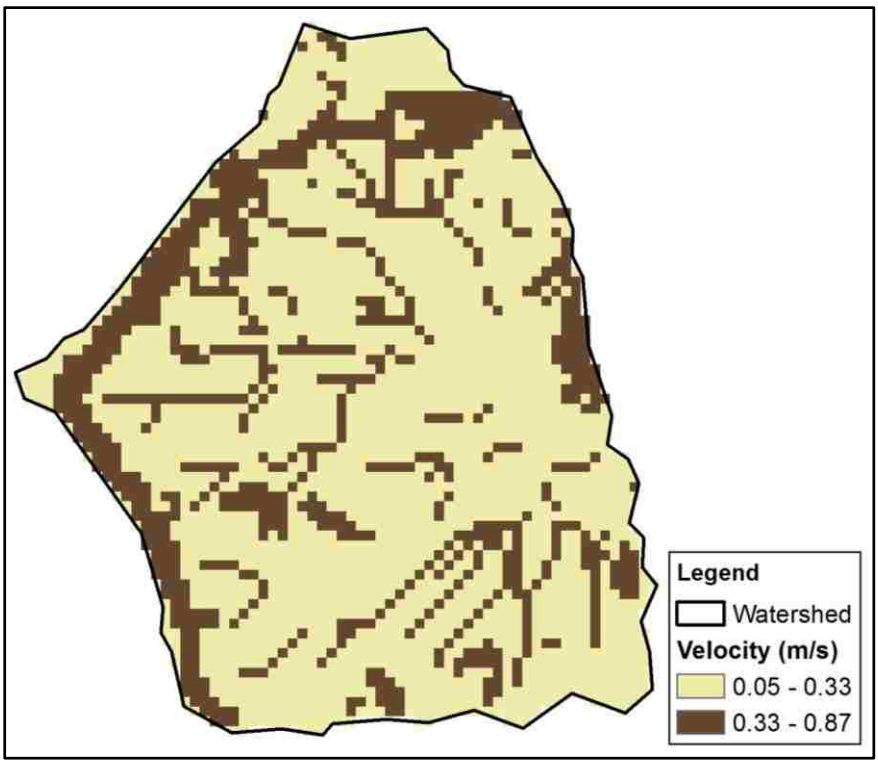

Figure 5.1-7: Velocity map of the Black lot watershed

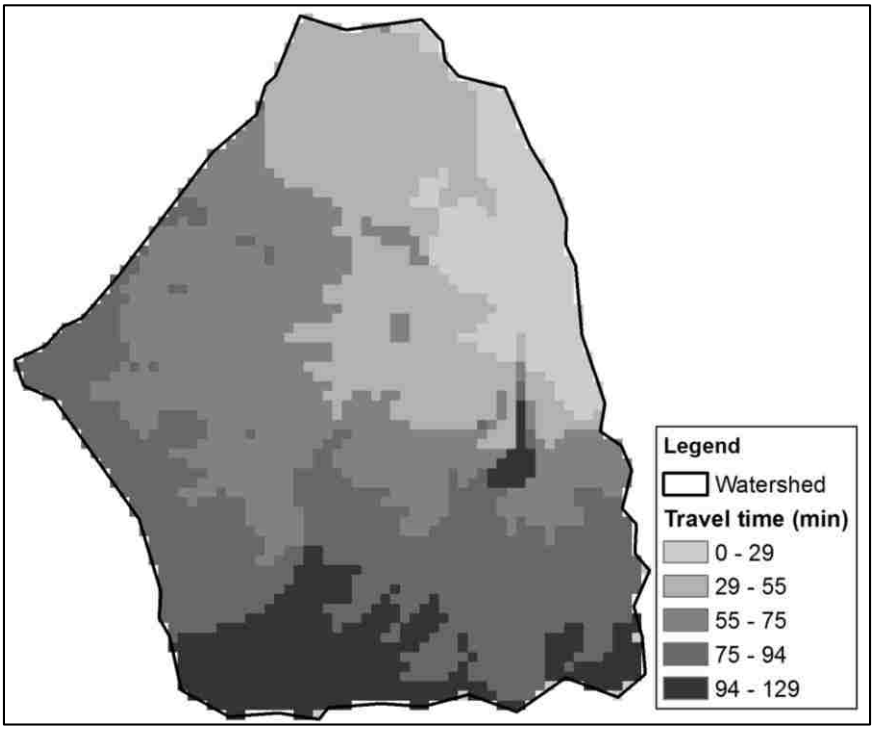

Figure 5.1-8: Travel time map of the Blacklot watershed

produced that is shown in figure 5.1-7. It shows that the lowest velocity the cell possesses is 0.05 m/s, and the highest velocity the cell possesses is 0.87 m/s.

A weight map is produced using this velocity map by dividing the resolution or length of each cell (5 meter) by its corresponding velocity. This intermediate weight map along with the pre-developed flow direction map of the study area as inputs to the Flow Length tool of GIS, travel time for the grid cells to the watershed outlet is estimated. The travel time map is demonstrated in figure 5.1-8. It shows that the longest time the cells take to reach the outlet is 129 minutes, and this implies that the time of concentration of the watershed is 129 minutes. These values of travel times were divided by the duration

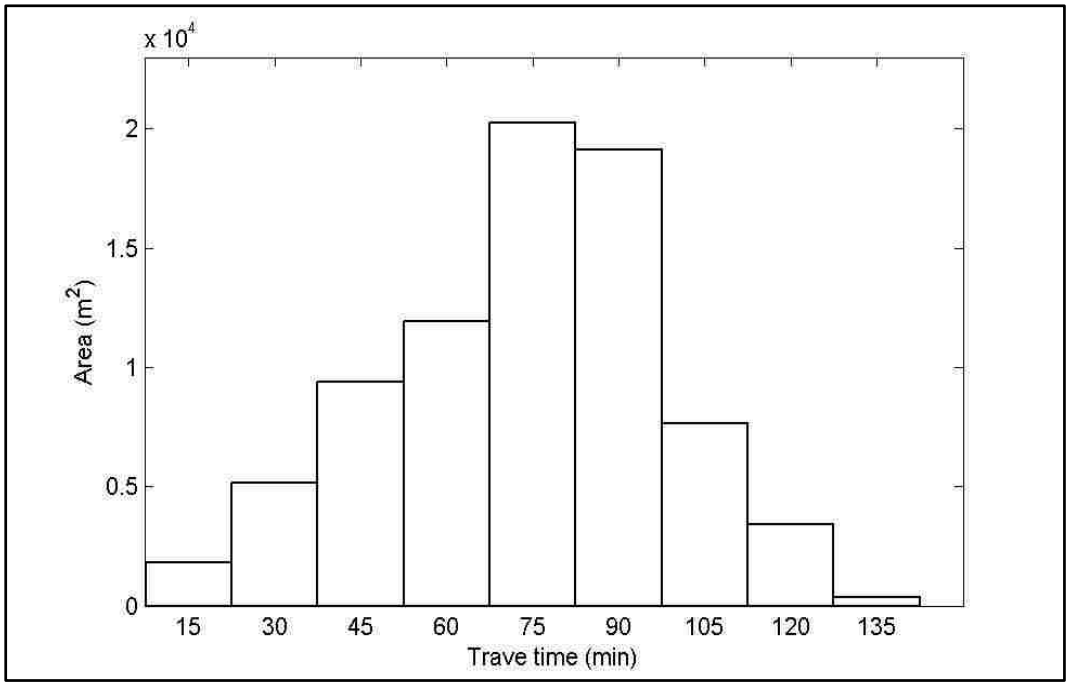

Figure 5.1-9: Time area histogram of the Blacklot watershed

of rainfall sub-event of 15 minutes to produce isochrones. Thus, there exist 9 isochrones for the watershed, and their contributing areas are estimated to produce time area histogram for the watershed [See Figure 5.1-9]. It demonstrates that the 75th minute

isochrone would produce the highest amount of runoff, since its contributing area is the largest (2.10×10^4 m^2). The area of this histogram is multiplied by the runoff produced by the rainfall of each sub-event resulting in runoff volume which then divided by the duration to result runoff flow. These runoff flows are plotted against the corresponding time to generate a hydrograph for the sub-event. Figure 5.1-10 shows the runoff hydrograph for the first sub- event. The peak is found 0.21 m^3/s and the time to peak is 67 minutes after the rainfall started. All the runoff hydrographs of the rainfall subevents are

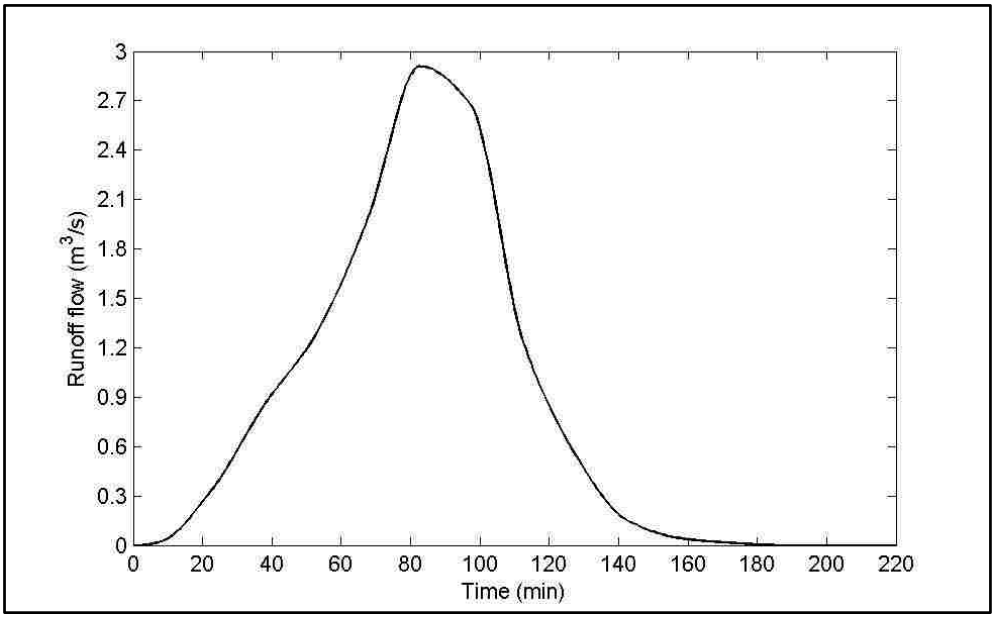

Figure 5.1-10: Runoff hydrograph for the 1st rainfall subevent in Blacklot watershed

accumulated and shifted according to their interval to result in final hydrograph [See Figure 5.1-11]. The peak of the hydrograph is found to be 2.91 m^3/s, and the time to peak is found 82 minutes after the rainfall. It is also noticed that the runoff ended after 203 minutes of rainfall.

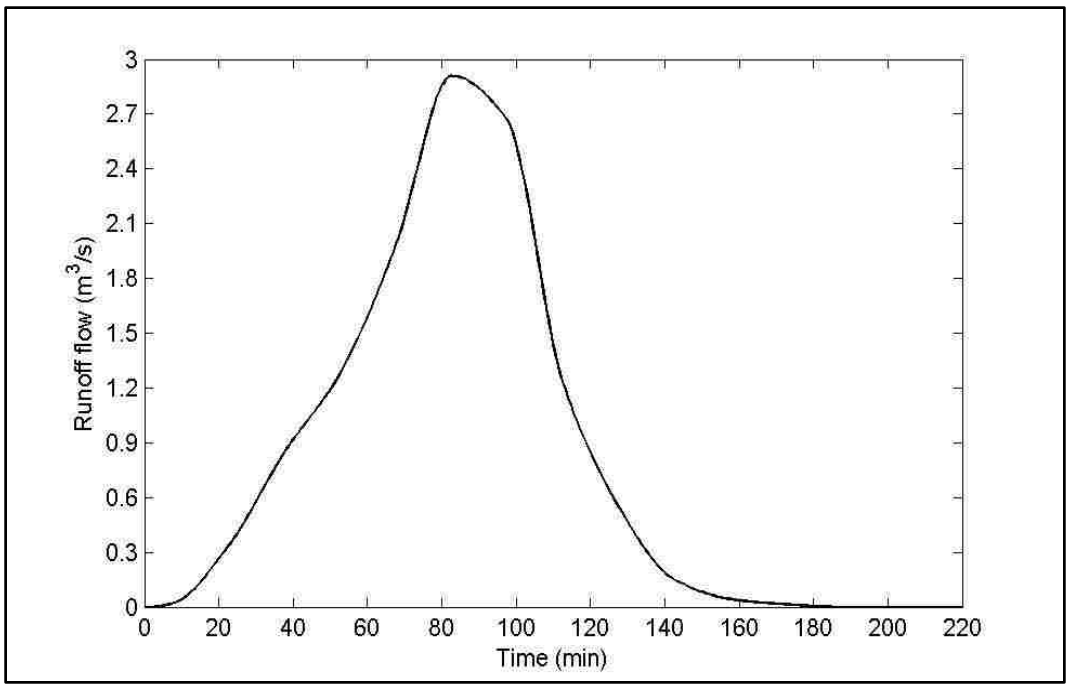

Figure 5.1-11: Hydrograph for the complete rainfall event

5.1.1.4. Inundation Estimation and Mapping

For inundation estimation, stage discharge curve for the drain inlet is constructed. The curve is shown in figure 5.1-12. Equations (13) through (16) are used to find out the

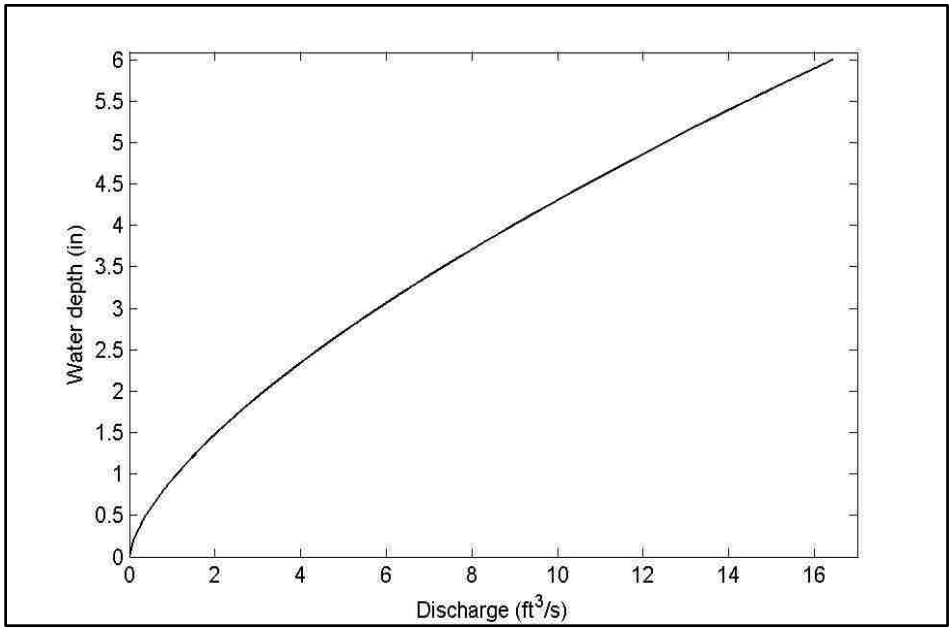

Figure 5.1-12: Stage discharge curve for Blacklot drain inlet

interception capacities as weir and orifice flows for the grate and curb opening segments of the inlet, while equations (11) and (12) are used to estimate the interception capacities as mixing flow through the segments. The values of N_w, N_o, C_{wg}, C_{wc}, and C_o are 0.62, 0.32, 0.30, 0.46 and 0.67, while the values of C_m is 0.93 (Guo et al., 2009). Using equations (9) and (10) the capacities for grate and curb inlets are estimated. As the drainage inlet has four units of grate and curb opening inlet each, and clogging effect is considered, equation (17) is used to estimate the clogging factor for the grate and curb inlet segments. The value of K for N=4 is 1.88 and 1.33, and the value of F is 0.5 and 0.1 respectively for grate and curb opening (Urban Storm Drainage Criteria Manual, 2002). Then equation (21) is used to estimate the clogging factor for our combination storm drain inlet that is estimated as 0.28. Finally, equation (20) is used to estimate the effective discharge capacity of the inlet for water depth (d) of 0 in to 6 in. The effective discharge

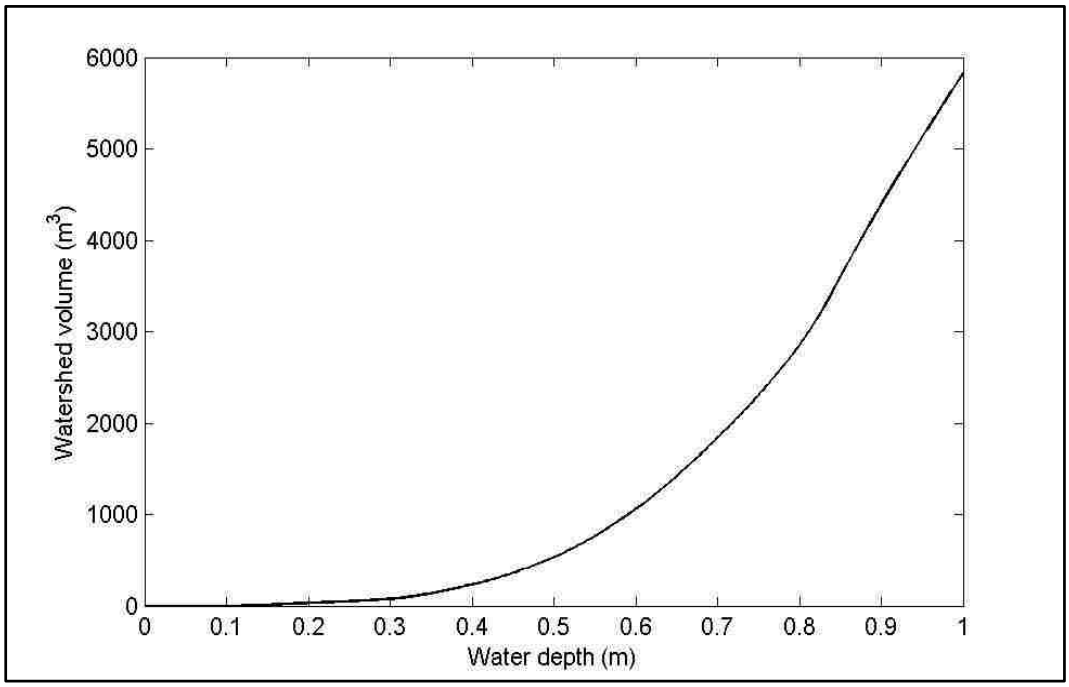

Figure 5.1-13: Stage capacity curve for the Blacklot watershed

capacity at the maximum allowable water depth of 6 in is found as 11.82 ft^3/s (0.33 m^3/s). This maximum allowable capacity of the inlet is compared to the runoff hydrograph shown in figure 5.1-11 to find out the flooding runoff, i.e., the runoffs that caused flooding. These runoffs are accumulated, and multiplied by their corresponding times to estimate the flood volumes over time, which are compared to the stage capacity curve of the watershed [See figure 5.1-13]. The maximum flood volume is estimated as

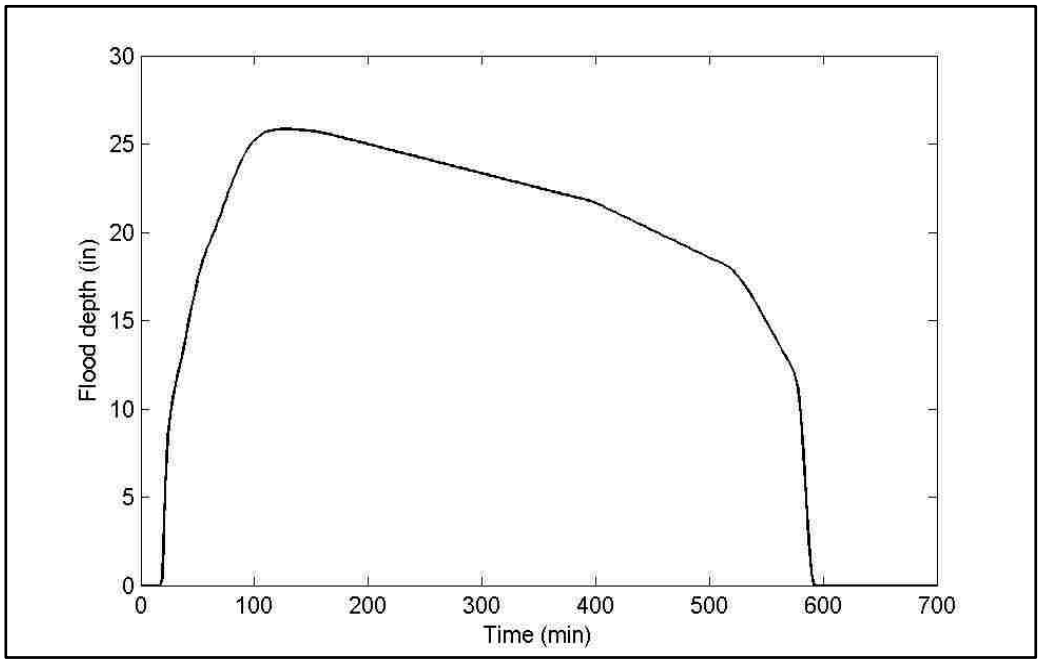

Figure 5.1-14: Flood depth variation over time in Blacklot watershed

700 cubic meters after 124 minutes of rainfall. However, from figure 5.1-13 it is observed that the watershed can hold a volume of 5800 cubic meters for a water depth of 1m. Thus, if the flood or ponding depth in the watershed is 1m, the corresponding volume will be 5800 cubic meters, and in case of the maximum flood volume which is 0.66 meter (26 inch) Therefore, the estimated flood volumes are compared to the volumes shown in figure 5.1-13, to find out the corresponding depths. The resulting flood depths at various

time intervals are shown in figure 5.1-14. It is found that the peak flood depth is 26 in near the inlet. The peak depth occurred after 124 minutes of rainfall. It is also noticed that the flooding started after 22 minutes of rainfall, and ended after 590 minutes (9.8 hours) of rainfall. Thus, the duration of the flooding was around 9.5 hours. These flood depths were contoured in GIS to produce the inundation extents. Figures 5.1-15 through 5.1-19 shows some of the inundation extents at various times in the watershed. From the

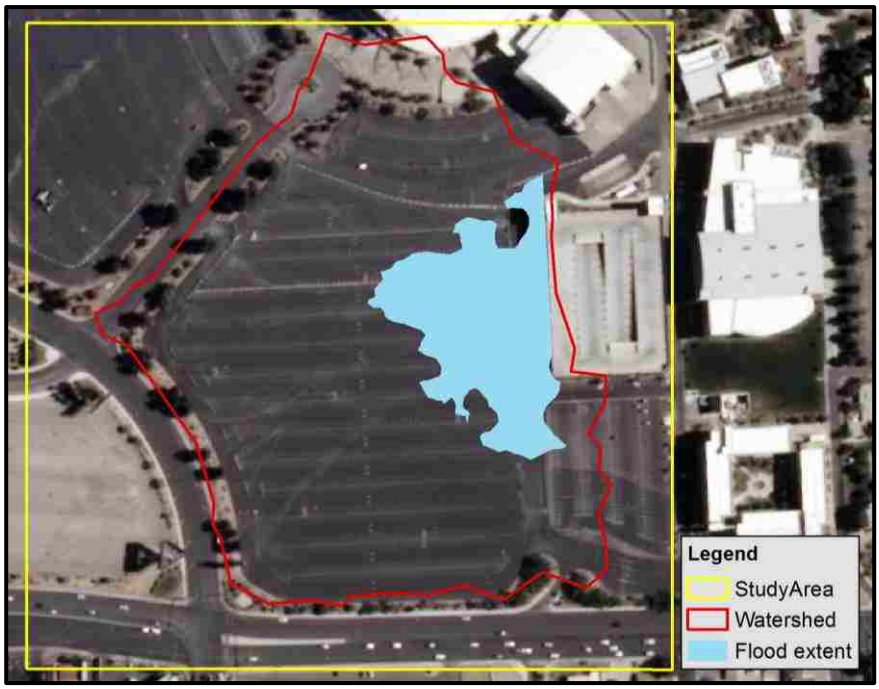

Figure 5.1-15: Inundation extent at 30 minute after rainfall in Black lot watershed

inundation extents, inundated areas at these times are found using GIS. For example, inundated areas at 30 minutes is found as 11172 m^2, at 60 minutes 14672 m^2, at 124 minutes 17834 m^2 (maximum flooded area), at 500 minutes 13855 m^2, and 5841 m^2 towards the end of the flooding respectively.

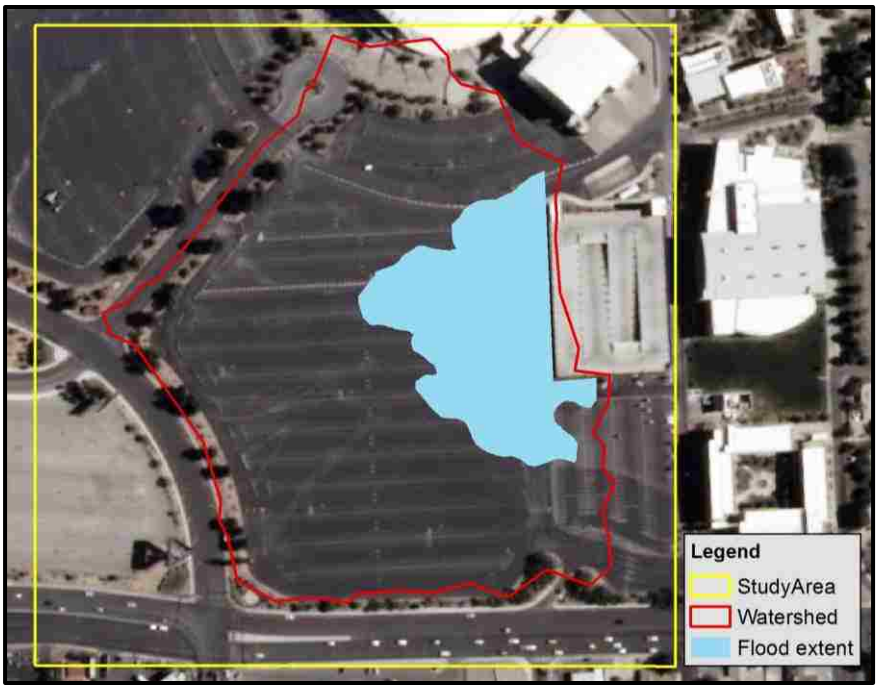

Figure 5.1-16: Inundation extent at 60 minutes after rainfall in Blacklot watershed

Figure 5.1-17: Inundation extent after 124 minutes of rainfall in Blacklot watershed

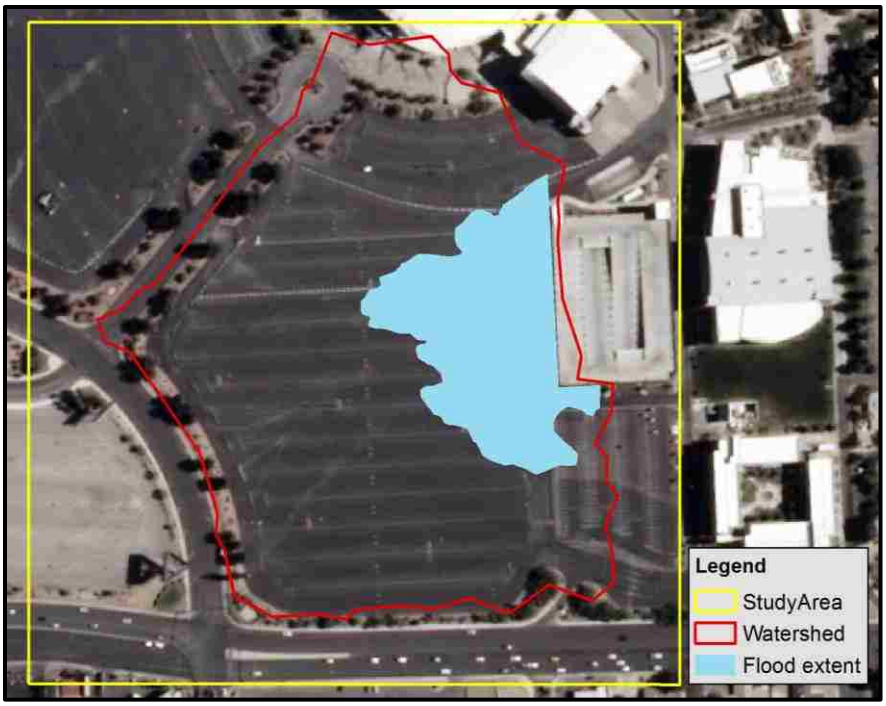

Figure 5.1-18: Inundation extent after 590 minutes of rainfall in Blacklot watershed

Figure 5.1-19: Inundation extent after 500 minutes of rainfall in Blacklot watershed

5.1.1.5.Calibration and Validation

The urban flood model of the GIS-framework is run for various DEM resolution of the study area in order to calibrate and validate the model against the DEM resolution. DEM resolutions of 1m to 10m is tested. The observed peak flood depth at and around the inlet is found as 34 inch from the ground. The peak flood depth is estimated for each DEM resolution, and compared to this actual peak depth to estimate errors. Figure 5.1-20

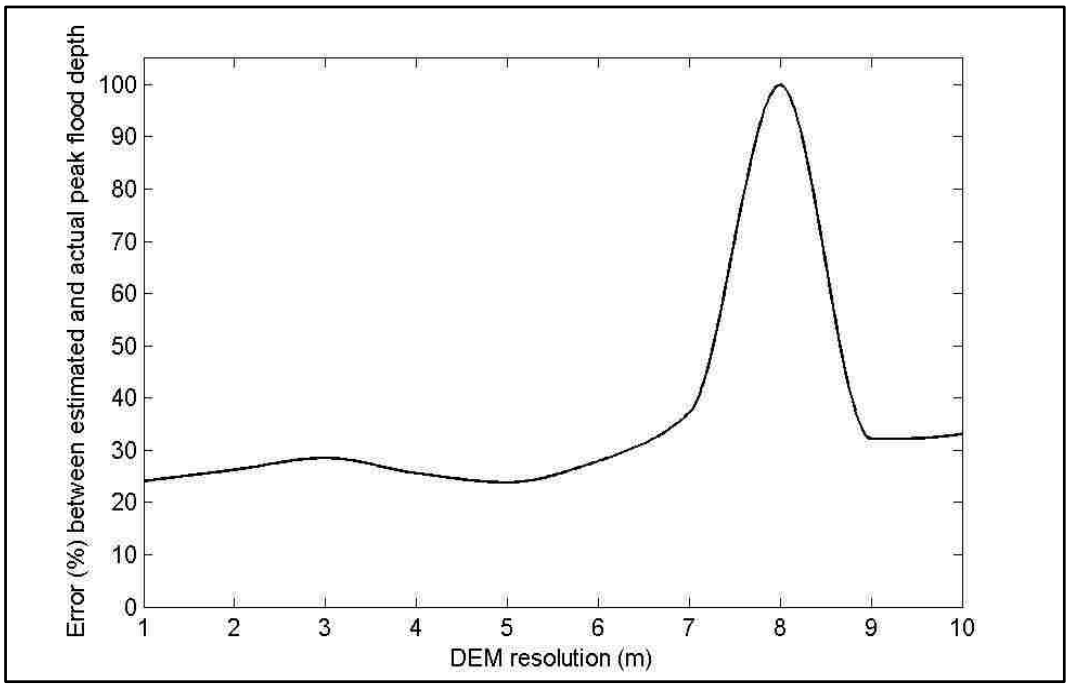

Figure 5.1-20: Calibration and validation against DEM resolution in Blacklot watershed

demonstrates the error against the corresponding DEM. It is observed that the DEM 5m produces the lowest error of 24%, and the 8m DEM produces the highest error of 100%. Figure 5.1-21 shows the error between the actual and calculated peak flood depths against the interpolated rainfall temporal distribution for the 5m DEM. It is observed that the 15 minutes resolution, i.e., the original distribution produces the lowest error of 24% while 1 minute resolution produces the largest error (100%). Figure 5.1-22 shows the error

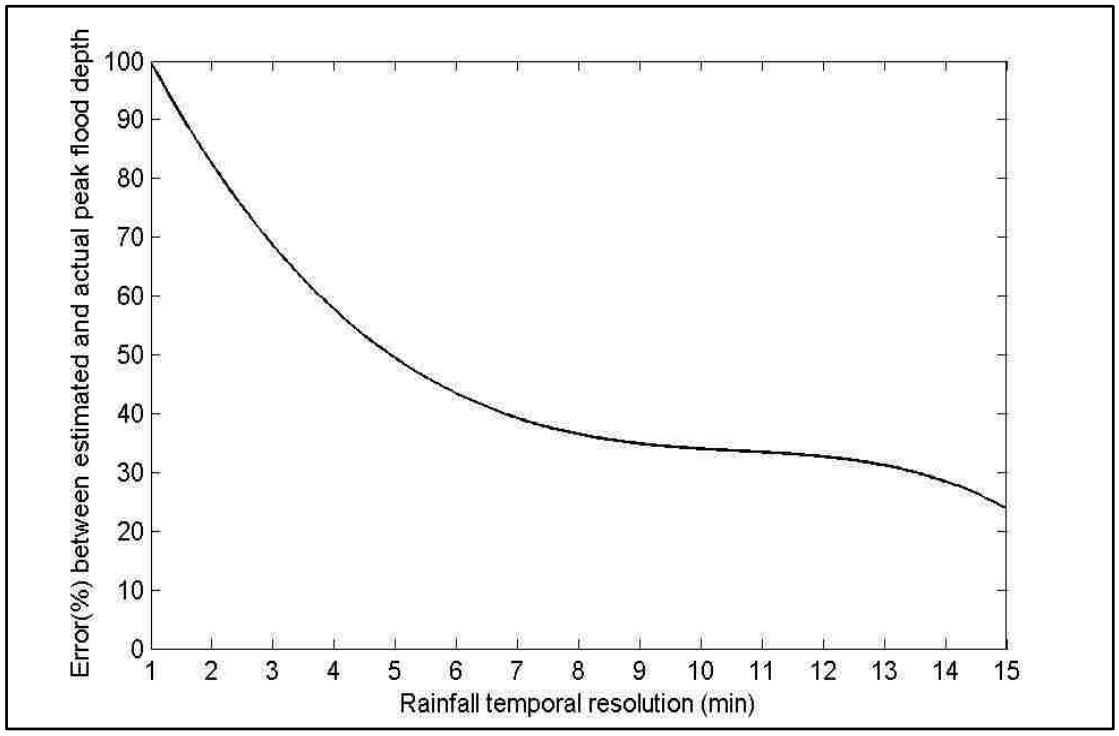

Figure 5.1-21: Calibration and validation against rainfall resolution in Blacklot watershed

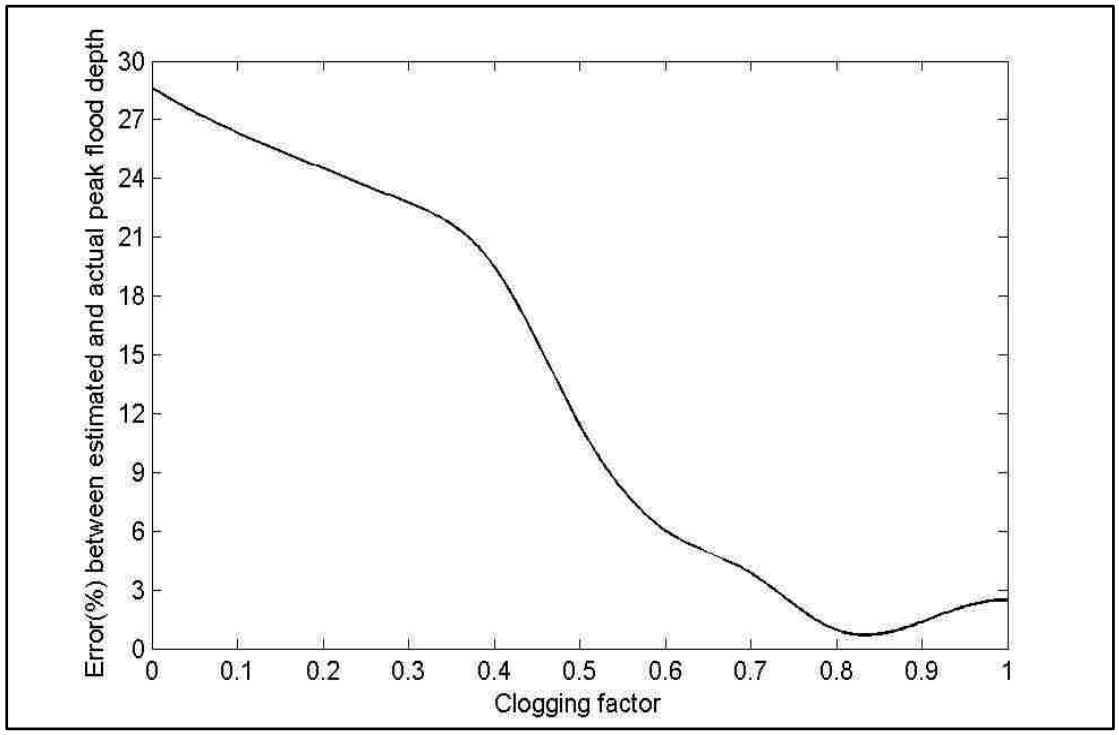

Figure 5.1-22: Calibration and validation against clogging factor in Blacklot watershed

between the actual and calculated peak flood depths against the clogging factor of the drain inlet for 5m DEM and 15 minutes rainfall distribution. It is found that the error is lowest (0.72%) for a clogging factor of 0.83, and the error is largest (29%) when no clogging effect is considered.

Figure 5.1-23 (UNLVRebelYell, 2013), shows couple of inundation points and

Figure 5.1-23: Image used for validation and calibration in Blacklot (RebelYell, 2013)

the peak flood level. The locations of the known flood inundation points (figure 5.1-23) are found as 36° 6' 10.83" N & 115° 8' 38.39" W, 36° 6' 10.43" N & 115° 8' 38.01" W and 36° 6' 10.94" N & 115° 8' 37.47" W through the field visit [See Figure 5.1-24]. All these points are found to be within the inundation extents of 5m DEM. It is reported in UNLV's student newspaper Rebel Yell (2013) that the flooding started around 2 pm, i.e., after 15 minutes of rainfall. It is found that for the 5m DEM flooding started after 20

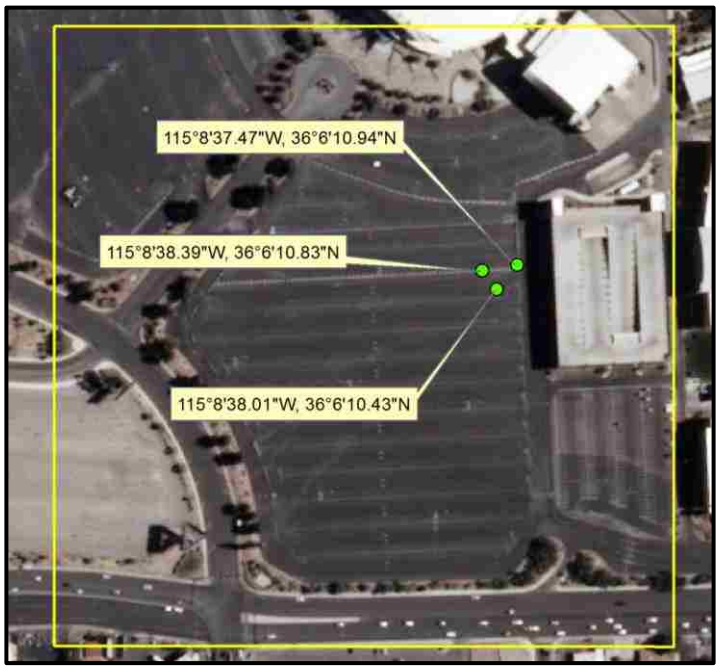

Figure 5.1-24: Geographic location of inundation points at Black parking lot

minutes of rainfall [See figure 5.1-14], which is very close to the approximate actual flooding start time. However, no information is found available about when the flooding ended. Thus, no calibration or validation can be performed against the duration of flooding.

5.1.2. Discussion

This sub-section describes the results of the corresponding components of the developed GIS-framework produced by the testing of the framework in the Black lot study area.

DEM resolution of 5 meters is chosen arbitrarily to start with for testing the GIS-framework. There is no profound basis for choosing this resolution since it is up to the user to choose a resolution to start with for a study area that is not calibrated against DEM resolution. However, this resolution is chosen because the study area is small, and

as well as for smaller resolution like 20m, 30 m or 40 m the details of the study area might be lost in great extent. It is not preferred to start with very high resolution of 1m or 2m since these resolutions may induce unnecessary or redundant details, and hamper the outputs. The higher elevations in the DEM mostly represent the buildings and trees in the area while lower elevations mostly represent the ground. However, a field visit was made to the study area to have a general idea about the elevation in the study area, and to check the accuracy of the DEM. It is noticed that the DEM is showing some abnormal peaks at locations where actually no tall structure is found, and the heights of some trees are misrepresented with the buildings. Bedsides, in the parking area elevations are noticed to fluctuate a lot, while in reality the parking area is found to be relatively flat. It is later discovered that the fluctuations or abnormal elevations originate from the height of existing parking vehicles. It may be because the parking vehicles were there when the LiDAR data were collected. However, the errors or irregularities of the DEM are minimized through reconditioning. The stream network produced by this reconditioned DEM looks fine since the streams are converging to the point near the inlet, i.e., the pour point, where the elevation is lower than the inlet (lowest in the watershed), and thus have higher flow accumulation. However, it is observed that the location of the drain inlet is on a secondary stream line, and an inlet located on a secondary or tertiary streamline is always supposed to produce such a small watershed shown in figure 5.1-3. The curve numbers in the watershed are found as 86 and 95 from the data, but actually the curve number should be higher and uniform throughout the watershed, since it has a single land cover which is uniform throughout the watershed. The curve number for asphalt land cover varies between 97 and 100 with an average of 99 (Pandit and Heck, 2009), and that

results in soil retention value of 0.3 in to 0 in. Therefore, conservatively a curve number of 99 instead of 95 is considered along the watershed's developed with high intensity land cover area, and that results in a soil retention values of 0.1 in throughout the 88% of the total watershed area. However, due to the SCS Curve Number rainfall-runoff equation, it is observed that considerable amount of rainfall might be lost even in a small and impervious watershed like the Blacklot watershed. For example, for the first subevent of the rainfall, the total volume of rainfall in the watershed is 476 m^3, while the total amount of runoff produced by the event is 425 m^3 resulting in 10% of rainfall lost. This is due to the fact that, SCS rainfall-runoff equation considers initial abstraction that includes infiltration, evaporation and other losses, but this is not applicable for a watershed like Blacklot watershed since it is covered with water impenetrable asphalt layer, and no evapotranspiration losses as there is no existence of vegetation in the watershed, and as well as very small evaporation losses are found in such urban watershed (only 0.003% of the total watershed area) (Chen et al., 2009). The slope map of the watershed shows that the watershed has horizontal areas with 0% slope. The elevations of these low lying horizontal grid cells need to be elevated to elevate their slopes, otherwise they would create internal ponding in the area even before the runoff reaches the outlet, and thus, would hamper the final outputs of the model. Therefore, the elevations of these horizontal cells are elevated to elevate their slopes to 0.1% from 0%. The velocity map shows that the cells that higher velocity coefficient and/or higher slope values produce larger velocities. From the travel time map, it is found that the time of concentration of the watershed is 129 minutes. Since there is no previous calibrated watershed available for this study area, this value of time of concentration could not be verified. From the time

area histogram, it is observed that the watershed should produce the highest amount of runoff at 75th minute isochrone, i.e., between 60 minutes and 75 minutes after initial rainfall. This assumption is found to come out as true which is observed in the runoff hydrograph for the first sub-event. This is due to the fact that the watershed area that contains the 75th minute isochrone has a uniform and the highest curve number of 95, which produces uniform and highest amount of runoff. The stage discharge curve is shown for a maximum water depth of 6 inch, and it increases exponentially with the increment in water depth. This is due to the fact that the curb opening height of the Blacklot drain inlet is 6 inch, and as well as flooding or ponding starts as soon as the waters depth crosses the curb opening height. Therefore, it is considered that the maximum allowable water depth for the inlet is 6 inch, and the discharge at this depth is considered to be the threshold discharge for non-flooding. The stage volume curve shows that the volume of the watershed increases exponentially to its depth. The curve is shown for a depth of 1 meter because the maximum flood depth is below 1 meter. This 5m DEM shows the minimum error of 23.92% ≈ 24% of error between the estimated and actual peak flood depth, while the 1m DEM also produces almost the same amount of error of 24.17%. The reason why DEM 5 meter shows the minimum error than the higher resolution of 1 meter completely depends on the GIS default DEM reconditioning processes. It is assumed that higher the resolution is, the more accurate the results are. But it is not found true in this case. For example, 3m DEM produces more error than the 4m DEM by 2.94%, and 7m DEM produces more error than the 10m DEM by 4.11%. The 8m DEM does not even produce flood and thus, results in 100% of error. The interpolated rainfall distributions are found to have opposite impact on the outputs. With

the increasing resolution, the error between the peak flood depths are found to get increased. This is because with the increasing resolution, the original amount of rainfall is distributed into smaller values that do not produce runoff, and thus do not contribute to flooding. For illustration, 1 inch rainfall with a duration of 5 minutes and a soil retention value of 1 produces runoff. But if the rainfall is distributed equally into 1 minute duration the amount would be 0.2 inch per minute, and this amount would not produce runoff for soil retention value of 1 according to the SCS rainfall-runoff equation condition. The clogging factor of 0.83 produces the lowest amount of error, which indicates that the inlet was 83% clogged. This amount does not seem reasonable since the watershed is completely urbanized and contains parking lot. If the inlet was in a garden or in other densely vegetated area this clogging factor would make more sense since in a vegetated area more debris are available than a complete water impenetrable parking lot. Both the clogging factor and the percent error would be lower if any other hydrologic method other than the SCS Curve Number method, like unit hydrograph method would be used for this impermeable watershed. This is because, SCS method introduces huge amount of rainfall losses through its initial abstraction, and thus produces low amount of runoff and consequently, low amount of flooding. However, it can be concluded that the watershed derived from the 5m DEM is the right one for the Blacklot drain inlet, original rainfall should not be interpolated into higher temporal resolution when using SCS Curve Number method, and clogging factor and as well as use of SCS Curve Number method for such an impenetrable watershed as a hydrologic method needs to be investigated for future flood modeling in the Blacklot study area.

5.2. East Mall

This section highlights and describes the important outputs derived from the testing of the developed GIS-framework in the East Mall area of UNLV. The final outputs of the flood model of the GIS-framework along with other important intermediate results are demonstrated in the Results sub-section, while they are elaborately explained in the Discussion sub-section.

5.2.1 Results

This sub-section highlights the results of the corresponding components of the developed GIS-framework produced by the testing of the framework in the East Mall study area.

5.2.1.1. Watershed Delineation

Figure 5.2-1 shows the reconditioned DEM of the East Mall study area. Like the Blacklot study area, we choose a DEM of 5m to start with, and the DEM had identical

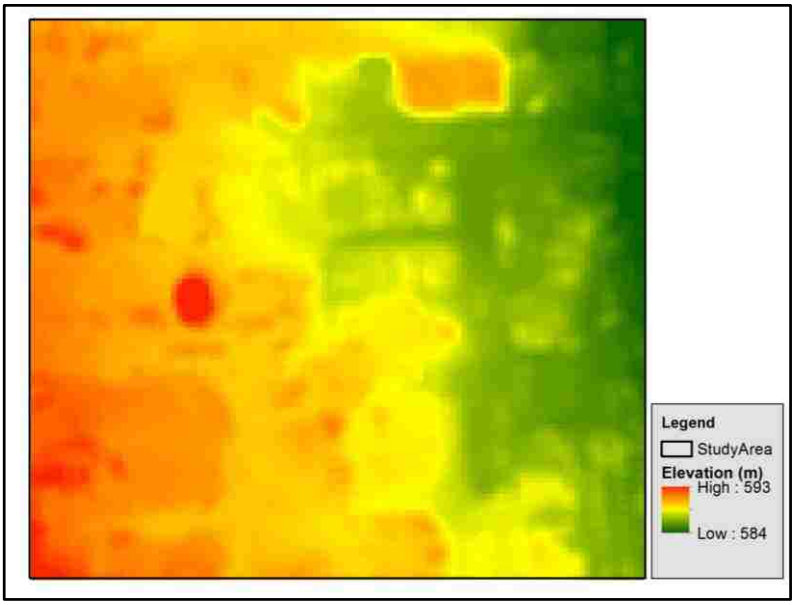

Figure 5.2-1: Reconditioned 5m DEM of the East Mall study area

errors as the Blacklot DEM. The errors were removed through the filtering and filling process to recondition the DEM which is used to delineate watershed for the storm drain inlet in the study area. This 5m reconditioned DEM is found to vary between 584 m and 593 m of elevation. Like the Blacklot, the elevation in the area decreases from west to east, and that suggests runoff in the area flow from west to east where the drain inlet lies. Using this reconditioned DEM, flow direction of the grid cells is delineated that are used to estimate the flow accumulation value of the cells. Using the flow accumulation values, and an accumulation threshold value of 20, the stream network in the study area is created. The delineated watershed for the

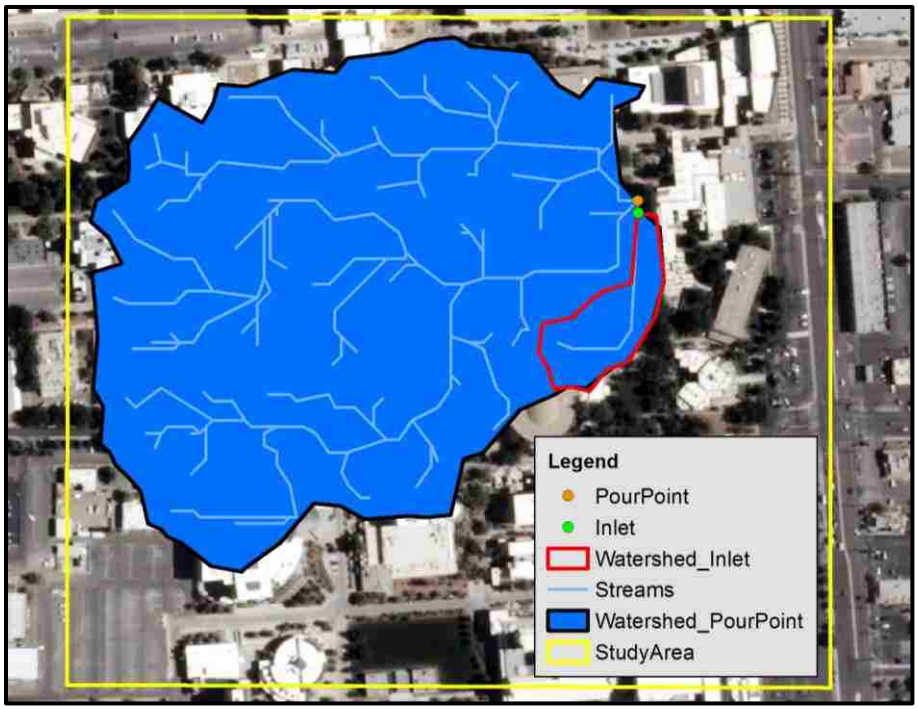

Figure 5.2-2: Delineated watershed for the East Mall area

inlet is shown in figure 5.2-2 along with the stream network in the watershed. Like the Blacklot area, the watershed delineated for the inlet is too small. That is why, Snap Pour Point tool of GIS is utilized to find out the highest flow accumulation cell to the nearest

of the inlet. Snap distance of 15 meters is used to find the new pour point. The delineated watershed for this pour point along with the point is also shown in figure 5.2-2. The area of the watershed is 131143 m^2 (32.42 acres).

5.2.1.2. Rainfall to Runoff Conversion

The soil and land cover data are extracted to the watershed to estimate the curve number for the watershed. The soil group of the watershed is found to be A, and the land covers are Developed with open space, and Developed with high, medium and low intensity. Thus, there exist four curve numbers in the watershed, and they are 49, 66,86 and 95 for Developed with open space, low, medium and high intensity respectively. 2% of the total watershed cells possess a curve number of 49, 24% of them possess a curve number of 66, 48% of them possess a curve number of 86, and the remaining 26% possess 95. The original rainfall data are converted to runoff using equation (4), and the soil retention values are estimated using equation (5), that range from 0.53 to 10.40. The value of 0.53 is considered to be zero like the Blacklot study area. Using equation (4) it is found that the first rainfall event produces runoff that range from 0 in (no runoff) to 0.15 in, for the second one the range varies from 0 in to 0.64 in of runoff, the third one produces 0 in to 0.05 in of runoff, the fourth one produces 0 in to 0.023 in runoff, and the fifth one produces 0 in to 0.12 in of runoff.

5.2.1.3.Runoff to Flow

The runoffs are converted to flow using time area approach. In order to estimate the travel time of the watershed grid cells, a velocity map needs to be produced that requires velocity coefficient (K) and slope values of the cells (in percent) beforehand

according to equation (6). The K map is produced by distributing the K values of 1.2 and 0.48 along

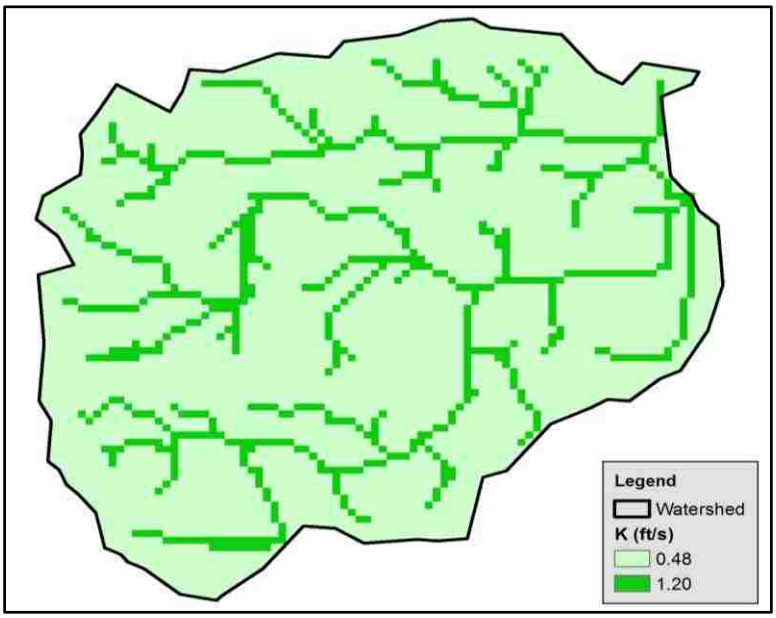

Figure 5.2-3: Velocity coefficient map for the East Mall watershed

the stream and overland flow cells of the watershed respectively [See figure 5.2-3]. The slope map is produced using the watershed DEM as input for Slope tool of GIS. The map

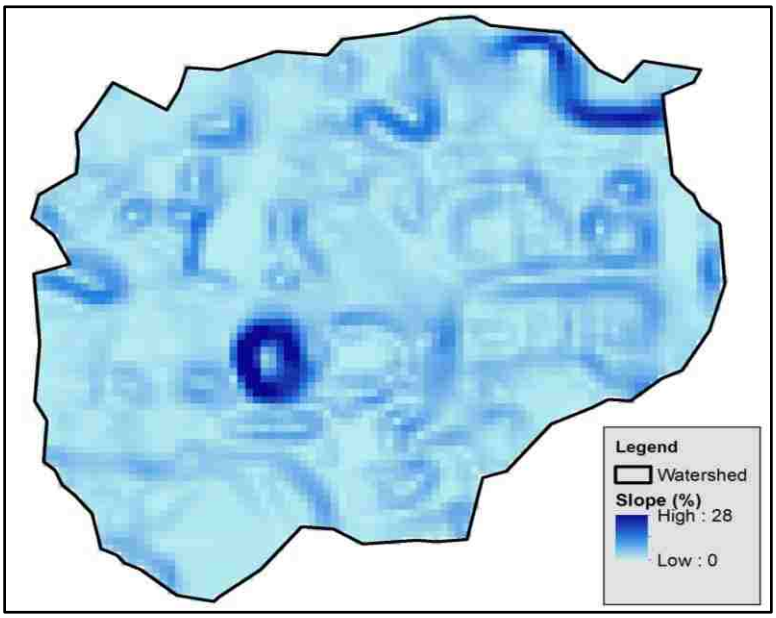

Figure 5.2-4: Slope map of the East Mall watershed

is shown in figure 5.2-4. It shows that the watershed has horizontal areas with 0% slope, and high areas with 19% slope. Using the two intermediate k and slope maps, the velocity map of the watershed is produced that is the velocity map of the watershed is produced, shown in figure 5.2-5. It shows that the lowest velocity the cell possesses is 0.15 m/s, and the highest velocity the cell possesses is 6.36 m/s. A weight map is produced using this velocity map by dividing the resolution of each cell (5 meter) by its corresponding velocity. This intermediate weight map along with the pre-developed flow direction map of the study area as inputs to the Flow Length tool of GIS, travel time for the cells to reach the watershed outlet is estimated. The travel time map is shown in figure 5.2-6. It shows that the longest time the cells take to reach the outlet is 210 minutes, and this implies that the time of concentration of the watershed is 210 minutes. These values of travel times were divided by the duration of rainfall sub-event of 15 minutes to produce isochrones. Thus, there exist 14 isochrones for the watershed, and their contributing areas are estimated to produce time area histogram for the watershed [See Figure 5.2-7].

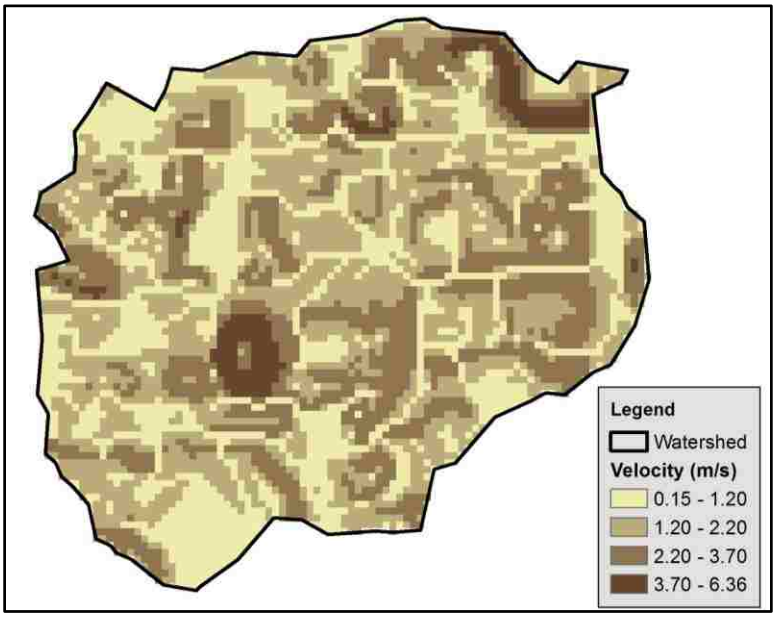

Figure 5.2-5: Velocity map of the East Mall watershed

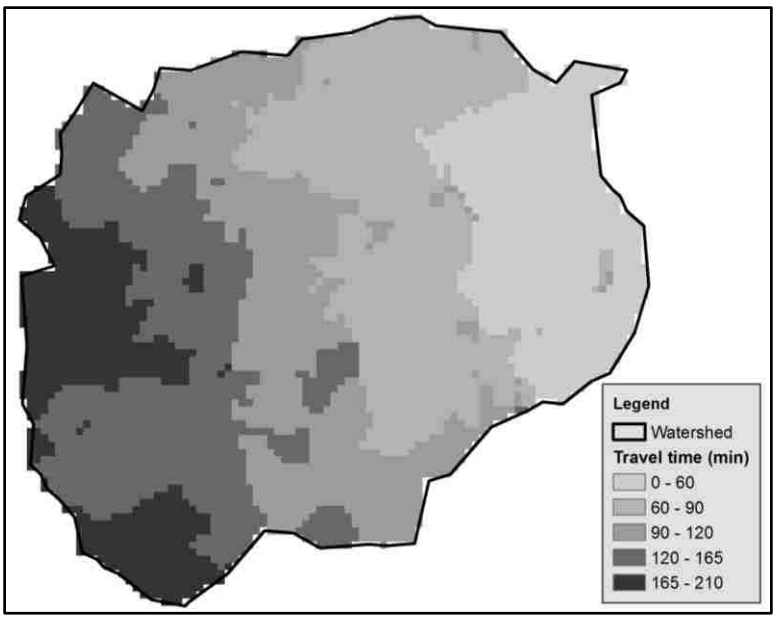

Figure 5.2-6: Travel time map of the East Mall watershed

It is observed that the watershed should produce the highest amount of runoff between 75 minutes and 90 minutes after initial rainfall since the contributing area at 90th minute isochrone, i.e., for the duration of 15 minutes between 75 minutes and 90 minutes is the

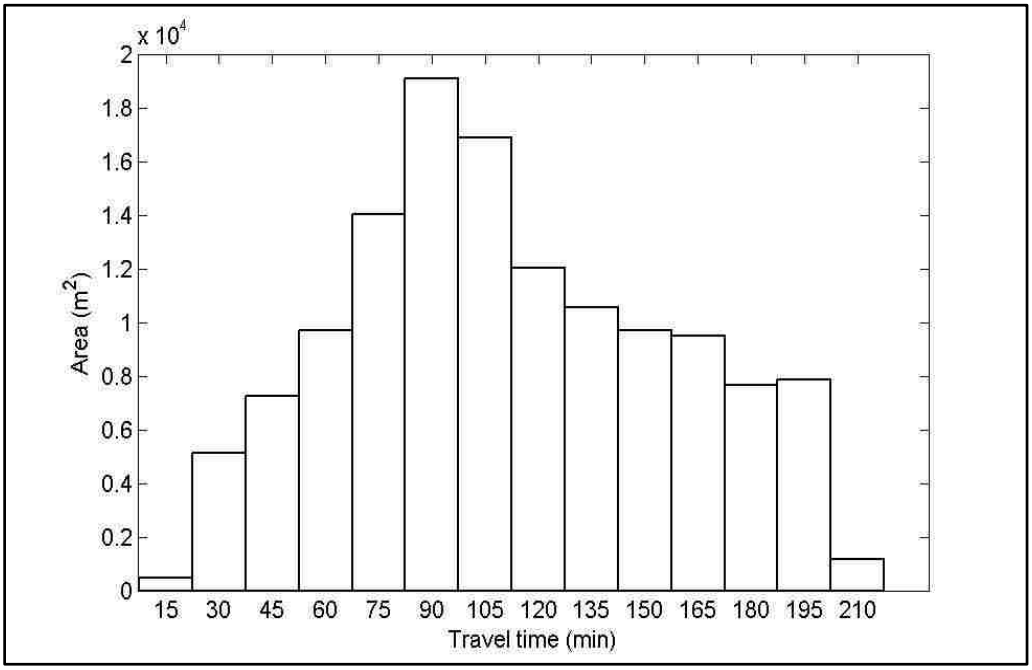

Figure 5.2-7: Time area histogram of the East Mall watershed

largest (1.90 x 10^4 m^2). The areas of this histogram are multiplied by the runoff of the corresponding isochrones produced by each sub-event of rainfall, and results in runoff volume which then divided by the duration of the isochrone to result runoff flow. These runoff flows are plotted against the corresponding time to generate a hydrograph for the sub-event. Figure 5.2-8 shows the runoff hydrograph for the first sub-event. The peak is found 0.06 m^3/s and the time to peak is 112 minutes after the rainfall started. All the

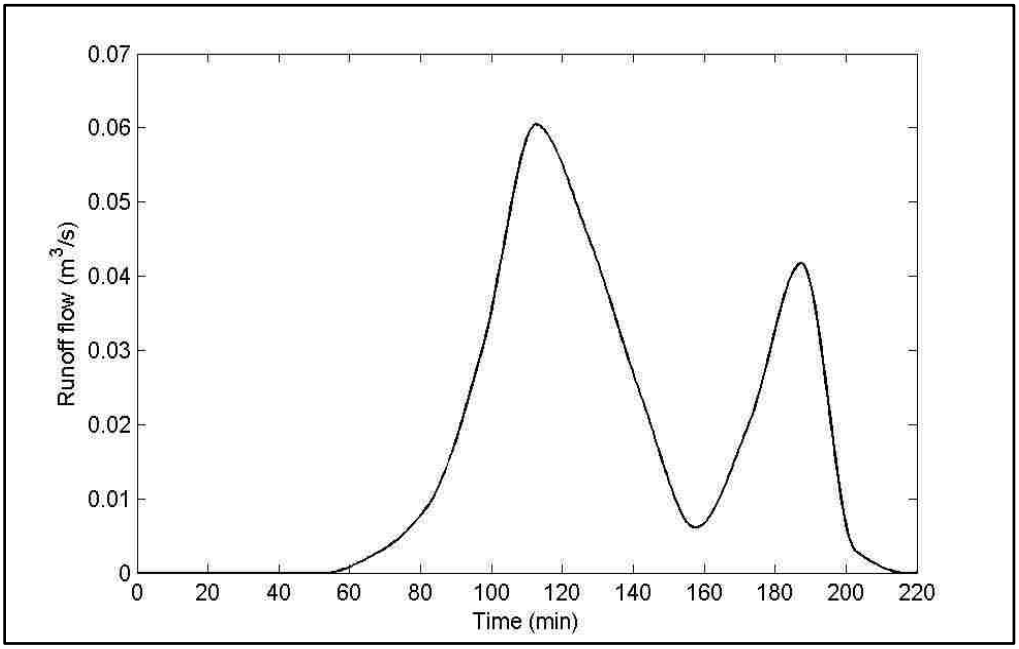

Figure 5.2-8: Runoff hydrograph for the 1st rainfall subevent in East Mall watershed

runoff hydrographs of the rainfall subevents are accumulated and shifted according to their interval to result in final hydrograph [See Figure 5.2-9]. The peak of the hydrograph is found to be 0.99 m^3/s, and the time to peak is found 120 minutes after the rainfall. It is also noticed that the runoff ended after 270 minutes of rainfall.

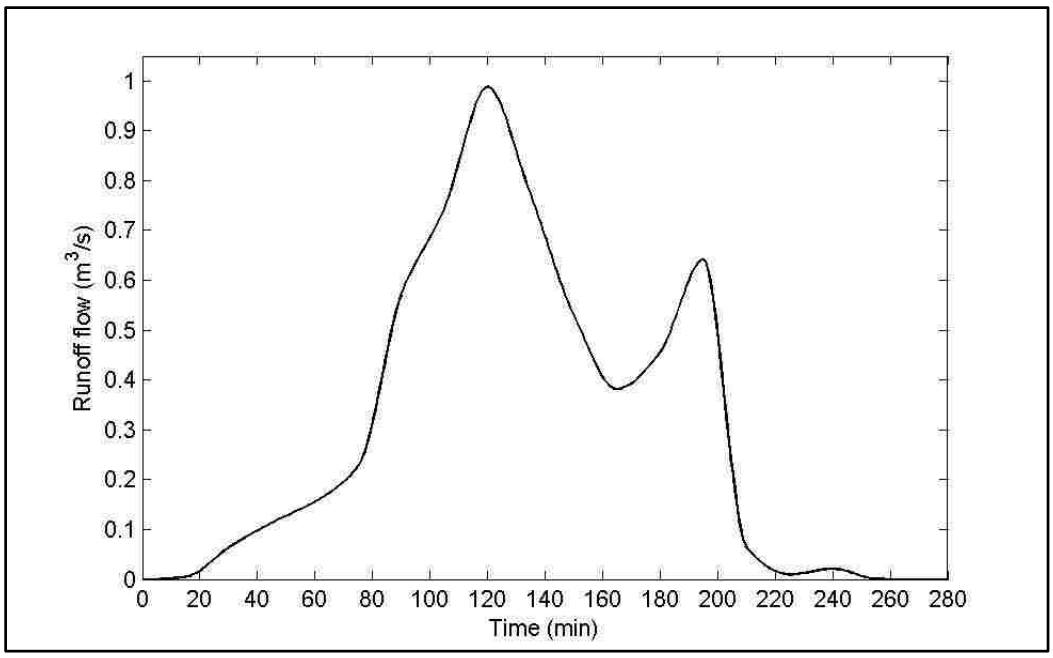

Figure 5.2-9: Final runoff hydrograph for the East Mall watershed

5.2.1.4.Inundation Estimation and Mapping

For inundation estimation, stage discharge curve for the drain inlet is constructed.

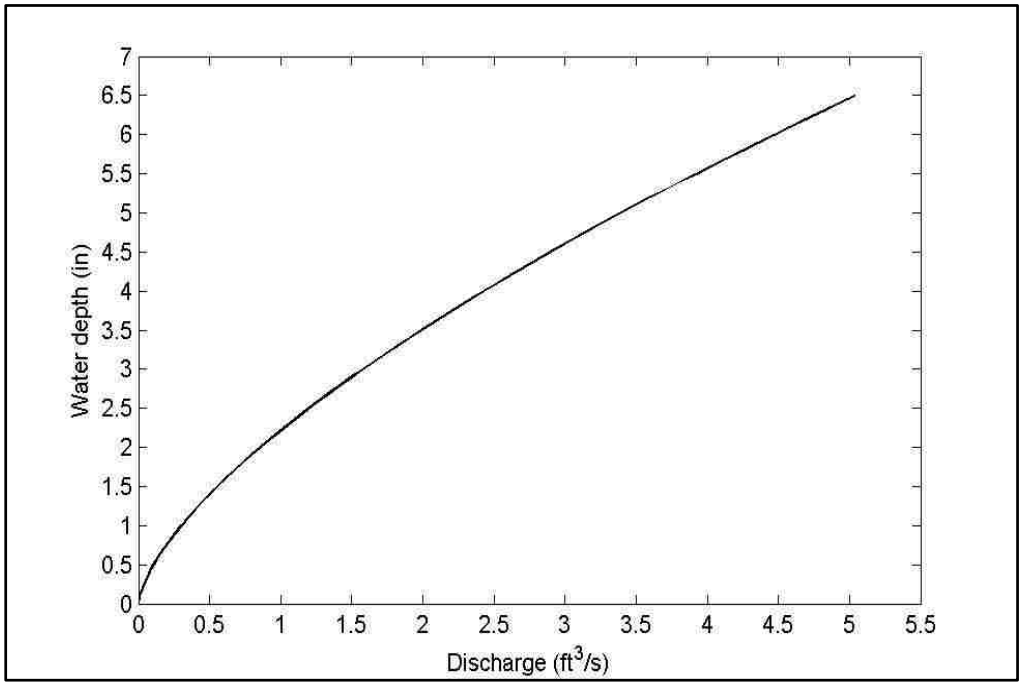

Figure 5.2-10: Stage discharge curve of the East Mall drain inlet

The curve is shown in figure 5.2-10. Equations (15) and (16) are used to find out the interception capacities as weir and orifice flows for the inlet, while equation (12) is used to estimate the interception capacities as mixing flow through the inlet. The values of C_{wc}, and C_o are 0.45 and 0.67, while the values of C_m is 0.93 (Guo et al., 2009). Using equations (10) the capacities for the inlet is estimated. The clogging effect is considered, and equation (17) is used to estimate the clogging factor for the inlet. The value of K for N=1 is 1, and the value of F is 0.1(Urban Storm Drainage Criteria Manual, 2002), and the clogging factor is estimated to be 0.10. Finally, equation (19) is used to estimate the effective discharge capacity of the inlet for water depth (d) of 0 in to 6.5 in. The effective discharge capacity at the maximum allowable water depth of 6.5 inch is found as 4.45 ft^3/s (0.126 m^3/s). This maximum allowable capacity of the inlet is compared to the hydrograph shown in figure 5.2-9 to find out the flooding runoff, i.e., the runoffs that

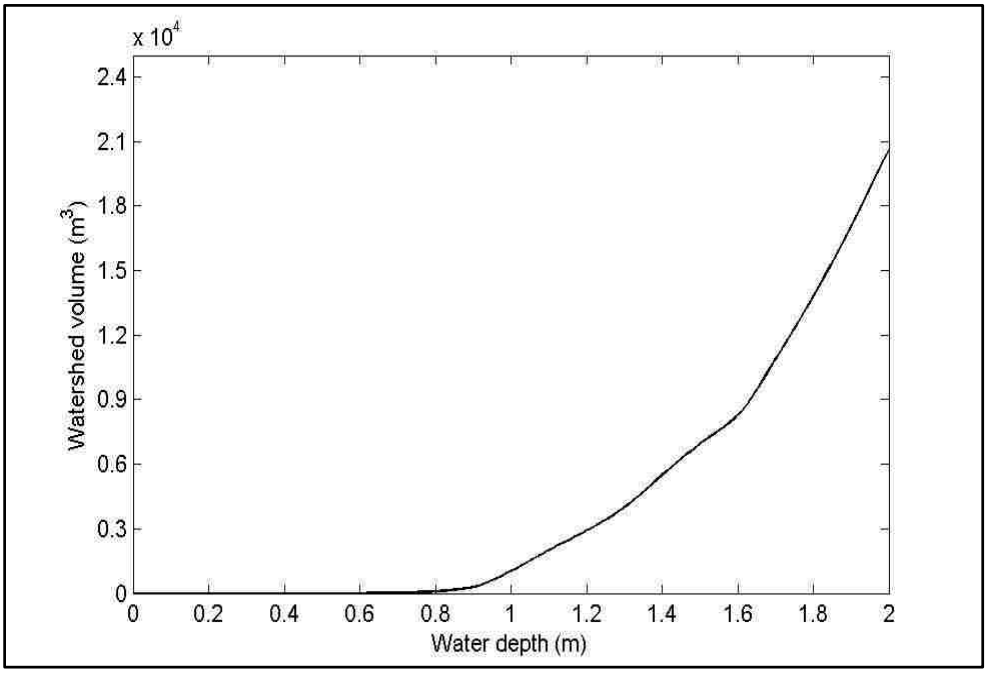

Figure 5.2-11: Stage capacity curve of the East Mall watershed

caused flooding. These runoffs are accumulated, and multiplied by their corresponding times to estimate flood volumes over time, that are compared to the stage capacity curve of the watershed [See figure 5.2-11]. It is found that the watershed can hold a volume of 20000 cubic meters of water for a water depth of 2m. Thus, if the flood or ponding

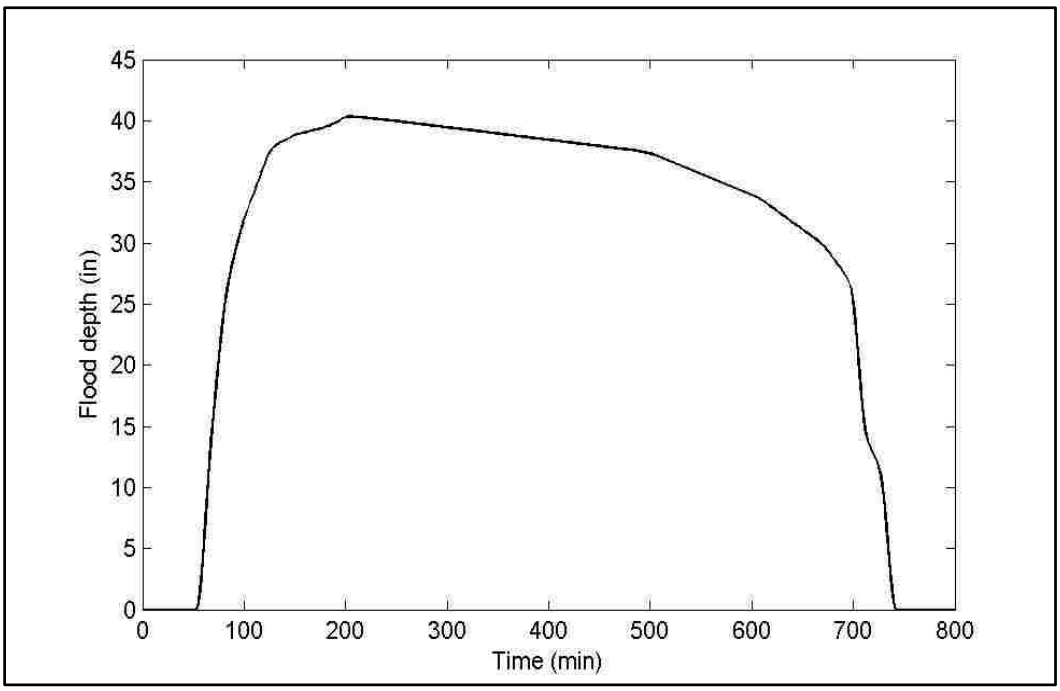

Figure 5.2-12: Flood depth variation over time in East Mall watershed

depth in the watershed is 2m, the corresponding volume will be 20000 cubic meters. Therefore, the estimated flood volumes are compared to the volumes shown in figure 5.2-11, to find out the corresponding depths. The resulting flood depths at various time intervals are shown in figure 5.2-12. It is found that the peak flood depth is 35 inch near the inlet. The peak depth occurred after 187 minutes of rainfall. It is also noticed that the flooding started after 52 minutes of rainfall, and ended after 745 minutes (12.40 hours) of rainfall. Thus, the duration of the flooding was around 11.5 hours. These flood depths were contoured in GIS to produce the inundation extents. Figures 5.2-13 through 5.2-17

show some of the inundation extents at various times in the watershed. From the inundation extents, inundated areas at these times are found using GIS. For example, inundated areas at 60 minutes is found as 6365 m^2, at 187 minutes 14957 m^2 (maximum

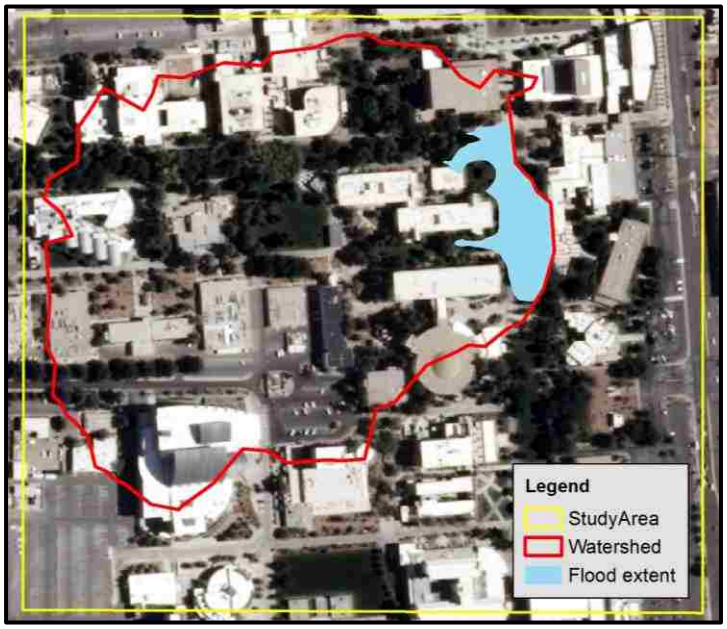

Figure 5.2-13: Inundation extent after 60 minutes of rainfall in East Mall watershed

Figure 5.2-14: Inundation extent after 185 minute of rainfall in East Mall watershed

flooded area), at 480 minutes 13197 m^2 , at 650 minutes 10336 m^2, and 4750 m^2 at 700 minutes respectively.

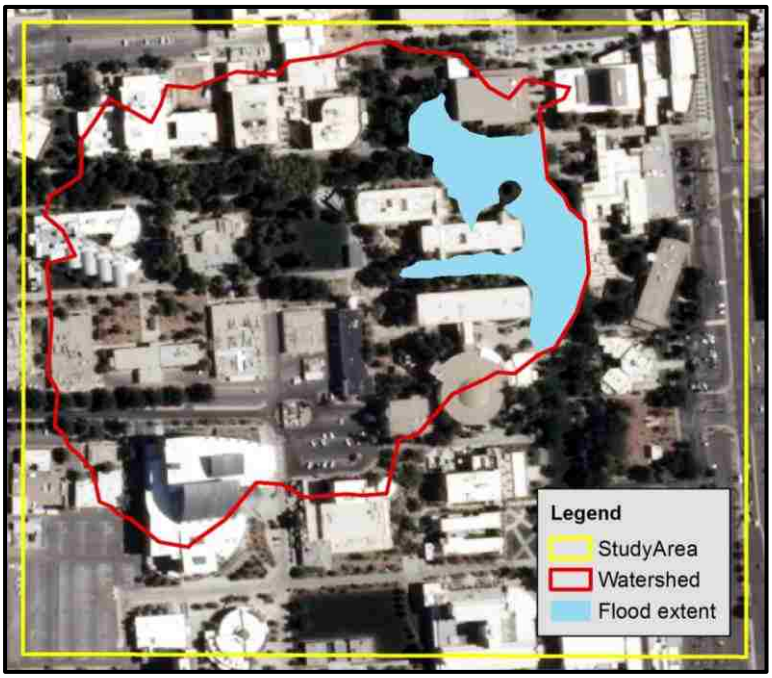

Figure 5.2-15: Inundation extent after 480 minute of rainfall in East Mall watershed

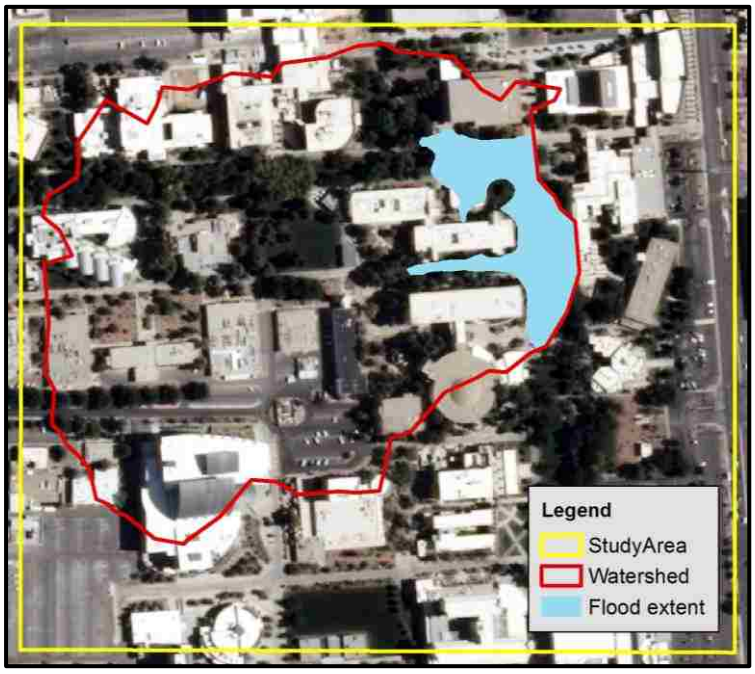

Figure 5.2-16: Inundation extent after 650 minute of rainfall in East Mall watershed

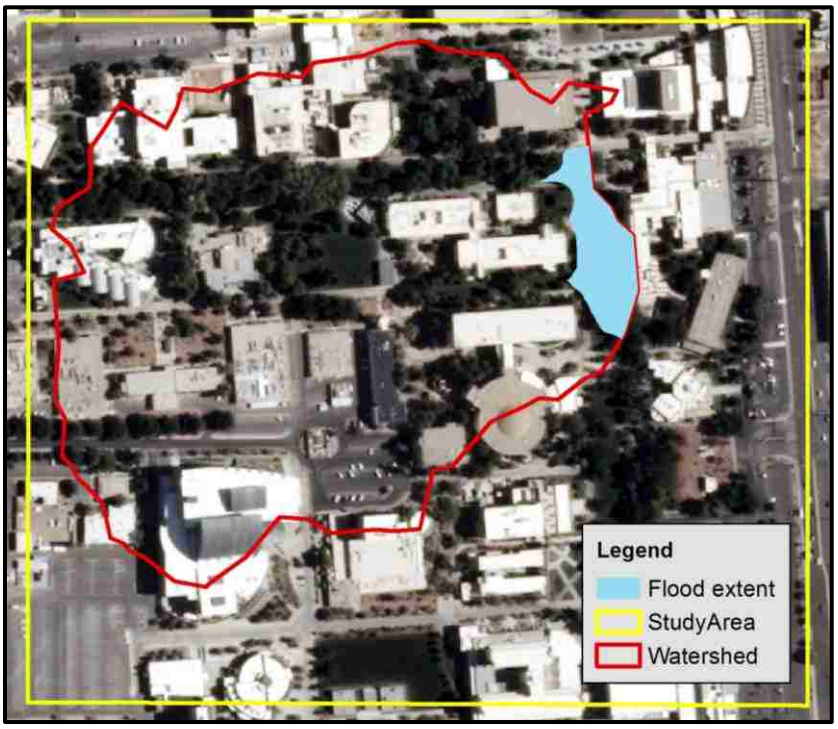

Figure 5.2-17: Inundation extent after 700 minute of rainfall in East Mall watershed

5.2.1.5.Calibration and Validation

The urban flood model of the GIS-framework is run for various DEM resolution of the study area in order to calibrate and validate the model against the DEM resolution. DEM resolutions of 1m to 10m is tested. The observed peak flood depth at and around the inlet is found as 20 inch from the ground. The peak flood depth is estimated for each DEM resolution, and compared to this actual peak depth to estimate errors. Figure 5.2-18 demonstrates the error against the corresponding DEM. It is observed that the DEM 5m produces the highest error of around 100%, and the 1m DEM produces the lowest error of only 5%.

Several flood imageries like figure 5.2-19 are collected and analyzed to calibrate and validate the approach for this study area. It is measured through the field visit that the

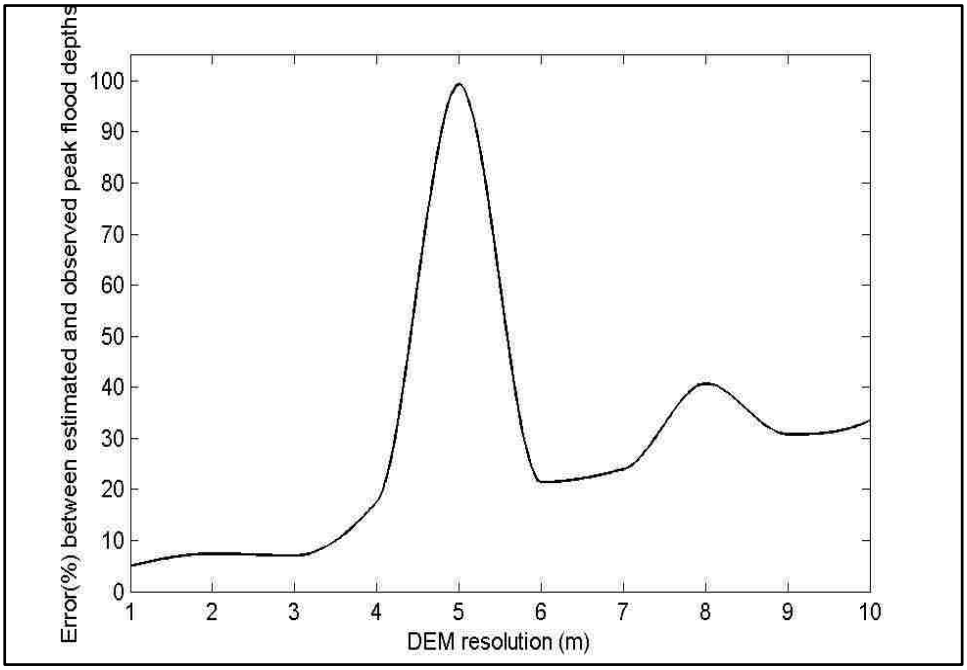

Figure 5.2-18: Calibration against DEM resolution for East Mall watershed

Figure 5.2-19: Image for calibration and validation in East Mall (RebelYell, 2013)

approximate maximum flood depth [See Figure 5.2-19] occurred at the inlet was 14" above the curb opening. Unfortunately, no profound newspaper reports or articles, and reports from flood management authorities on the flood depth, extent and duration are found available.

5.2.2. Discussion

DEM resolution of 5 meters is chosen arbitrarily to start with for testing the GIS-framework in this East Mall study area like the Blacklot study area. Again, there is no profound basis for choosing this resolution since the study area is not calibrated against DEM resolution. However, this resolution is chosen because the study area is small, and as well as for smaller resolution like 20m, 30 m or 40 m the details of the study area might be lost in great extent. It is not preferred to start with very high resolution of 1m or 2m since these resolutions may induce unnecessary or redundant details, and hamper the outputs. The DEM had identical irregularities or errors like the DEM of the Black lot area. However, the errors of the DEM are minimized through reconditioning. The stream network produced by this reconditioned DEM looks fine since the streams are converging to the point near the inlet, i.e., the pour point, where the elevation is lower than the inlet (lowest in the watershed), and thus have higher flow accumulation. However, it is observed that the location of the drain inlet is on a secondary stream line, and an inlet located on a secondary or tertiary streamline is always supposed to produce such a small watershed shown in figure 5.2-2. Due to the SCS Curve Number rainfall-runoff equation, it is observed that considerable amount of rainfall might be lost even in a small watershed like the East Mall watershed. For example, for the first subevent of the rainfall, the total volume of rainfall in the watershed is 800 m^3, while the total amount of runoff produced

by the event is only 380 m^3 resulting in 53% of rainfall lost. This is due to the fact that, SCS rainfall-runoff equation considers initial abstraction that includes infiltration, evaporation and other losses. Since almost 50% of the watershed is covered with vegetation, 53% of losses through infiltration and evapotranspiration might sound reasonable. The slope map of the watershed shows that the watershed has horizontal areas with 0% slope. The elevations of these low lying horizontal grid cells need to be elevated to elevate their slopes, otherwise they would create internal ponding in the area even before the runoff reaches the outlet, and thus, would hamper the final outputs of the model. Therefore, the elevations of these horizontal cells are elevated to elevate their slopes to 0.1% from 0%. The velocity map shows that the cells that higher velocity coefficient and/or higher slope values produce larger velocities. From the travel time map, it is found that the time of concentration of the watershed is 210 minutes. Since there is no previous calibrated watershed available for this study area, this value of time of concentration could not be verified. From the time area histogram, it is observed that the watershed should produce the highest amount of runoff at 90^{th} minute isochrone, i.e., between 75 minutes and 90 minutes after initial rainfall. This assumption is not found to come out as true which is observed in the runoff hydrograph for the first sub-event that the peak of the hydrograph occurs after 112 minutes of rainfall. This is due to the fact that the watershed area that contains the 90^{th} minute isochrone has lower curve number than the isochrone of 120^{th} minute, and thus results in higher soil retention value and consequently, lower amount of runoff. The stage discharge curve is shown for a maximum water depth of 6.5 inch, and it increases exponentially with the increment in water depth. This is due to the fact that the curb opening height of the East Mall drain

inlet is 6.5 inch, and as well as flooding or ponding starts as soon as the waters depth crosses the curb opening height. Therefore, it is considered that the maximum allowable water depth for the inlet is 6.5 inch, and the discharge at this depth is considered to be the threshold discharge for non-flooding. The stage volume curve shows that the volume of the watershed increases exponentially to its depth. The curve is shown for a depth of 2 meter because the estimated maximum flood volume equates to a flood depth of above 1 meter. This 5m DEM shows the maximum error of 99% between the estimated and actual peak flood depth, while the 1m DEM produces the lowest amount of error of only 5%. It is assumed that higher the resolution is, the more accurate the results are. But it is not found true in this case. For example, 2m DEM produces more error than the 3m DEM by 0.40%, and 7m DEM produces more error than the 8m DEM by 16%. Since it is found from the previous case study that by using SCS method interpolated higher rainfall distributions are found to have opposite impact on the outputs, calibration using the rainfall temporal resolution is not performed for this case study area. Besides, calibration against clogging factor is not conducted for this drain inlet, since it is a single curb opening inlet, and there is a recommended value of 0.10 is established. It can be concluded that the watershed derived from the 1m DEM is the right one for the East Mall drain inlet, original rainfall should not be interpolated into higher temporal resolution, and clogging factor of 0.10, and as well as SCS Curve Number method can be used a hydrologic method can be used for future flood modeling in the East Mall study area.

5.3 Sensitivity Analysis

This research only considers the temporal variation of rainfall for flood modling. Spatial variation of rainfall is not considered as calibrating parameter, i.e., only one

rainfall station data is used in this study. However, spatial variation of rainfall can be a vital parameter, and can be very sensitive to the outputs. For example, if there are two rain gage stations, and the total rainfall amount readings for them are 1.5 inches and 2 inches, then the average rainfall would be 1.75 inches, but if only one rainfall gage would be considered it might underestimate or overestimate the rainfall amount for the study site. To show how sensitive this research is to the amount of rainfall, runoff hydrographs and flood depth variation over time plots are produced using the GIS framework for

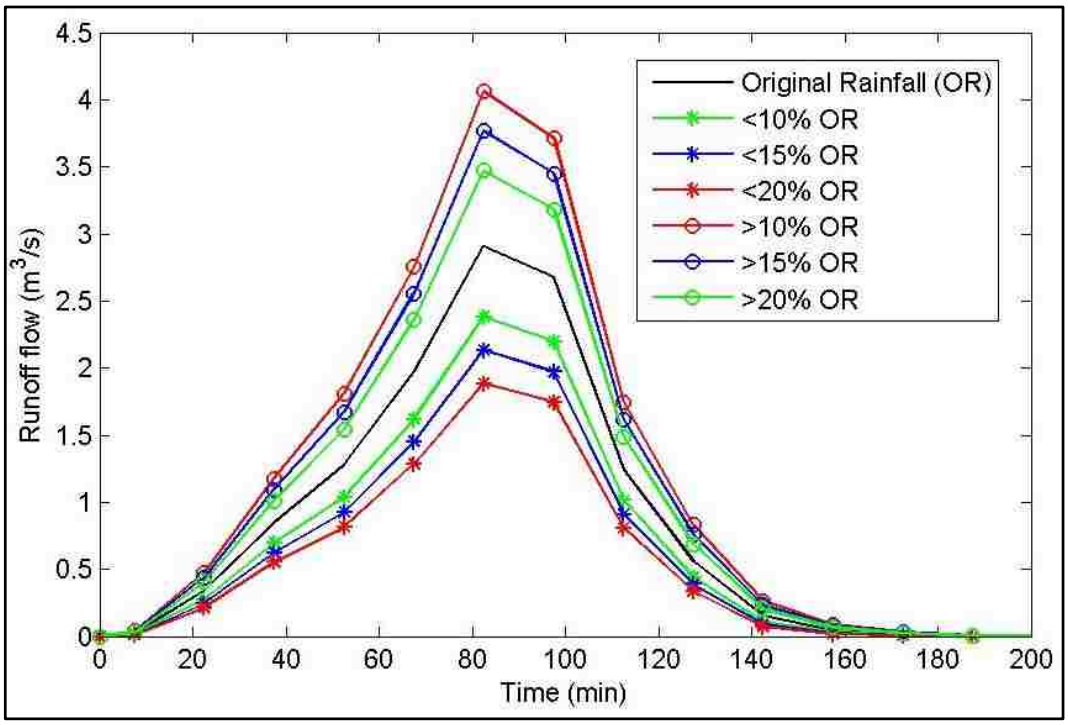

Figure 5.3-1: Runoff sensitivity to the total rainfall

various amount of rainfall where already obtained calibrated DEM, rainfall resolution, and clogging factors are considered as inputs. Blacklot case study site is utilized for this sensitivity analysis. Six rainfall scenarios are considered. They are: i) 10% more in total rainfall than the original total rainfall, ii) 15% more in total rainfall than the original total rainfall, iii) 20% more in total rainfall than the original total rainfall, iv) 10% less in total

rainfall than the original total rainfall, v) 15% less in total rainfall than the original total rainfall, and vi) 20% less in total rainfall than the original total rainfall. Figure 5.3-1 shows how sensitive runoff is to the total amount of rainfall. With the increase in total rainfall, the runoff flow increases, and *vice versa.* Figure 5.3-2 shows the flood sensitivity to the total amount of rainfall. Same pattern like the runoff sensitivity to the rainfall is observed for the flood depths. With the increase in total rainfall, flood depths and duration increase, and *vice versa*. Thus, it can be said if other nearby rainfall stations are

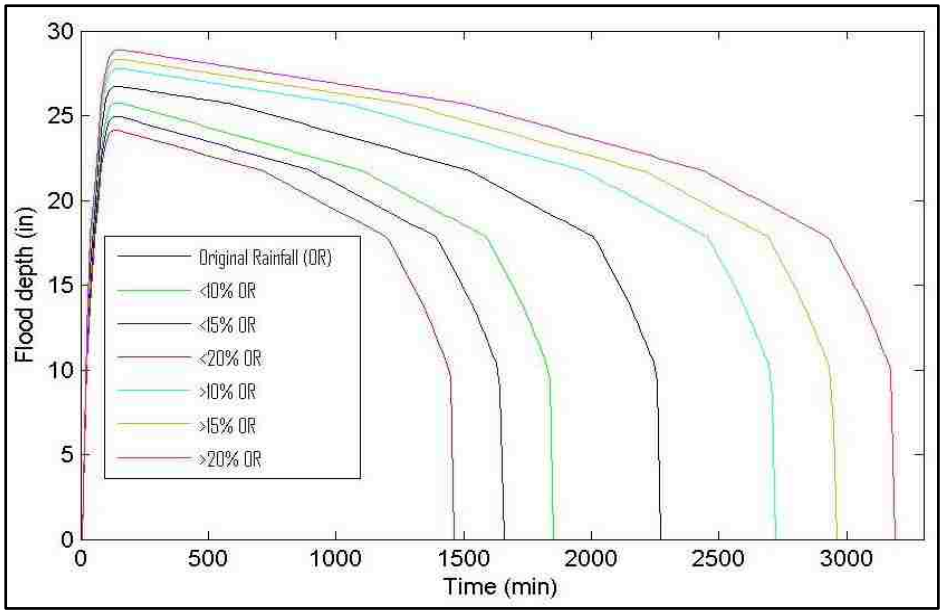

Figure 5.3-2: Flooding sensitivity to the total rainfall

considered that have varying rainfall, the outputs change. That is what exactly observed in this research. To evaluate how sensitive the flood model of the research to the rainfall, the outputs of the model, namely: peak runoff, peak flood depth and flood duration generated for original rainfall event are compared to the ones of rainfall scenarios. For peak flood depth, 4%, 6%, and 7.4% change or increment is observed for >10%, >15% and >20% rainfall while they are 3.7%, 6.6% and 9.6% when the same amount of rainfall are reduced respectively. It can be said that peak flood depth is sensitive to the change in

rainfall. For flood duration, 19%, 30% and 40% of increase is found when the rainfall is increased by 10%, 15% and 20% respectively, and it is decreased by 18.50%, 28% and

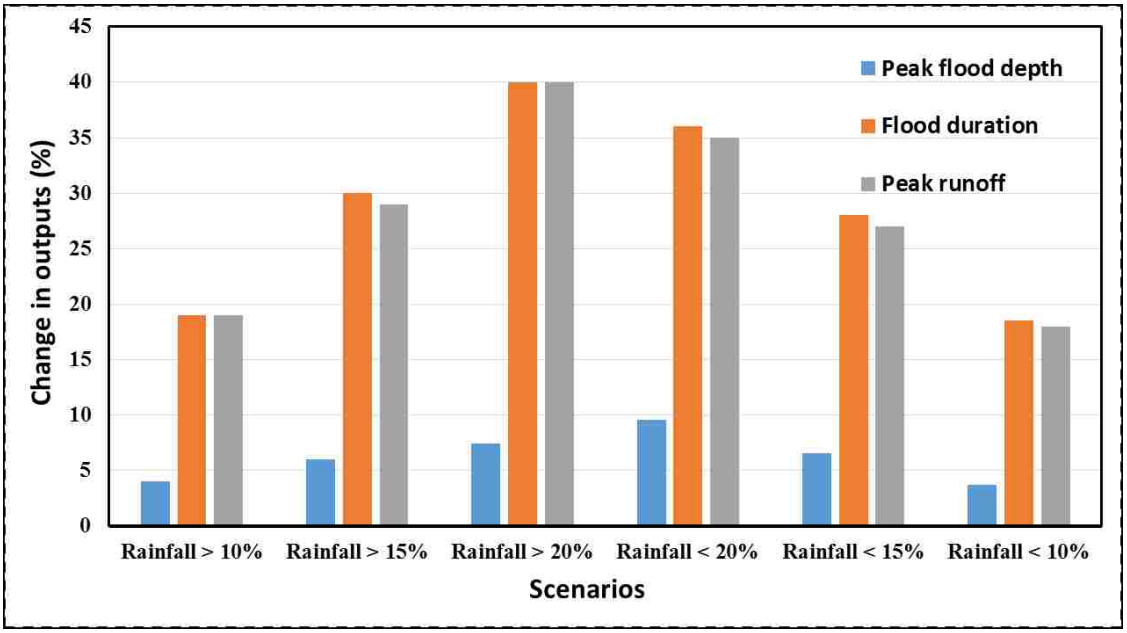

Figure 5.3-3: Sensitivity of peak flood depth, flood duration and peak runoff to rainfall

36% for the decrease in same amount of rainfall respectively. Thus, it can be said that the flood duration is very sensitive to the rainfall. The peak runoff is found to be also very sensitive to the total rainfall. Overall, it can be considered that the model is very sensitive to the total rainfall.

5.4 Summary of Discussion

DEM of 5 meter resolution produces the most representable watershed for the Blacklot drain inlet while DEM of 1 meter resolution produces the most representable watershed for the East Mall drain inlet. Due to the initial abstraction factor, SCS Curve Number method is more suitable for a watershed like East Mall watershed that is covered with vegetation than a watershed like Blacklot watershed that has impenetrable water surface like asphalt and concrete. In case of Blacklot watershed, unit hydrograph method

might produce better results. Obtaining high temporal resolution of rainfall through data interpolation does not produce meaningful results when using SCS Curve Number method. It is assumed that when the water depth reaches the curb opening of the inlet, the discharge does not change afterwards. But in real situation, the discharge increases with the increase in water depth. Results might be more accurate if this condition would be considered. Clogging factor of 0.10 is found considerable for the drain inlet of the East Mall area, and this value may be used for future flood modeling in the area. However, clogging factor of 0.83 for Blacklot study area inlet should be investigated. The sensitivity analysis show that the flood model inside the GIS framework is sensitive to the total amount of rainfall that can be attributed to the spatial variability of rainfall.

CHAPTER 6: RELATING THE WATERSHED'S HYDROLOGIC RESPONSE TO THE LAND COVER CHANGE

6.1 Introduction

Urban flooding is a common problem in cities around the globe due to the dominance of impervious surface and lack of sufficient drainage. Urban floods create hazardous situations by affecting daily life of people, disrupting utility services, and damaging property. In an urban area, parking lot watersheds like Blacklot watershed are vulnerable to flooding because of the existence of excessive impermeable surfaces, and often underperforming drains. Therefore, retrofitting an urban parking watershed is often necessary to modify the hydrologic response of the area to reduce or prevent flooding. Typically, land cover alteration is done to modify parking watershed's hydrograph, which is primarily lowering and delaying the peak discharge. In this research, we aim to estimate the variation in hydrologic response when a parking lot watershed like the Blacklot watershed is retrofitted with flood-reducing surfaces like pervious porous asphalt, grass pavers, concrete grid pavers etc.

6.2 Research Approach and Methodology

This section contains the following two sub-sections: i) Research approach and ii) Methodology that talk about the approach to conduct the research, and detail about the approach with methods respectively.

6.2.1 Research Approach

To relate the watershed's hydrologic response to the change in land cover in the

watershed, the land cover type of the watershed is changed to various other land covers. The same GIS-based approach that is used to develop the GIS-framework for the original land cover to estimate flood depths and inundated areas, is also utilized for estimating flood depths and inundated areas for other land covers. The only exceptions to the approach for achieving this objective are that urban watershed needs not to be delineated, stage discharge curve for the inlet needs not to be constructed, and calibration and

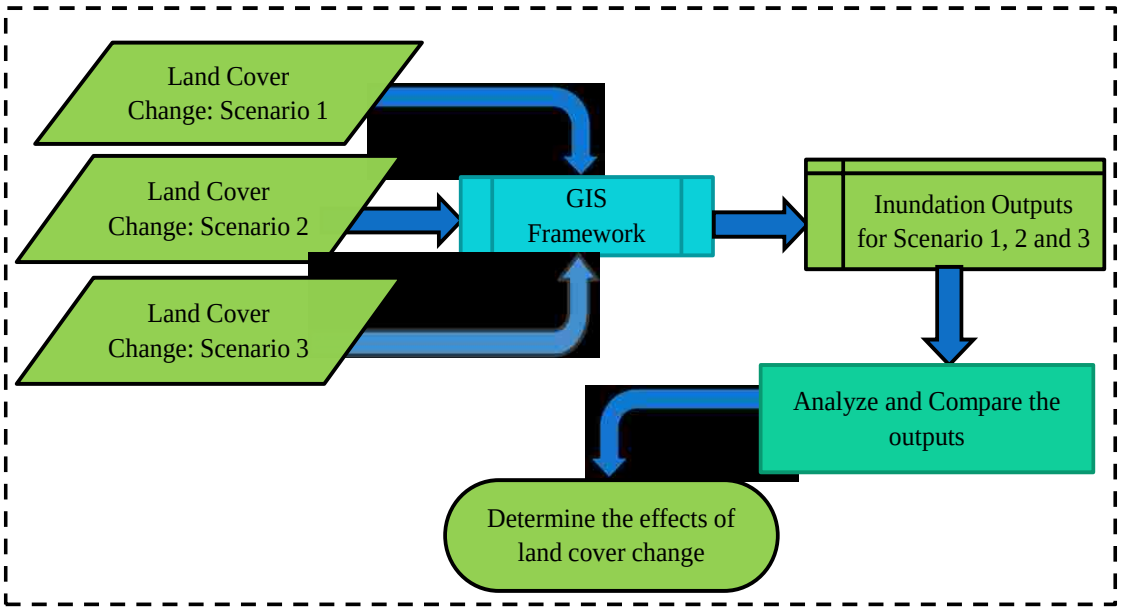

Figure 6.2-1: Flowchart of research methodology for determining impacts of land cover change on flooding

validation is not needed since these tasks are already done for the watershed of interest, and its indigenous land cover. However, the outputs, that are the flood depths, areas, durations along with the runoff hydrograph for each land cover are analyzed, and compared to the same outputs of the original land cover. These outputs are chosen to compare since they closely reflect the hydrologic response of a watershed against flooding when there is a change in land cover. Finally, analyses are made for several iterations of combining the land covers to find out the optimal land cover for avoiding

floods. Figure 6.2-1 shows the research approach to ascertain the impacts of land cover change on the watershed behavior in simplistic way.

6.2.2 Methodology

Five scenarios are run to ascertain the effects of land cover change in a watershed. All the land cover change analyses are conducted on the watershed of Black parking lot study area. The scenarios are:

i) porous asphalt by replacing the existing land cover of the watershed

ii) gravel pavers along the main streamlines of the watershed;

iii) grass pavers along the main streamlines of the watershed;

iv) grass paver along the parking space aisles along with the porous asphalt; and

v) concrete grid pavers (CGP) throughout the watershed

Table 6.2-1: Area coverage and curve numbers for land covers

Land Cover Scenarios	Area Covered (%)	Curve Number
Porous asphalt	100	88
Gravel swale strip	5	76
Grass swale strip	5	68
Grass pavers	25	68
Concrete grid pavers	100	77.50

These land covers, i.e., porous asphalt, gravel and grass pavers, and concrete pavers are chosen because they are found to be used in the parking lot as pervious pavement system material in order to reduce runoff (Hunt and Collins, 2008). Gravel and grass paver along the main flowpath lines of the watershed are chosen conservatively. The main difference

in using the flood model built in the GIS-framework between the original land cover and the new land cover scenarios are the changes in curve number due to changes in land covers. Thus, among the intermediate outputs of the framework's flood model only the soil retention maps differ from the original soil retention map, and consequently the runoff maps that result in different hydrographs to produce different time series of inundation. Porous or pervious asphalt helps in minimizing the runoff by reducing the surface imperviousness. The curve number for such land cover in the Black parking lot watershed is found 88 (Pandit and Heck, 2009), which is significantly lower than the existing curve numbers of 99 (impervious asphalt) in the area. For a lower curve number, the capacity of underlying soil cover to hold the water increases which results in lower amount of runoff, and consequently lower amount of flooding. Thus, it is assumed that the watershed in the area will behave better in favor of reducing flood than the original land cover if the land cover in the watershed is changed to porous asphalt. Therefore, based on this hypothesis the existing impervious land cover of the watershed with pervious asphalt is considered. Runoff hydrograph is constructed, and time series of inundation for this land cover is estimated, i.e., for a curve number of 88.

A land cover made of gravel is considered as a good alternative land cover to reduce flooding in a highly dense impervious area like the Black parking lot since gravels have lower curve number than impervious materials. However, they may hamper the parking activities since their surfaces are not as smooth as other recognized land covers for parking like asphalt and concrete. The interruption gets bigger with the higher amount of gravel and vice versa. Therefore, the amount of gravel land cover in a parking area should be estimated carefully, and in this sense, a swale like strip filled with gravel built

along the main stream lines or flow paths in the watershed can act as an optimum land cover to reduce flooding. To accomplish this, the stream network for the watershed is created by extracting the pre-generated stream network grid of the study area to the watershed boundary. From the stream network, the main streamlines are determined. A main streamline is a primary streamline where the secondary streamlines are connected.

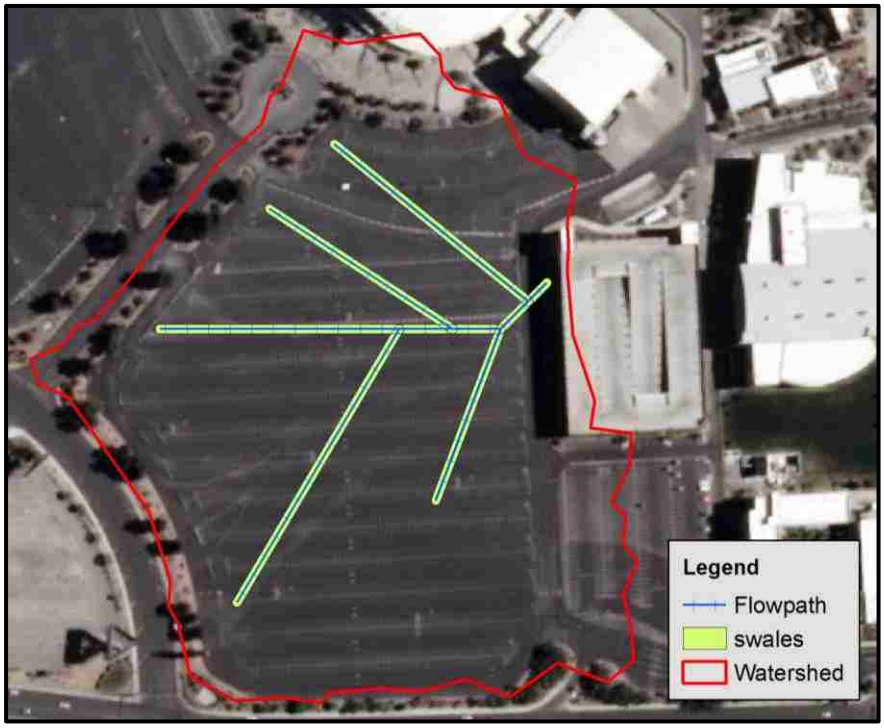

Figure 6.2-2: Schematic map of gravel and grass swale strip along main flowpath

The length and width of the swale strip are determined based on the criterion that the total surface area of the swale should be at least one percent of the watershed area (Swales, 1999). Since the curve number for a surface made of gravel, and for underlying soil hydrologic group of A is 76 (Cronshey, 1986), a curve number of 76 is distributed along the gravel swale strip. It is assumed that the swale strip is rectangular in shape, and its hydrograph is constructed, and time series of inundation for this land cover is estimated,

i.e., for a combination of curve number of 76 and the remaining current curve numbers of the watershed. Figure 6.2-2 shows the schematic map for the swale strip filled with gravel pavers. Like a gravel swale strip, a grass swale strip constructed along the main flow path lines of a watershed can be considered as an excellent alternative land cover to reduce flooding in the watershed. Again, it is due to the fact that the grass has low curve

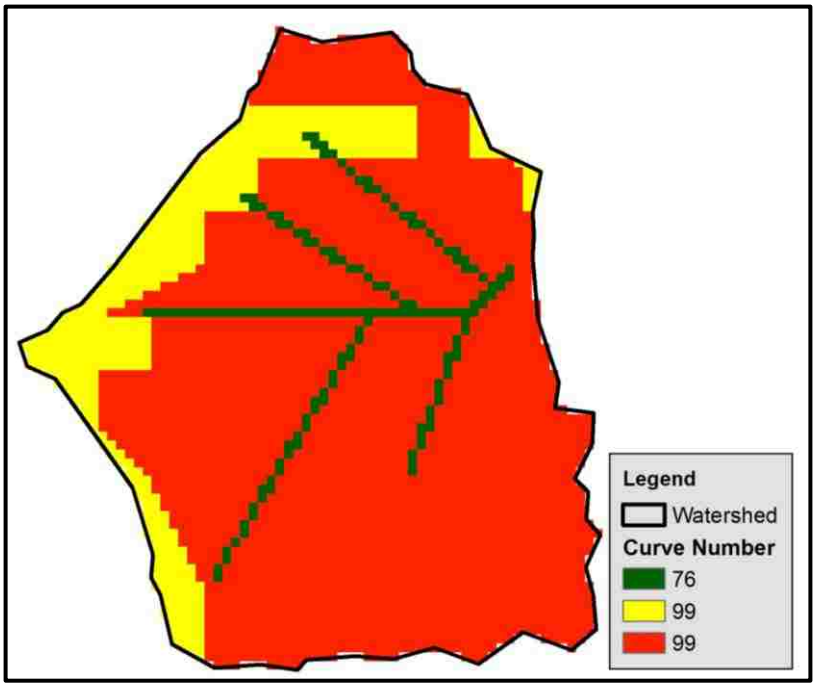

Figure 6.2-3: Curve number distribution map for gravel and grass swale strips

number. The size and shape of this grass swale strip is considered to be same as the gravel swale strip. However, in case of a grass swale, it should be considered that the height of the grass used should be more than the depth of the storm runoff to treat runoff efficiently (Swales, 1999). Since, the highest amount of rainfall is 0.75 inch, the grass height of the swale is 1 inch is considered. For this grass, and for underlying soil group of A, the curve number is found 68 (Cronshey, 1986) which is distributed along the grass

swale. Runoff hydrograph is constructed, and time series of inundation for this land cover is estimated, i.e., for a combination of curve number of 68 and the remaining current curve numbers of the watershed. Figure 6.2-2 shows the schematic map for the swale strip filled with grass pavers that is same as for gravel pavers. Figure 6.2-3 shows the curve number distribution map for both the gravel swale strip which is also identical to

Figure 6.2-4: Schematic presentation of parking aisle filled with grass pavers

the grass swale strip. The fourth type of land cover that is applied is the parking space aisles of the watershed covered with grass pavers, and the remaining part is covered by the porous asphalt. Figure 6.2-4 shows the schematic presentation of this land cover type. A curve number of 68 is distributed along the parking aisle patches, and 88 is distributed along the remaining porous asphalt layer. The last type of land cover treatment applied is the concrete grid pavers (CGP) throughout the whole watershed. A curve number of 77.5 is distributed throughout the whole watershed for this land cover type (Hunt and Collins, 2008).

6.3 Results

This section highlights the findings of the analyses of changing land covers in the Blacklot watershed.

6.3.1 Porous Asphalt Pavement

Figure 6.3-1 shows the runoff hydrograph developed for the porous asphalt

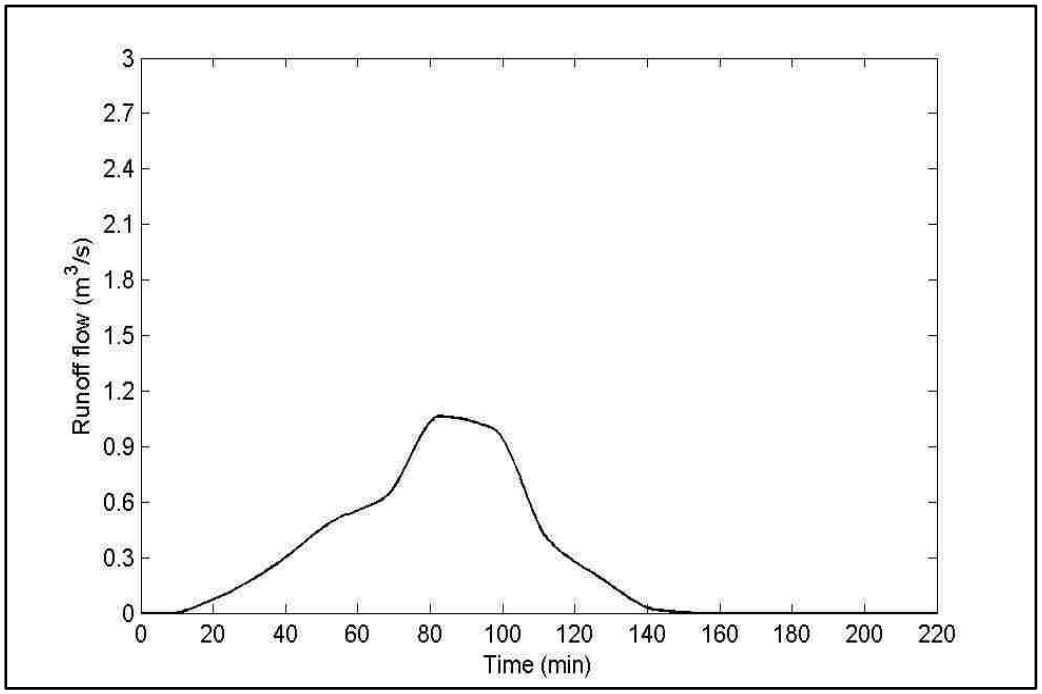

Figure 6.3-1: Runoff hydrograph for the porous asphalt land cover

pavement land cover. The peak of the hydrograph is 1.10 m^3/s and the time to peak is after 82 minutes of rainfall. The runoff ended after 142 minutes of rainfall. The peak is reduced by 62% from the peak of 2.91 m^3/s of the original impervious asphalt land cover. The duration of the runoff is also reduced by 27%. Figure 6.3-2 shows the flood depth variation over time for this land cover treatment. The peak flood depth is 19 inch, and the time to peak is after 97 minutes of rainfall. The flooding starts after 37 minutes of

rainfall, and ends after 232 minutes of rainfall resulting in a flood duration of 195 minutes (3.25 hours). Thus, the peak depth is reduced by 26%, and the duration of flooding is reduced by 63% from the original impervious asphalt land cover. The maximum inundated area for this land cover treatment is shown in figure 6.3-3. The estimated area is 14325 m^2 (18% of the total watershed area). The inundated area is also reduced by 3500 m^2 (5%).

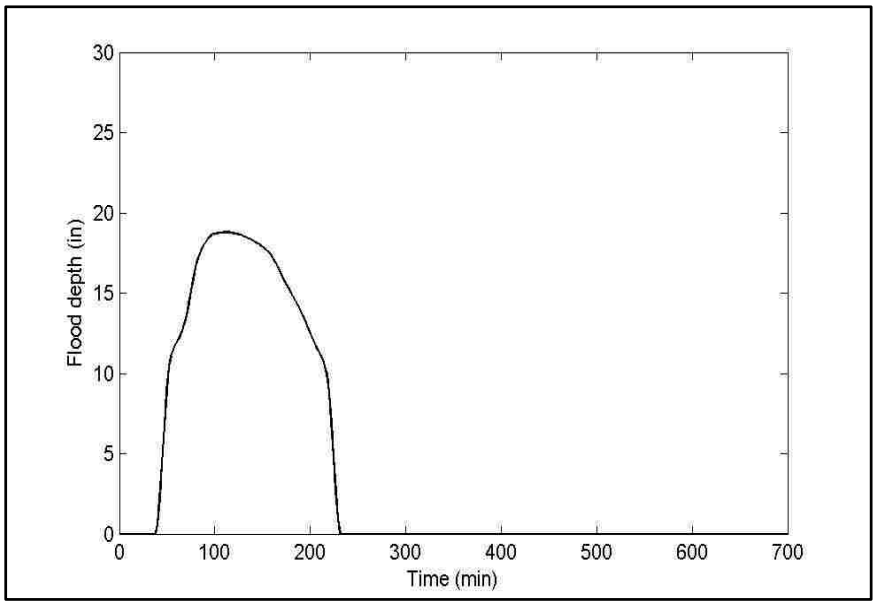

Figure 6.3-2: Flood depth variation over time for porous asphalt land cover

Figure 6.3-3: Peak inundation extent for the porous asphalt land cover

6.3.2 Gravel Swale Strip

Figure 6.3-4 shows the runoff hydrograph developed for the gravel swale strip constructed along the main flowpath lines of the watershed. The peak of the hydrograph is 2.64 m^3/s and the time to peak is after 82 minutes of rainfall. The runoff ended after 203 minutes of rainfall. The peak is reduced by only 10% from the peak of 2.91 m^3/s of the original impervious asphalt land cover. The duration of the runoff is not reduced at all. Figure 6.3-5 shows flood depth variation over time for this land cover treatment. The peak flood depth is 25.24 inch, and the time to peak is after 127 minutes of rainfall. The flooding starts after 22 minutes of rainfall, and ends after 542 minutes of rainfall resulting

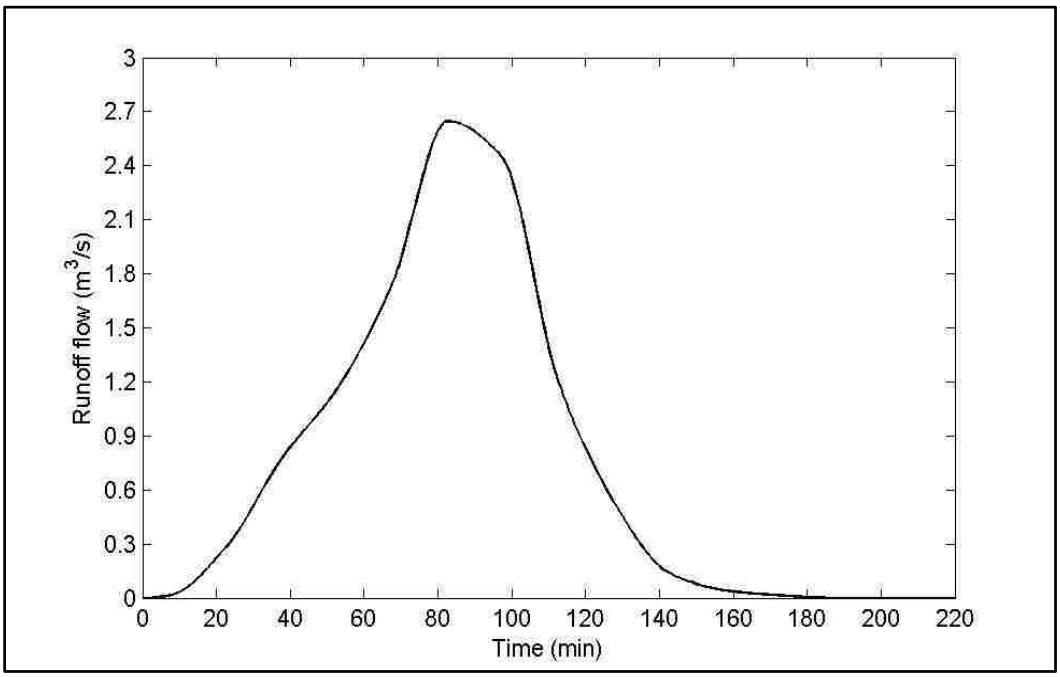

Figure 6.3-4: Runoff hydrograph for the gravel swale strip

in a flood duration of 520 minutes (8.5 hours). Thus, the peak depth is reduced by 2.90%, and the duration of flooding is reduced by only 11% from the original impervious asphalt

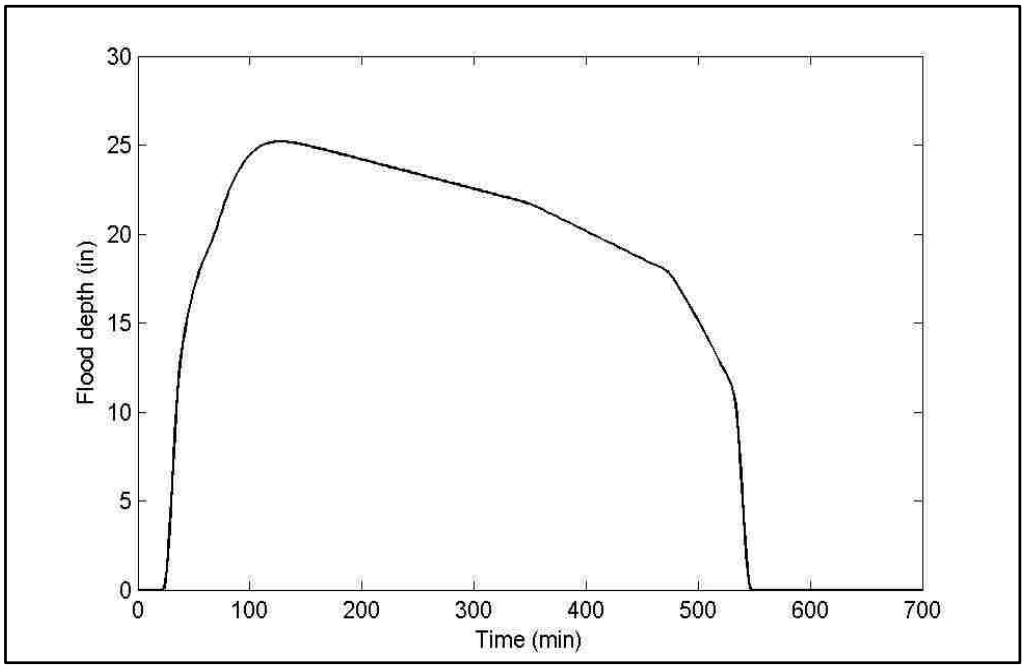

Figure 6.3-5: Flood depth variation over time for gravel swale strip

land cover. The maximum inundated area for this land cover treatment is shown in figure 6.3-6. The estimated area is 17435 m^2 (22% of the total watershed area). The peak inundated area is also reduced by 400 m^2 (0.50%).

Figure 6.3-6: Peak inundation extent for gravel swale strip

6.3.3 Grass Swale Strip

Figure 6.3-7 shows the runoff hydrograph developed for the grass swale strip constructed along the main flowpath lines of the watershed. The peak of the hydrograph is 2.64 m^3/s and the time to peak is after 82 minutes of rainfall. The runoff ended after 187 minutes of rainfall. The peak is reduced by only 10% from the peak of 2.91 m^3/s of the original impervious asphalt land cover. The duration of the runoff is reduced by 8%. Figure 6.3-8 shows the flood depth variation over time for this land cover treatment. The peak flood depth is 25.24 inch, and the time to peak is after 112 minutes of rainfall. The flooding starts after 22 minutes of rainfall, and ends after 542 minutes of rainfall resulting

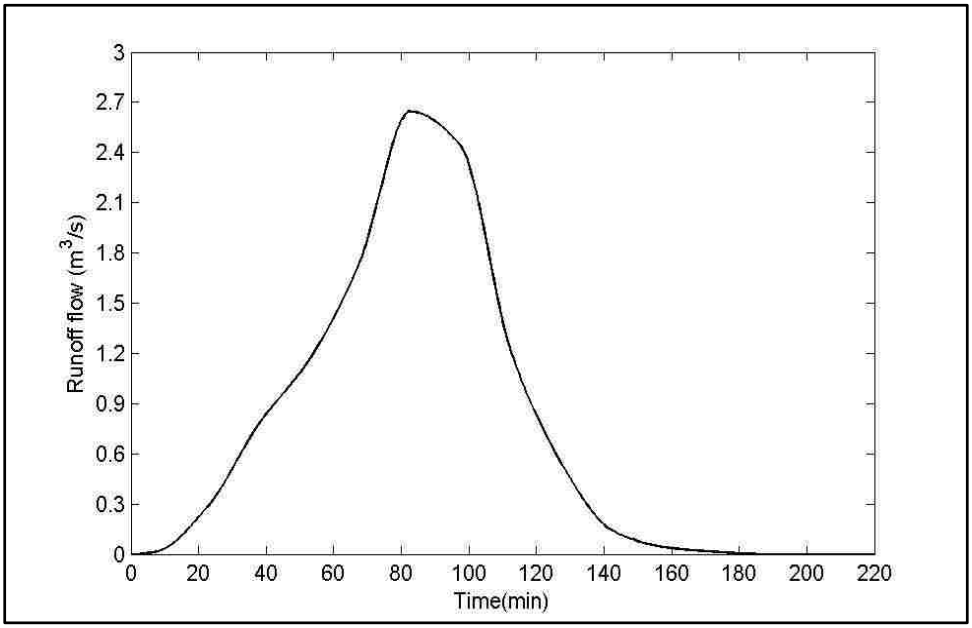

Figure 6.3-7: Runoff hydrograph for the grass swale strip

in a flood duration of 510 minutes (8.5 hours). Thus, the peak depth is reduced by 2.90%, and the duration of flooding is reduced by only 11% from the original impervious asphalt land cover. The maximum inundated area for this land cover treatment is shown in figure

6.3-9. The estimated area is 17435 m^2 (22% of the total watershed area). The peak inundated area is also reduced by 400 m^2 (0.50%).

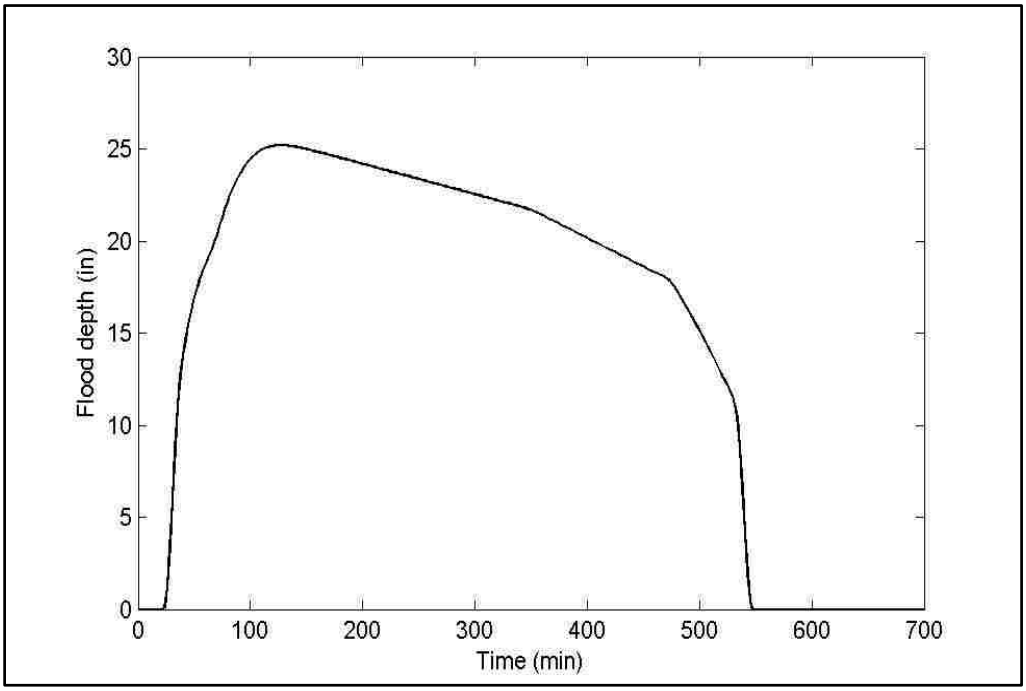

Figure 6.3-8: Flood depth variation over time for grass swale strip

Figure 6.3-9: Peak inundation extent for grass swale strip

6.3.4 Grass Pavers along the Parking Aisles

Figure 6.3-10 shows the runoff hydrograph developed for the grass pavers along the parking aisles of the watershed, and the remaining area of the watershed is covered with porous asphalt. The peak of the hydrograph is 0.40 m^3/s and the time to peak is after 52 minutes of rainfall. The runoff ended after 158 minutes of rainfall. The peak is reduced by 86% from the peak of 2.91 m^3/s of the original impervious asphalt land cover.

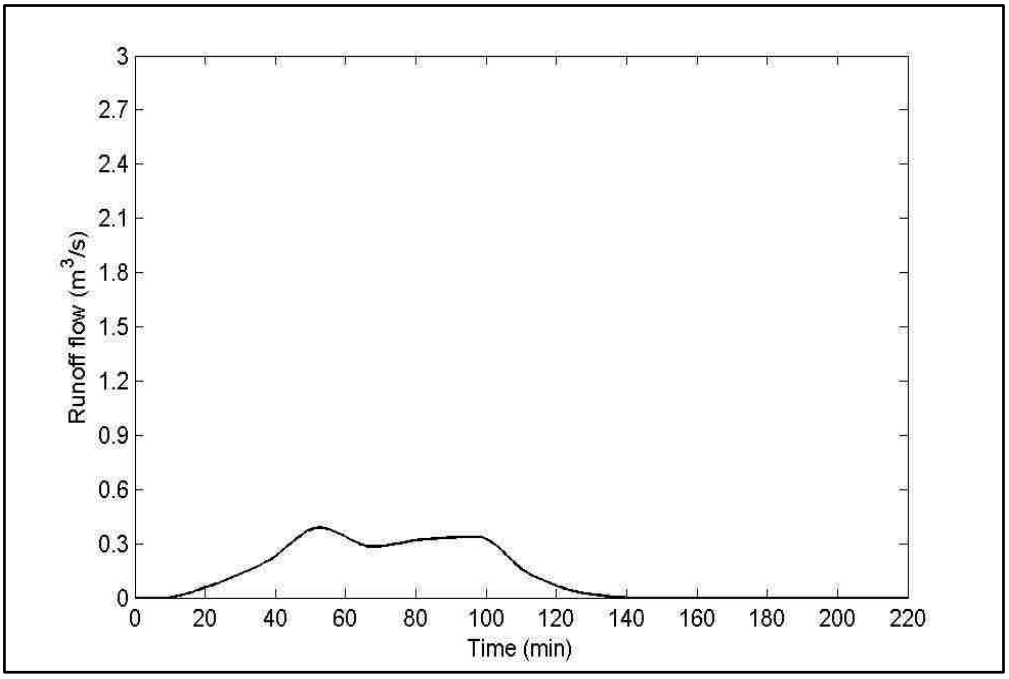

Figure 6.3-10: Runoff hydrograph for the gravel pavers along the parking aisles

The duration of the runoff is reduced by 30%. Figure 6.3-11 shows the flood depth variation over time for this land cover treatment. The peak flood depth is 10.24 inch, and the time to peak is after 97 minutes of rainfall. The flooding starts after 52 minutes of rainfall, and ends after 112 minutes of rainfall resulting in a flood duration of only 60 minutes (1 hour). Thus, the peak depth is reduced by 46%, and the duration of flooding is reduced by only 90% from

the original impervious asphalt land cover. The maximum inundated area for this land cover treatment is shown in figure 6.3-12. The estimated area is 8032 m^2 (10% of the total watershed area). The peak inundated area is also reduced by 9800 m^2 (13%).

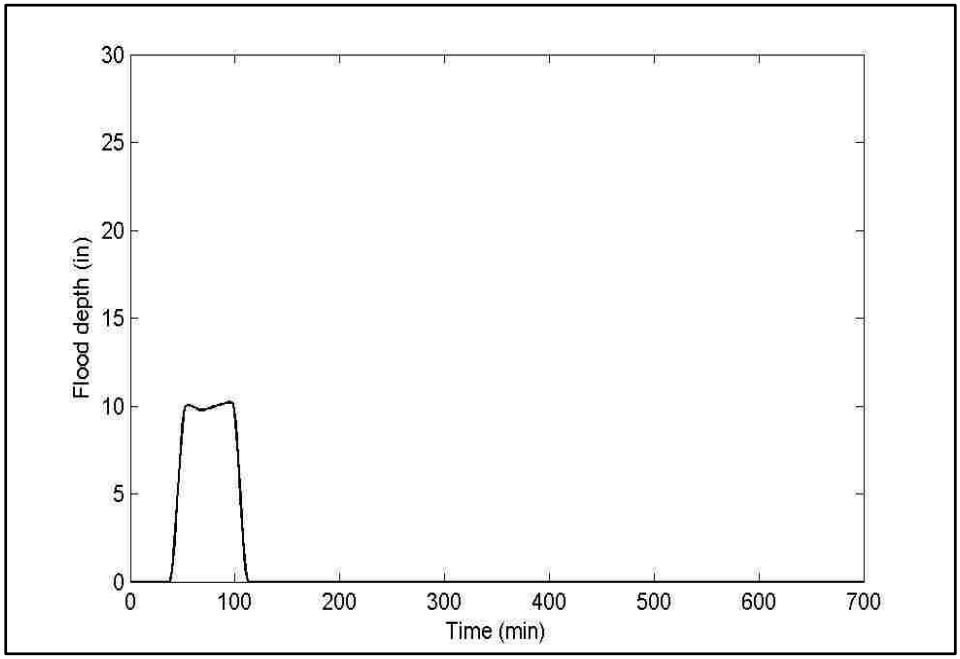

Figure 6.3-11: Flood depth over time for the grass pavers along the parking aisles

Figure 6.3-12: Peak inundation extent for the grass pavers along the parking aisles

6.3.5 Concrete Grid Pavers (CGP)

Figure 6.3-13 shows the runoff hydrograph developed for the concrete grid pavers lain throughout the watershed. The peak of the hydrograph is 0.08 m^3/s and the time to peak is after 82 minutes of rainfall. The runoff ended after 157 minutes of rainfall. The peak is reduced by 97% from the peak of 2.91 m^3/s of the original impervious asphalt land cover. The duration of the runoff is reduced by 30%.

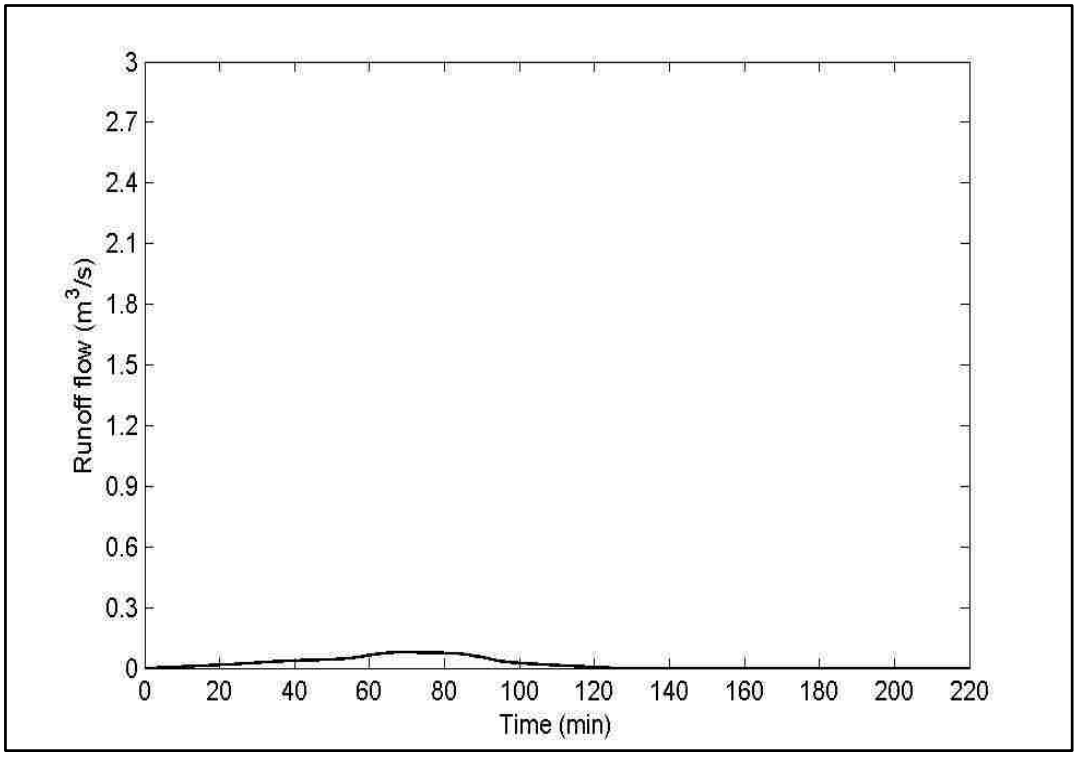

Figure 6.3-13: Runoff hydrograph for the concrete grid pavers

Figure 6.3-14 shows the flood depth variation over time for this land cover treatment. It is observed that the flood depth is 0 inch, and thus there is no flooding for concrete grid pavers. This can be attributed to the lower curve number of concrete grid pavers, and the coverage of the watershed by the concrete grid pavers.

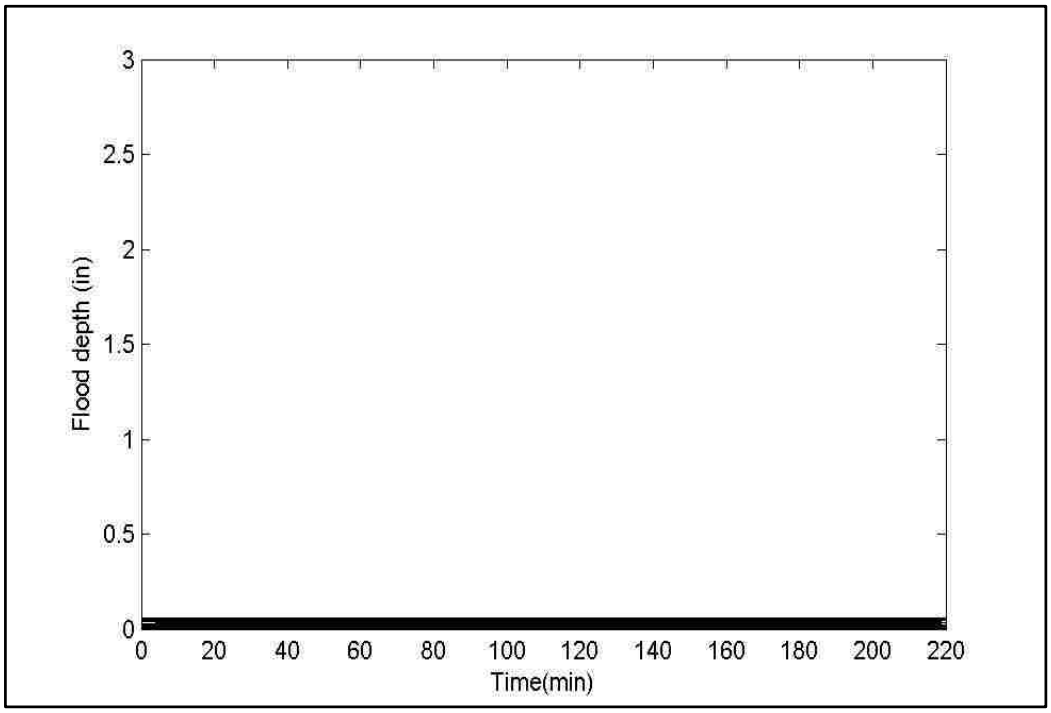

Figure 6.3-14: Flood depth variation over time for concrete grid pavers

6.4 Discussion

Table 6.4-1: Summary of outputs for land cover analysis

Land cover treatment	Peak runoff reduction (%)	Peak flood depth reduction (%)	Inundated area reduction (%)	Flood duration reduction (%)
Porous asphalt pavement system	62	26	5	67
Gravel swale strip	10	2.90	0.50	11
Grass swale strip	10	2.90	0.50	11
Grass pavers	86	46	13	90
Concrete grid paving system	97	100	100	100

Table 6.4-1 shows the summary of outputs for land cover analysis. For the first land cover change, i.e., the porous asphalt, the peak runoff is reduced by 62%, peak flood depth and inundated area are found to be reduced by 26% and 5% respectively, and the

duration of flooding is also found to be reduced by 67% from the peak runoff, peak flood depth, maximum inundated area and flood duration resulted from the original impervious asphalt land cover respectively. This is due to the fact that the porous asphalt has voids (15-20%) in it that permits the runoff to infiltrate into the ground. Therefore, it has lower curve number, and consequently higher abstraction losses through the infiltration than the impervious one. Thus, this land cover treatment produces less runoff, and consequently less flooding. However, the reduced amounts are not that much significant in terms of flood depth and inundated area, and this is due to the fact that the curve number of porous asphalt (88) is not significantly lower than the impervious one (99). It is also noticed that there is no delay in the peak runoff time (82 minutes after rainfall) between the pervious and impervious asphalt. But in real situation, the peak runoff time should be higher for the pervious asphalt since it is rougher than the impervious one. This is because the surface friction of the porous asphalt layer is not considered while calculating velocity of the cells, and thus no delay is observed For the gravel swale strip along the main flow path lines, the peak runoff is reduced by only 10%, peak flood depth and inundated area are found to be reduced by only 2.90% and 0.50% respectively, and the duration of flooding is also found to be reduced by 11% from the peak runoff, peak flood depth, maximum inundated area and flood duration resulted from the original impervious asphalt land cover respectively. The reduction through using this land cover is not significant at all. The gravel swale strip acts almost like the impervious asphalt. This is due to the fact that, though the gravel has lower curve number but the gravel swale strip only contains 5% of the total watershed area. Thus, there is not considerable amount of abstraction losses through infiltration. Besides, as surface friction of the land cover is not

considered in the velocity calculation, no delay is observed in peak runoff or flooding time. Since the gravel swale has the same area as the grass swale, and grass has little less curve number than the gravel, it is observed that the grass swale strip has no effect on reducing flood in the watershed. For the grass pavers along the parking aisles of the watershed, the peak runoff is reduced by 86%, peak flood depth and inundated area are found to be reduced by only 46% and 13% respectively, and the duration of flooding is also found to be reduced by 90% from the peak runoff, peak flood depth, maximum inundated area and flood duration resulted from the original impervious asphalt land cover respectively. It is observed that the putting grass pavers along the parking aisle works better than putting grass pavers along the primary flowpath lines. The main reason behind this is the amount of grass pavers (44% of the total watershed area) is more than the grass pavers along the swale strip. Due to the high existence of grass pavers, more abstraction losses occur through infiltration resulting in less runoff and flooding. For this land cover, it is observed that the peak runoff and flooding occur earlier than the impervious asphalt though the amount is far lower than the impervious asphalt. This is because of the location of the grass pavers [See Figure 6.3-4] that are little bit away from the drain inlet. The areas near the inlet is still covered with porous asphalt, and that produce considerable amount of runoff in quick time greater than the inlet capacity which results in quick flooding. However, since the amount of these areas are not large enough, the amount of peak runoff and flooding is significantly lower than the impervious asphalt. For the concrete grid pavers, the peak runoff is reduced by 97% from the peak runoff resulted from the original impervious asphalt land cover. The peak runoff is only 0.08 m^3/s which is significantly lower than the drain inlet capacity of 0.33 m^3/s, and thus no

flooding is observed for this land cover. This is because, concrete grid pavers have significantly lower curve number than the impervious asphalt that barely produces runoff. However it is observed that the peak runoff occur after 82 minutes of rainfall, the same peak runoff time as for the impervious asphalt. This is because surface friction is not considered in velocity calculation of the grid cells. However, it can be concluded that the concrete grid pavers throughout the watershed performs better than the other land covers considered since it does not produce flooding.

Through the analyses of outputs, it is observed that since the flood model of the GIS-framework is based on the SCS Curve Number method, curve numbers play the most important role in producing runoff and thus, in flooding. Thus, watershed's response to the land cover change against flooding actually originate from the various curve numbers of the land cover materials. The lower the curve number, the less the watershed is favorable to produce flooding. Since grass has the lowest curve number of 68 among the land cover materials, around 50% covering of the watershed through putting the grass pavers along the parking aisles reduce the flooding significantly. It can easily assumed that if the whole watershed is covered with the grass pavers, there would be no flooding. But this type of land cover configuration is not suitable for an urban parking lot like Blacklot parking watershed where there is considerable traffic in the driveways, and the grass pavers cannot handle such traffic load (Brattebo and Booth, 2003). Besides, grass pavers are more vulnerable to clog the drain inlet than the impervious asphalt though dislodging (Brattebo and Booth, 2003). Although, both the grass and gravel pavers have low curve numbers, but swale strips built using them are found be least effective mainly due to their coverage area. If they would cover more

areas, the outputs would be different. The competition is left between the porous asphalt and concrete grid pavers. Concrete grid pavers produce less runoff and flooding than the porous asphalt because of its lower curve number. In terms of structural (load bearing capacity) and surface performance (clogging, raveling etc.) they are equally good (Putman, 2010). Therefore, concrete grid pavers would be the most suitable for flood reduction in Blacklot study site among the land covers considered in this research regardless of other constraints like financial considerations, and besides, they are best used in urban parking lot (Hunt and Collins, 2008).

6.5 Summary

Watershed's hydrologic response to the land cover change is observed through producing the outputs for the land covers of interests using the flood model of the GIS-framework, and analyzing and comparing them with the same outputs of other land covers. The outputs that are chosen to analyze and compare are flood depths, areas, durations, and peak runoff. Though the analyses, it is found that the concrete grid pavers is the only land cover treatment among the land cover of interests that do not produce any flooding. Watershed's response in favor of producing floods becomes negative with the decreasing curve numbers of the land cover materials. This is because, the flood model of the GIS-framework is based on the SCS Curve Number method, and according to the rainfall-runoff equation of the method there will be more runoff, and consequently more flooding for higher curve number. However, no delays are observed in terms of peak runoff and flooding time since surface friction is not considered in velocity calculation of the watershed cells. It is assumed that if surface friction would be considered along with the curve numbers, the results would be different.

CHAPTER 7: SUMMARY AND CONCLUSION

7.1 Summary

Urban floods cause serious economic, structural damages along with environmental damages. In extreme cases, the floods may become fatal too. In order to prevent such damages, flooding in an urban watershed should be well studied to avoid future flooding in the watershed. This research is undertaken to study flooding in urban watersheds using GIS. This research uses GIS techniques and tools to develop a GIS-framework for flood modeling, and mapping the spatiotemporal behaviors of the floods in urban micro watersheds. This research also utilizes the GIS-framework to relate the watershed's hydrologic response to the flood remediation measures through land cover change in the watershed.

In order to develop the GIS-framework, a two-step methodological approach is devised. According to the approach, the framework is first divided into five components: i) Urban watershed delineation, ii) Rainfall to runoff conversion, iii) Runoff to flow conversion, iv) Inundation estimation and mapping, and v) Calibration and validation. Secondly, methods are formulated to produce outputs for each of the components. For the first component of the framework, DEM is used to delineate watershed considering the drain inlet of the study area as a pour point. Rainfall is converted to runoff in the watershed using gridded SCS Curve Number method. Runoff is converted to flow at the drain inlet, i.e., a runoff hydrograph is constructed using time area approach. The runoff hydrograph is compared to the stage discharge curve of the drain inlet to result in inundation, and the flood depths are contoured in GIS to produce inundation maps. The

outputs of the flood model are compared with the observed data to calibrate and validate the model. For calibration, three parameters are used: i) DEM resolution, ii) rainfall temporal resolution, and iii) clogging factor of the drain inlet.

The above mentioned GIS-framework is tested in two study areas: i) Blacklot parking area of UNLV, and ii) East Mall area of UNLV for a flood event occurred in UNLV main campus on September 11, 2012 resulted from a 25-year 1-hour rainfall. These two study sites are chosen for their extensive flood damages, and available flood information. For the Blacklot study site, 5m DEM produces accurate watershed resulting the lowest peak error between the calculated and actual peak flood depth (24%). This calibrated DEM is used for calibration against the interpolated rainfall temporal resolution. The rainfall resolution is observed to have higher errors with increasing resolution resulting lowest error for 15-minutes resolution. The calibrated DEM and rainfall resolution are utilized to calibrate against the clogging factor of the inlet. The lowest peak error of only 0.72% is obtained for a clogging factor of 0.83. For East Mall, 1m DEM produces accurate watershed, and no calibration against the rainfall resolution and clogging factor are done for this study site since it is observed for the previous study site that rainfall resolution does not have any meaningful impact on the outputs, while a recommended value of 0.10 is used as a clogging factor for the drain inlet. The flood model of the GIS framework is found to be very sensitive to the total amount of rainfall.

In order to relate the watershed hydrologic response to the flood remediation measures through land cover change, the original land cover of the Blacklot watershed is changed to: i) Porous asphalt pavement system throughout the watershed, ii) Gravel swale strip constructed along the central flowpath lines of the watershed, iii) Grass swale

strip built along the central flowpath lines of the watershed, iv) Gravel pavers along the parking aisles of the watershed, and v) Concrete grid paving system throughout the watershed. For the porous asphalt, peak flood depth, total inundated area and flood duration are found to be reduced by 26%, 5% and 67% respectively. The gravel and grass swale strips, reduce flood depth by only 2.90%, and flood area and duration by only 0.50% and 11% respectively. For the grass pavers, the peak depth, inundated area, and duration of flooding are reduced by 46%, 13% and 90% respectively. For the concrete grid pavers, no flooding is observed in the study site.

7.2 Conclusions

The conclusions can be summarized as:

1) This research has developed a GIS-framework for urban flood modeling, and spatiotemporal mapping in micro watersheds. It has been able to devise methods, and produce outputs for each of the framework's components.
2) This research has also analyzed urban watershed hydrologic response to the flood remediation land covers. As a byproduct, it has been able to find out the optimum land cover in the study site to reduce flooding.
3) The major findings through the testing of the GIS-framework in the are provided below:
    I. DEM of 5 meter resolution produces the accurate watershed for the drain inlet of the Blacklot parking area, while 1m DEM produces the accurate one for the East Mall drain inlet. Therefore, these

resolutions can be used for future hydrologic modeling in these areas.

II. A clogging factor of 0.10 can be used as a clogging factor for East Mall inlet for future hydrologic modeling, while clogging factor of 0.83 obtained for the Blacklot drain inlet needs investigation.

III. When using SCS Curve Number method, interpolated rainfall distribution does not have any meaningful impacts on the outputs of the flood model. Therefore, it is suggested not to interpolate rainfall distribution to higher resolution when using SCS method.

IV. The peak error between the estimated and actual flood depth for the Blacklot watershed is found 24%. This high amount of error is mainly attributed to the SCS Curve Number method since the method considers initial abstraction losses through infiltration and evaporation that should be negligible for a small watershed covered with highly impervious asphalt layer like the Blacklot watershed. Therefore, this method should be applied with care in highly impermeable micro watersheds.

V. The peak error between the estimated and actual flood depth for the East Mall watershed is found only 5%. The method produces better results for East Mall watershed since its 50% area is covered with vegetation, and considerable abstraction losses occur mainly through infiltration losses. Therefore, it can be said that the SCS

Curve Number method can be used successfully in a vegetative micro watershed.

VI. Regardless of cost or any other constraints, concrete grid pavers can be used in the Blacklot watershed to minimize flooding. Porous asphalt also reduces flooding but less than the concrete grid pavers. Grass or gravel pavers lain throughout the watershed also would not produce flooding, but they are not suggested over concrete grid pavers due to their lower wheel load handling capacity and stability.

VII. A study site should be calibrated against DEM resolution when the DEMs are created from the point cloud elevation data like LiDAR data. This is because, through the calibration an irregular trend of DEM resolution is observed against the peak flood depth error. For example, in case of Blacklot watershed, 3m DEM produces more error that the 4m DEM, and 8m DEM produces more error than 9m DEM.

VIII. Finally, apart from the hydrologic method used in the research, the errors produced may be attributed to the accuracy of the data. The LiDAR elevation data are found to have errors that are minimized but not removed completely while creating DEM. In some cases, the data are found in either high resolution (e.g. LiDAR point data) or moderate resolution (e.g. rainfall data), while in some cases they are found in low resolution (e.g. Landcover data, soil data).

Further, in some cases the data are considered uniform, which is not true in real situation (e.g. spatial distribution of rainfall data is not considered). Also, the errors may come from the assumptions used. For instance, it is assumed that the discharge of the inlet does not change when the water depth reaches the curb opening of the inlet, though in reality the discharge increases with the increase in depth.

7.2.1 Limitations

The limitations of the research are as follows:

1) Though this research considers only the watersheds that drain into storm drain inlets, but it can be extended for other watersheds.
2) Street drain inlet on grade were not considered but the appropriate equations can be adopted into the framework.
3) Due to the low rainfall intensity, the research does not consider wet and dry moisture condition while estimating runoff using SCS method. Besides, SCS Curve Number method is not applicable for big watershed, and thus limiting the research into small watersheds.
4) While reusing the research for another flood event in the study sites, the clogging factors for the drain inlets might need to be investigated.

7.3 Recommendations

The recommendations would be as follows:

1) The GIS-framework developed in this research can be utilized to any other uncalibrated small urban study area that has a storm drain inlet so that the delineated watershed would drain into the inlet.
2) When using the GIS-framework for modeling floods in micro watersheds covered with highly impenetrable material like asphalt or concrete, SCS Curve Number method should be applied with proper caution, instead other hydrologic method like distributed instantaneous unit hydrograph method might get preference.
3) When using the SCS Curve Number method as the hydrologic method for flood model of the framework, dry and wet moisture condition should be taken into account for estimating runoff in case of high rainfall intensity.
4) Elevation, rainfall, soil and land cover data should be of high resolution as much as possible since these are the four most important parameters of the GIS-framework flood model. Therefore, before utilizing the GIS-framework for another study site or another rainfall event it should be made sure that these data are of high resolution and error free as much as possible.
5) This research can be improved by considering the true situation that the discharge increases with the water depth when constructing the stage discharge curve of the inlets.

APPENDIX

Curve Number table for NLCD classes along with HSGs

Class No.	General Description of Classes	Hydrologic Condition	Curve Number			
			HSG A	HSG B	HSG C	HSG D
11	Open Water	ALL	100	100	100	100
12	Perennial Ice/Snow	ALL	100	100	100	100
21	Developed, Open Space (lawns, parks, golf courses, cemeteries etc.)	Good	39	61	74	80
		Fair	49	69	79	84
		Poor	68	79	86	89
22	Developed, Low Intensity (Impervious surfaces = 20% to 49%)	ALL	66	79	86	89
23	Developed, Medium Intensity (Impervious surfaces = 50% to79%)	ALL	86	91	94	95
24	Developed, High Intensity (Impervious surfaces = 80% to 100%)	ALL	95	96	97	98
31	Barren Land (Rock/Sand/Clay)	ALL	77	86	91	94
41	Deciduous Forest	Good	30	55	70	77
		Fair	36	60	73	79
		poor	45	66	77	83
42	Evergreen Forest	Good	30	55	70	77
		Fair	36	60	73	79
		poor	45	66	77	83
43	Mixed Forest	Good	30	55	70	77
		Fair	36	60	73	79
		poor	45	66	77	83
51	Dwarf Scrub	Good	35	56	70	77
		Fair	48	56	70	77
		poor	48	67	77	83
52	Shrub/Scrub	Good	35	56	70	77
		Fair	48	56	70	77
		poor	48	67	77	83
71	Grassland/Herbaceous	Good	49	69	79	84
		Fair	54	74	84	87
		poor	58	78	88	91
72	Sedge/Herbaceous	Good	49	69	79	84
		Fair	54	74	84	87
		poor	58	78	88	91

73	Lichens	Good	49	69	79	84
		Fair	54	74	84	87
		poor	58	78	88	91
74	Moss	Good	49	69	79	84
		Fair	54	74	84	87
		poor	58	78	88	91
81	Pasture/Hay	Good	67	78	85	89
		Fair	70	80	87	90
		poor	72	81	88	91
82	Cultivated Crops	Good	67	78	85	89
		Fair	70	80	87	90
		poor	72	81	88	91
90	Woody Wetlands	ALL	100	100	100	100
95	Emergent Herbaceous Wetlands	ALL	100	100	100	100

REFERENCES

Ahmad, M. M., Ghumman, A. R., & Ahmad, S. (2009). Estimation of Clark's instantaneous unit hydrograph parameters and development of direct surface runoff hydrograph. Water resources management, 23(12), 2417-2435.

Ahmad, M. M., Ghumman, A. R., Ahmad, S., & Hashmi, H. N. (2010). Estimation of a unique pair of Nash model parameters: an optimization approach. Water resources management, 24(12), 2971-2989.

Ahmad, S., & Simonovic, S. P. (1999). Comparison of one-dimensional and two-dimensional hydrodynamic modeling approaches for Red River Basin. [report] Ottawa, Washington: International Joint Commission-Red River Basin Task Force, pp. 1-51.

Ahmad, S., & Simonovic, S. P. (2001). Developing runoff hydrograph using artificial neural networks. Paper presented at ASCE conference in Bridging the Gap: Meeting the World's Water and Environmental Resources Challenges, Orlando, FL. doi: 10.1061/40569(2001)54

Ahmad, S., & Simonovic, S. P. (2001). Modeling Dynamic Processes in Space and Time--A Spatial System Dynamics Approach. Paper presented at ASCE conference in Bridging the Gap: Meeting the World's Water and Environmental Resources Challenges, Orlando, FL. doi: 10.1061/40569(2001)88

Ahmad, S., & Simonovic, S. P. (2004). Spatial system dynamics: new approach for simulation of water resources systems. Journal of Computing in Civil Engineering, 18(4), 331-340.

Ahmad, S., & Simonovic, S. P. (2005). An artificial neural network model for generating hydrograph from hydro-meteorological parameters. Journal of Hydrology, 315(1), 236-251.

Aronica, G., Freni, G. & Oliveri, E. (2005) Uncertainty analysis of the influence of rainfall time resolution in the modelling of urban drainage systems. Hydrol. Processes 19, 1055–1071.

Ashour, R. A. (2000). Description of a simplified GIS-based surface water model for an arid catchment in Jordan. In Proceedings of 20th Annual International ESRI User Conference, held in San Diengo, CA, USA, on June (pp. 26-30).

Brattebo, B. O., & Booth, D. B. (2003). Long-term stormwater quantity and quality performance of permeable pavement systems. Water research, 37(18), 4369-4376.

Brown, S. A., Stein, S. M., & Warner, J. C. (1996). URBAN DRAINAGE DESIGN MANUAL: HYDRAULIC ENGINEERING CIRCULAR NO. 22 (No. FHWA-SA-96-078).

Bryant, S. D., Carper, K. A., & Nicholson, J. (2001). GIS Tools for Proactive Urban Watershed Management. In Urban Drainage Modeling (pp. 638-648). ASCE.

Carrier, C., Kalra, A., & Ahmad, S. (2011). Using proxy reconstructions for streamflow forecasting. Paper presented at ASCE conference in World Environmental and Water Resources Congress: Bearing Knowledge for Sustainability (pp. 3124-3133), Palm Spring, CA. doi: 10.1061/41173(414)326

Carrier, C., Kalra, A., & Ahmad, S. (2013). Using paleo reconstructions to improve streamflow forecast lead time in the western United States. JAWRA Journal of the American Water Resources Association, 49(6), 1351-1366.

CCRFCD (2013). History of Flooding in Clark County. Retrieved from: http://www.ccrfcd.org/03-history.htm

Chen, J., Hill, A. A., & Urbano, L. D. (2009). A GIS-based model for urban flood inundation. Journal of Hydrology, 373(1), 184-192.

Cronshey, R. (1986). Urban hydrology for small watersheds. US Dept. of Agriculture, Soil Conservation Service, Engineering Division.

Dawadi, S., & Ahmad, S. (2012). Changing climatic conditions in the Colorado River Basin: Implications for water resources management. Journal of Hydrology, 430, 127-141.

De Smedt, F., Liu, Y. B., & Gebremeskel, S. (2000). Hydrologic modeling on a catchment scale using GIS and remote sensed land cover information. Risk analysis II, 295-304.

DeVantier, B. A., & Feldman, A. D. (1993). Review of GIS applications in hydrologic modeling. Journal of Water Resources Planning and Management, 119(2), 246-261.

Drainage, U. (2002). Flood Control District. 2001. Urban storm drainage criteria manual-volume 1. Retrieved from: http://www.udfcd.org/downloads/down_critmanual_volI.htm

Ellis, J. B., & Viavattene, C. (2013). Sustainable Urban Drainage System Modeling for Managing Urban Surface Water Flood Risk. CLEAN–Soil, Air, Water.

Estiri, H., Rottle, N., & Batten, L. (2012, March). Stormwater estimation for management in urban watersheds: a landuse-based GIS model. In AWRA 2012 Spring Specialty Conference.

Feyen, L., Barredo, J. I., & Dankers, R. (2008). Implications of global warming and urban land cover change on flooding in Europe. Water and urban development paradigms–Towards an integration of engineering, design and management approaches, 217-225.

Forsee, W. J., & Ahmad, S. (2011). Evaluating urban storm-water infrastructure design in response to projected climate change. Journal of Hydrologic Engineering, 16(11), 865-873.

Forsee, W., & Ahmad, S. (2011). Using HEC-HMS for Stormwater Infrastructure Assessment in Response to Changes in Design Storm Depths Calculated from Climate Projections. Paper presented at ASCE conference in World Environmental

and Water Resources Congress: Bearing Knowledge for Sustainability (pp. 1318-1327), Palm Spring, CA. doi: 10.1061/41173(414)326

Genovese, E. (2006). A methodological approach to land use-based flood damage assessment in urban areas: Prague case study. Technical EUR Reports, EUR, 22497.

GISHydroNXT User's Manual. (2014).Retrieved from: http://www.gishydro.eng.umd.edu/documents/mdsha_reports/GISHydroNXT_documentation2011.pdf.

Goforth, G. F. (1983). AN ADVANCEMENT IN HYDRAULIC MODELING OF POROUS PAVEMENT FACILITIES. In Proceedings of Stormwater and Water Quality Model Users Group Meeting, January 27-28, 1983 (Vol. 83, No. 15, p. 237). Environmental Research Laboratory, Office of Research and Development, US Environmental Protection Agency.

Goulden, T., Hopkinson, C., Jamieson, R., & Sterling, S. (2014). Sensitivity of watershed attributes to spatial resolution and interpolation method of LiDAR DEMs in three distinct landscapes. Water Resources Research.

Greene, R. G., & Cruise, J. F. (1995). Urban watershed modeling using geographic information system. Journal of water resources planning and management, 121(4), 318-325.

Grimaldi, S., Petroselli, A., & Nardi, F. (2012). A parsimonious geomorphological unit hydrograph for rainfall–runoff modelling in small ungauged basins. Hydrological Sciences Journal, 57(1), 73-83.

Guo, J. C. Y., & MacKenzie, K. (2012). Hydraulic Efficiency of Grate and Curb-opening Inlets Under Clogging Effect (No. CDOT-2012-3). Colorado Department of Transportation, DTD Applied Research and Innovation Branch.

Guo, J. C., MacKenzie, K. A., & Mommandi, A. (2009). Design of Street Sump Inlet. Journal of Hydraulic Engineering, 135(11), 1000-1004.

Guo-an, T., Yang-he, H. U. I., Strobl, J., & Wang-qing, L. I. U. (2001). The impact of resolution on the accuracy of hydrologic data derived from DEMs. Journal of Geographical Sciences, 11(4), 393-401.

Hunt, W. F., & Collins, K. A. (2008). Permeable pavement: Research update and design implications. North Carolina Cooperative Extension Service. Raleigh, NC.

Huong, H. T. L., & Pathirana, A. (2013). Urbanization and climate change impacts on future urban flooding in Can Tho city, Vietnam. Hydrology and Earth System Sciences, 17(1), 379-394.

Jing, Z. H. U. (2010, December). GIS Based Urban Flood Inundation Modeling. In Intelligent Systems (GCIS), 2010 Second WRI Global Congress on (Vol. 2, pp. 140-143). IEEE.

Kalra, A., & Ahmad, S. (2012). Estimating annual precipitation for the Colorado River Basin using oceanic‐atmospheric oscillations. Water Resources Research, 48(6).

Kilgore, J. L. (1997). Development and evaluation of a GIS-based spatially distributed unit hydrograph model (Doctoral dissertation, Virginia Polytechnic Institute and State University).

Konrad, C. P. (2003). Effects of urban development on floods.

Kumar, P. S., Babu, M. J. R. K., & Praveen, T. V. (2010). Analysis of the Runoff for Watershed Using SCS-CN Method and Geographic Information Systems. International Journal of Engg. Sci. and Tech, 2(8), 3947-3954.

Lindsay, J. B., Rothwell, J. J., & Davies, H. (2008). Mapping outlet points used for watershed delineation onto DEM-derived stream networks. Water resources research, 44(8).

Links, N. O. A. A. Unit Hydrograph (UHG) Technical Manual.

Lu, D., Hetrick, S., & Moran, E. (2011). Impervious surface mapping with QuickBird imagery. International journal of remote sensing, 32(9), 2519-2533.

MacKenzie, K., & Guo, J. (2011). UDFCD Street Inlet Capacity Technical Memorandum. Retrieved from: http://www.udfcd.org/downloads/pdf/tech_papers/UDFCD%20Street%20Inlet%20Capacity.pdf.

Merwade, V. (2012). Downloading SSURGO Soil Data from Internet. Retrieved from: https://web.ics.purdue.edu/~vmerwade/education/ssurgo.pdf.

Miller, S. N., Semmens, D. J., Miller, R. C., Hernandez, M., Goodrich, D. C., Miller, W. P. ... & Ebert, D. (2002, July). GIS-based hydrologic modeling: the automated geospatial watershed assessment tool. In Proceeding of the Second Federal Interagency Hydrologic Modeling Conference (p. 12).

Mosquera-Machado, S., & Ahmad, S. (2007). Flood hazard assessment of Atrato River in Colombia. Water Resources Management, 21(3), 591-609.

National Asphalt Pavement Association. (2014). Retrieved from: http://www.asphaltpavement.org/

NRCS (2008). Urban Soil Erosion and Sediment Control. Retrieved from: http://www.nrcs.usda.gov/Internet/FSE_DOCUMENTS/nrcs141p2_034363.pdf.

Olivera, F., & Maidment, D. (1999). Geographic information systems (GIS)-based spatially distributed model for runoff routing. Water Resources Research, 35(4), 1155-1164.

Oregon Department of Transportation Hydraulics Manual. (2005). Retrieved from: ftp://ftp.odot.state.or.us/techserv/geoenvironmental/Hydraulics/Hydraulics%20Manual/Chapter_13/Chapter_13.pdf

Pandit, A., & Heck, H. H. Estimation of Curve Numbers for Concrete and Asphalt. In World Environmental and Water Resources Congress 2008@ sAhupua'A (pp. 1-1). ASCE.

Ponce, V. M., & Hawkins, R. H. (1996). Runoff curve number: Has it reached maturity?. Journal of hydrologic engineering, 1(1), 11-19.

Prodanović, D., Stanić, M., Milivojević, V., Simić, Z., & Arsić, M. (2009). DEM-based GIS algorithms for automatic creation of hydrological models data. Journal of Serbian Society for Computational Mechanics, 3(1), 64-85.

Putnam, B. J. (2010). Field performance of porous pavements in South Carolina.

Randerson, D. (1976). Meteorological analysis for the Las Vegas, Nevada, flood of 3 July 1975. Monthly Weather Review, 104(6), 719-727.

Sagarika, S., Kalra, A., & Ahmad, S. (2014). Evaluating the effect of persistence on long-term trends and analyzing step changes in streamflows of the continental United States. Journal of Hydrology, 517, 36-53.

Searcy, J. K., & Hardison, C. H. (1950). MANUAL OF HYDROLOGY: PART I, GENERAL SURFACE-WATER TECHNIQUES. Geological Survey Water-supply Paper, 31.

Sorrell, R. C., & Hamilton, D. A. (2003). Computing flood discharges for small ungaged watersheds. Geological and Land Management Division, Michigan Department of Environmental Quality, Lansing, Michigan.

Soulis, K. X., & Valiantzas, J. D. (2012). Identification of the SCS-CN Parameter Spatial Distribution Using Rainfall-Runoff Data in Heterogeneous Watersheds. Water Resources Management, 27(6), 1737-1749.

Sui, D. Z., & Maggio, R. C. (1999). Integrating GIS with hydrological modeling: practices, problems, and prospects. Computers, environment and urban systems, 23(1), 33-51.

Swales, V. (1999). Storm Water Technology Fact Sheet Vegetated Swales.

UNHSC Design Specifications for Porous Asphalt Pavement and Infiltration Beds. University of New Hampshire Stormwater Center (UNHSC). (2014).Retrieved from: http://www.unh.edu/erg/cstev

Urbonas, B. (2007). Stormwater Runoff Modeling; Is it as Accurate as We Think?. Keynote Address at the Engineering Conferences International Conference on Urban Runoff Modeling: Intelligent Modeling to Improve Stormwater Management, Humboldt State Univ., Arcata, CA.

Usul, N., & Yilmaz, M. (2002). Estimation of instantaneous unit hydrograph with Clark's Technique in GIS. In Proceedings of 2002 ESRI international user conference. ESRI on-line, San Diego. http://proceedings. esri. com/library/userconf/proc02.

Wang, X., Gu, X., Wu, Z., & Wang, C. (2010, May). Simulation of flood inundation of Guiyang City using remote sensing, GIS and hydrologic model. In Int Arch Photogramm Rem Sens Spat Inf Sci, Proc Comm VIII, ISPRS Congress, 3rd-11th

July, Beijing, China. http://www. isprs. org/proceedings/XXXVII/congress/tc8. aspx. Accessed (Vol. 1).

Wang, Y., Bin, H., & Keiji, T. (2009) Effects of temporal resolution on hydrological model parameters and its impact on prediction of river discharge. Hydrological Sciences Journal, 54:5, 886-898.

Watershed Delineation with ArcGIS 10. Trent University Library. (2014). Retrieved from: https://www.trentu.ca/library/data/DelineateWatersheds_V10.pdf.

Wehmeyer, L. L., Weirich, F. H., & Cuffney, T. F. (2011). Effect of land cover change on runoff curve number estimation in Iowa, 1832–2001. Ecohydrology, 4(2), 315-321.

Wilson, J. P., & Gallant, J. C. (Eds.). (2000). Terrain analysis: principles and applications. John Wiley & Sons.

Yuan, Y., Nie, W., McCutcheon, S. C., & Taguas, E. V. (2014). Initial abstraction and curve numbers for semiarid watersheds in Southeastern Arizona. Hydrological Processes, 28(3), 774-783.

Zhang, Y., McBroom, M., & Hung, I. (2011). Snapping a Pour Point for Watershed Delineation in ArcGIS Hydrologic Analysis. Retrieved from: http://www.faculty.sfasu.edu/zhangy2/download/Snapping%20a%20Pour%20Point%20forWatershed%20Delineation.pdf.

VITA

Graduate College
University of Nevada, Las Vegas

Sayed Joinal Hossain Abedin

Degrees:

Bachelor of Science, Water Resources Engineering, 2009
Bangladesh University of Engineering and Technology, Bangladesh

Thesis Title:

GIS FRAMEWORK FOR SPATIOTEMPORAL MAPPING OF URBAN FLOODING AND ANALYSIS OF WATERSHED HYDROLOGIC RESPONSE TO LAND COVER CHANGE

Thesis Examination Committee:

Chairperson, Dr. Haroon Stephen, Ph. D
Committee Member, Dr. Sajjad Ahmad, Ph. D
Committee Member, Dr. Jacimaria Batista, Ph. D
Graduate Faculty Representative, Zhongbo Yu, Ph. D